

PhD degree in Molecular Medicine, Curriculum in Molecular Oncology

*European School of Molecular Medicine (SEMM),*

*University of Milan and University of Naples "Federico II"*

Disciplinary sector BIO/11

**ROLE OF NUCLEAR ENVELOPE PROTEIN MAN1  
IN NUCLEAR ORGANISATION  
AND MAINTENANCE OF GENOME STABILITY**

*Stefania Bertora*

*IFOM, Milan*

*Matriculation number: R10736*

***Supervisor: Dr. Vincenzo Costanzo***

IFOM, Milan

***Added supervisor: Prof. Elisabetta Dejana***

IFOM, Milan

*Academic year 2017-2018*

# TABLE OF CONTENTS

Abbreviations.....	5
List of Figures.....	7
List of Tables.....	9
<b><u>ABSTRACT</u></b> .....	10
<b><u>INTRODUCTION..</u></b> .....	11
<b>1. The eukaryotic cell nucleus</b> .....	11
<b>2. Eukaryotic chromatin organization</b> .....	13
<b>3. Nuclear tethering</b> .....	15
3.1. Nuclear tethering and genomic stability.....	15
3.1.1. Nuclear organization and DNA repair.....	16
3.1.2. Nuclear tethering and Homology-directed Repair.....	17
3.1.3. Nuclear tethering and DNA replication stress.....	22
3.2. Cell cycle and chromatin organization.....	24
3.2.1. Effect of nuclear tethering on DNA replication.....	24
3.2.2. Nuclear assembly and disassembly during mitosis.....	27
3.3. Role of nuclear tethering in gene regulation and cell differentiation.....	28
<b>4. The nuclear lamina</b> .....	30
4.1. Lamins.....	30
4.2. Lamin-associated proteins: LEM-domain family.....	31
4.3. Barrier to autointegration factor (BAF).....	34
4.4. Man1.....	35
<b>5. Xenopus cell-free extract as model system to study nuclear assembly and         DNA metabolism</b> .....	37
<b><u>MATERIALS AND METHODS</u></b> .....	39
<b>1. Solutions</b> .....	39

<b>2. Growth media</b> .....	40
2.1. <i>Escherichia coli</i> growth media.....	40
2.2 Mouse embryonic stem cell media.....	41
<b>3. Molecular biology technique</b> .....	41
3.1 Agarose gel electrophoresis.....	41
3.2 Transformation of <i>E. coli</i> .....	42
3.3. Cloning of <i>Xenopus</i> Man1.....	42
3.4. Preparation of recombinant xMan1 proteins.....	43
3.5. SDS-page.....	43
3.6. Western blot analysis.....	43
3.6.1. Antibodies.....	44
<b>4. <i>Xenopus</i> techniques</b> .....	44
4.1. <i>Xenopus</i> sperm and egg extracts.....	44
4.1.1. Interphase extracts.....	45
4.1.2. Mitotic (CSF-arrested) extracts.....	45
4.1.3. Cycling extracts.....	47
4.1.4. Demembranated sperm preparation.....	47
4.2. Nuclear assembly in interphase extracts.....	48
4.3. Assay for the nuclear envelope integrity.....	48
4.4. Nuclear pore assembly assay.....	49
4.5. Immunofluorescence on isolated <i>Xenopus</i> nuclei.....	49
4.6. Replication assay.....	50
4.7. Visualization of nascent single stranded DNA on alkaline agarose gel.....	50
4.8. Chromatin binding experiment.....	51
4.9. Halo assay.....	52
4.10. Nuclear assembly in CSF extracts.....	52
4.11. Analysis of the cell cycle using <i>Xenopus</i> cycling extracts.....	53

<b>5. Cell culture techniques</b> .....	53
5.1 ESC cell lines.....	53
5.2. Generation of CRISPR-Cas9 Man1 ko clones.....	53
5.3. PCR screening of CRISPR-Cas9 clones.....	55
5.4. Preparation of whole cell extracts for western blotting.....	56
5.5. Total RNA extraction.....	57
5.6. Reverse-transcriptase quantitative PCR(RT-qPCR).....	57
5.7. Alkaline phosphatase staining.....	59
5.8. Embryoid bodies formation.....	59
<b><u>RESULTS</u></b> .....	60
<b>1. Man1 characterization using the <i>Xenopus</i> cell-free extract system</b> .....	60
1.2. Analysis of <i>X. Leavis</i> Man1 sequence and structure.....	60
1.3. Generation of Man1 derivative mutants.....	62
1.4. The N-terminal fragment of Man1 impairs nuclear assembly and chromatin decondensation.....	64
1.5. Man1 N-terminal fragment does not impair nuclear envelope enclosure but it affects nuclear pore formation.....	68
1.6. Man1 N-terminal domain inhibits DNA replication and causes accumulation of DNA damage.....	73
1.7. Man1 N-terminal fragment alters the chromatin organization inside the nucleus.....	79
1.8. Man1 N-terminal fragment alters cell cycle progression by inhibiting the exit from mitosis.....	81
<b>2. Characterization of man1 in mouse embryonic stem cells</b> .....	86
2.1. Generation of stable Man1-knockout cell lines .....	86
2.2. Man1-knockout mESCs display features of differentiating cells.....	90
2.3. Man1-knockout mESCs show an alteration of pericentromeric and	

telomeric RNA expression.....	93
<b><u>DISCUSSION</u></b> .....	95
<b><u>REFERENCES</u></b> .....	101

## ABBREVIATIONS

3C = Chromosome Conformation Capture

AP = Alkaline Phosphatase

BAF = Barrier to Autointegration Factor

BMP = Bone Morphogenetic Protein

BSA = Bovine Serum Albumine

CDK = Cyclin-Dependent Kinase

CRISPR = Clustered Regularly Interspaced Short Palindromic Repeats

DHCC = Dihexyloxacarboocyanine iodide

dHJ = double Holliday Junction

D-Loop = Displacement Loop

DNA = Deoxyribonucleic Acid

DSB = Double Strand Break

DSBR = Double Strand Break Repair

EB = Embryoid Body

EDMD = Emery-Dreyfuss Muscular Dystrophy

GCR = Gross Chromosomal Rearrangement

GFP = Green Fluorescent Protein

HGPS = Hutchinson-Gilford Progeria Syndrome

HR = Homologous Recombination

INM = Inner Nuclear Membrane

kbp = kilo base-pair

kDa = kilo Dalton

LAD = Lamin-Associated Domain

LEM = Lap2 $\beta$ -Emerin-Man1

LEM-D = LEM Domain

LIF = Leukaemia Inhibitory Factor

LOH = Loss of Heterozygosis

MCM = Minichromosome Maintenance

mESC = mouse Embryonic Stem Cell

MFHR = Maximum Fluorescence Halo Radius

MSC = Man1-Src 1p-C-terminal

NE = Nuclear Envelope

NGPS = Nestor-Guillermo Progeria Syndrome

NHEJ = Non Homologous End Joining

NLS = Nuclear Localization Signal

NPC = Nuclear Pore Complex

ONM = Outer Nuclear Membrane

ORC = Origin Recognition Complex

pcRNA = pericentromeric RNA

Pre-RC = Pre-Replication Complex

rDNA = ribosomal DNA

RNA = Ribonucleic Acid

RRM = RNA Recognition Motif

RT-qPCR = Reverse Transcriptase – quantitative PCR

SAC = Spindle Assembly Checkpoint

SDSA = Synthesis-Directed Strand Annealing

SSA = Single Strand Annealing

ssDNA = single-stranded DNA

TAD = Topological Associated Domain

TERRA = Telomeric Repeat-containing RNA

TGF $\beta$  = Transforming Growth Factor  $\beta$

## LIST OF FIGURES

<b>Figure 1.</b> The eukaryotic cell nucleus.....	12
<b>Figure 2.</b> Chromosome territories.....	14
<b>Figure 3.</b> Pathways of Homologous Recombination.....	20
<b>Figure 4.</b> Pre-Replication Complex (Pre-RC) assembly on DNA replication origin.	25
<b>Figure 5.</b> LEM-domain protein family.....	34
<b>Figure 6.</b> Sequence alignment between <i>X. laevis</i> and human Man1 proteins.....	62
<b>Figure 7.</b> Structure and functional domains of <i>Xenopus</i> Man1 and its recombinant derivatives.....	64
<b>Figure 8.</b> Effect of Man1 mutants on nuclear assembly and nucleotide incorporation.....	66
<b>Figure 9.</b> Dose-dependent effect of Man1 N-terminal fragment on nuclear assembly over time.....	67
<b>Figure 10.</b> Effect of recombinant LEM domain on nuclear assembly.....	67
<b>Figure 11.</b> Effect of Man1 N-terminal mutant on nuclear envelope integrity.....	69
<b>Figure 12.</b> Effect of Man1 N-terminal mutant on nuclear import.....	70
<b>Figure 13.</b> Nuclear pore assembly assay.....	71
<b>Figure 14.</b> Nup-153 immunostaining of assembled nuclei.....	72
<b>Figure 15.</b> Effect of Man1 mutants on DNA replication.....	74
<b>Figure 16.</b> Visualization of nascent ssDNA strands by alkaline gel electrophoresis..	75
<b>Figure 17.</b> Effect of Man1 N-terminal fragment on M13 ssDNA replication.....	76
<b>Figure 18.</b> Chromatin binding of DNA replication factors on nuclei assembled in the presence of Man1 N-terminal fragment.....	77
<b>Figure 19.</b> $\gamma$ H2A.X immunostaining of replicating nuclei.....	79
<b>Figure 20.</b> High order chromatin organization in nuclei assembled in presence of Man1 N-terminal fragment.....	80
<b>Figure 21.</b> Effect of Man1 N-terminal recombinant fragment and LEM domain on nuclear reformation after mitosis.....	82
<b>Figure 22.</b> Effect of recombinant LEM domain on cell cycle progression.....	84



<b>Figure 23.</b> Expression levels of Man1 in D1 Man1-Knockout mESCs.....	87
<b>Figure 24.</b> Western blot analysis of D1 Man1-KO cells.....	88
<b>Figure 25.</b> PCR screening for E14 Man1-KO positive clones.....	89
<b>Figure 26.</b> Western blot analysis of E14 Man1-KO clones.....	89
<b>Figure 27.</b> Phase-contrast microscopic analysis of E14 Man1-KO colonies morphology.....	90
<b>Figure 28.</b> Alkaline Phosphatase staining of E14 Man1 KO colonies.....	91
<b>Figure 29.</b> Expression of common stem cell markers in E14 Man1-KO clones.....	91
<b>Figure 30.</b> Embryoid Bodies formation.....	92
<b>Figure 31.</b> Expression of pericentromeric and telomeric transcripts.....	93
<b>Figure 32.</b> Schematic representation of the proposed mechanism of action of <i>Xenopus</i> Man1 N-terminal fragment.....	95
<b>Figure 33.</b> Schematic representation of the role of Man1 in <i>Xenopus</i> nuclear assembly, DNA replication and mitosis.....	99

## LIST OF TABLES

<b>Table 1.</b> List of PCR primers used for <i>Xenopus</i> Man1 cloning.....	42
<b>Table 2.</b> List of primary antibodies used for Western Blot analysis.....	44
<b>Table 3.</b> List of primary antibodies used for immunofluorescence on <i>Xenopus</i> nuclei.....	50
<b>Table 4.</b> List of ESC cell lines used in this study.....	53
<b>Table 5.</b> List of crRNA oligos used to knockout Man1 by CRISPR/Cas9.....	54
<b>Table 6.</b> List of primers used for Reverse-Transcriptase quantitative PCR (RT- qPCR).....	59

## ABSTRACT

The eukaryotic cell nucleus is characterized by a defined spatial organization of the chromatin, which relies on the physical tethering of many genomic loci to the inner surface of the nuclear envelope. This interaction is mainly mediated by lamins and lamin-associated proteins, which create a protein network at the nuclear periphery called nuclear lamina. Man1 is a member of a lamin-associated protein family known as LEM-domain proteins, which are characterized by the presence of a highly conserved domain, called LEM, that mediates the interaction with the chromatin. Data obtained with the yeast Man1 homolog Src1 underline the importance of this protein in different processes of the cell cycle, such as chromosome segregation, nuclear pores assembly, gene expression, chromatin organization and maintenance of genome stability, while in animal models, the function of Man1 has been associated to the regulation of developmental signalling pathways during embryogenesis. In this study, truncated recombinant mutants of Man1, containing the LEM domain, were shown to inhibit nuclear assembly and alter nuclear pore formation when added to *Xenopus laevis* cell-free extracts. Moreover, *Xenopus* nuclei assembled in the presence of Man1 truncated fragments were characterized by defects in chromatin organization, DNA replication and accumulation of DNA damage and, as a consequence, they failed to progress through mitosis. Furthermore, mouse embryonic stem cells (mESCs) depleted for Man1 showed evident signs of spontaneous differentiation, indicating inability in the maintenance of stem cell features. Intriguingly, preliminary analysis of Man1-knockout mESCs transcriptional profile showed an alteration of gene expression at the level of pericentromeric and telomeric regions, underlining a potential link between Man1 and genomic stability of these particular regions. In conclusion, this study illustrates the importance of Man1 in ensuring the proper chromatin organization necessary to support different cellular and DNA metabolic processes.

# INTRODUCTION

## 1. THE EUKARYOTIC CELL NUCLEUS

The acquisition of an intracellular membranous system marked the transition from prokaryotic to eukaryotic cells that occurred over a billion and a half years ago<sup>1</sup>. Since then, the complexity of the internal compartmentalization of cellular functions has increased in response to changes in environmental conditions, driving the evolution of modern eukaryotic organisms<sup>2</sup>.

As suggested by the origin of their name “Eukarya” (from ancient Greek εὖ “good” and κάρυον “nucleus”), the most striking feature of eukaryotic internal organization is the presence of the nucleus, which segregates the DNA from the cytoplasm, providing a more sophisticated control over gene expression and DNA metabolism.

The nucleus of eukaryotic cells is defined by the Nuclear Envelope (NE), that is constituted by two parallel membranes, the Inner and the Outer Nuclear Membranes (INM and ONM, respectively), separated by an aqueous perinuclear lumen. The ONM is dotted with ribosomes, it is continuous with the Rough Endoplasmic Reticulum and shares some functions with the latter. On the other side, the INM carries unique integral membrane proteins that are specific to the nucleus. The INM and the ONM are fused together at the nuclear pores, forming 100 nm-diameter channels associated to multiprotein complexes, named Nuclear Pore Complexes (NPCs), which regulate the bidirectional flux of molecules across the nuclear envelope<sup>3</sup> (Figure 1).

Although the nucleus is often represented as round-shaped, it has been observed that the nuclear envelope can reach the nuclear interior, forming a reticulum of membrane invaginations that can even cross the entire nucleus<sup>4</sup>. It is thought that these structures might increase the surface of interaction between the chromatin and the nuclear envelope, allowing the accomplishment of NE-specific functions in more internal regions<sup>5</sup>.

In animal cells, the molecular interactions occurring at the level of the nuclear periphery are mainly mediated by lamins, a family of proteins that create a mesh network (called nuclear lamina) linking the chromatin to the nuclear membrane<sup>6-9</sup>. Despite lamins are absent in plants and fungi, other proteins of the nuclear envelope and of NPCs exert their functions<sup>10,11</sup>.

The extensive interaction with the chromatin mediated by lamins together with proteins of the INM is crucial for the spatial organization of the genome, which is considered to have important regulatory roles in all the cell functions<sup>6,12</sup>.

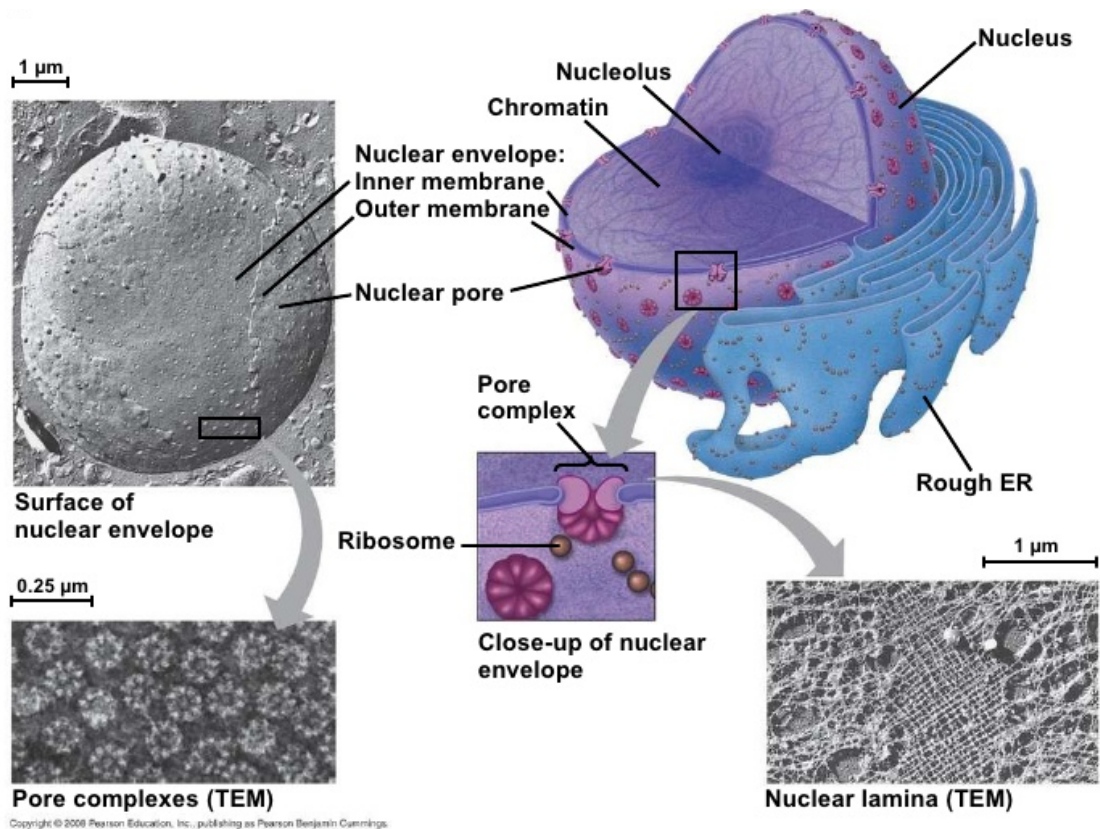


**Figure 1. The eukaryotic cell nucleus.**

*Eukaryotic genome is enclosed in the nuclear envelope, which separates the chromatin from the cytoplasm. The nuclear envelope is formed by the Inner and Outer Nuclear Membranes and it is constellated by nuclear pores. The internal surface of the nuclear envelope is also covered by the nuclear lamina, which creates a filamentous network that connects the chromatin to the nuclear periphery. (Picture taken from book chapter “Campbell biology-A tour to the cell”, Pearsons education, 2006<sup>13</sup>).*

## 2. EUKARYOTIC CHROMATIN ORGANIZATION

Despite the absence of internal compartments, the eukaryotic nucleus is characterized by a defined spatial organization, which allows cells to balance the extensive level of DNA folding with the regulation of gene expression. As cells progress through the cell cycle or as they differentiate into specialized cell types, their chromosomes undergo structural reorganizations that influence cell behaviour and function. Increasing evidences relate contacts between specific chromatin regions with gene expression and other important DNA transactions such as replication, recombination and repair<sup>14-18</sup>. Moreover, several human diseases are characterized by defects in nuclear architecture, underscoring a link between proper nuclear organization and normal cell function<sup>19,20</sup>.

Inside the eukaryotic nucleus, during the interphase of the cell cycle, the DNA is organized into chromosomes, that are packaged and folded through various mechanisms and occupy discrete positions called “chromosome territories”<sup>21,22</sup> (Figure 2). The three-dimensional disposition of chromosome territories is not random inside the nucleus, but they are organized into patterns. Interestingly, analysis of chromosome territories in many cell types and tissues revealed that patterns of relative chromosome arrangement are both cell- and tissue-specific<sup>23,24</sup>.

The first evidence of the non-random organization of the chromatin was described by Carl Rabl, which noticed that centromeres, which are the chromatin structures required for proper segregation of chromosomes during mitosis and meiosis, were often associated to the nuclear envelope in some cell types<sup>25</sup>. The same configuration has also been described for telomeres, that are DNA sequences covered by nucleoprotein structures which protect the ends of eukaryotic chromosomes. Telomeres are often found clustered at one pole of the nucleus in mitotic cells and in some interphase cells. This “Rabl-like” configuration has been observed in fungi, plants and mammals, though it is more often occurring transiently before or during mitosis and meiosis<sup>26,27</sup>.

Since many studies suggest that both centromeres and telomeres play important roles in aging and cancer<sup>28-31</sup>, the evidence of nuclear tethering of these elements provides important links between the spatial disposition of the genome and the maintenance of its stability.

Moreover, chromosome territories repositioning has been observed in some clinical conditions, as Alzheimer's disease and cancer<sup>32-35</sup>, providing novel insights into the relationship between chromatin organization and the alteration of gene expression that occurs in pathology.

Analysis of chromatin structure by Chromosome Conformation Capture (3C) technique revealed that chromosome territories can be further divided in "Topological Associated Domains" (TADs), which are genomic regions that are enriched with intra-domain interactions generated by the multiple levels of DNA folding<sup>36</sup>.

Given the high degree of conservation between different cell types and species, it has been proposed that TADs represent the fundamental unit of physical organization of the genome<sup>37</sup>.

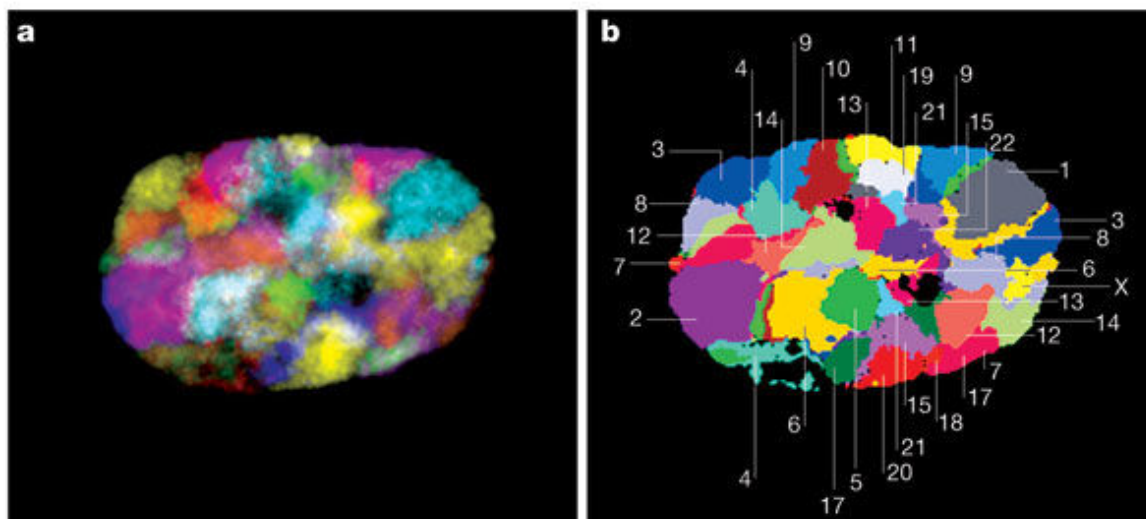


**Figure 2. Chromosome territories.**

*Visualization of human chromosome territories in an interphase nucleus by fluorescence microscopy (left panel) and automated karyotyping (right panel) of all the 23 chromosomes. Dark spots represent unstained nucleoli. (Image from Speicher et al.<sup>38</sup>).*

### 3. NUCLEAR TETHERING

Nuclear organization of the DNA is achieved through generic factors, like the physical properties of chromosomes (considered as semi-flexible polymers confined in a restricted space), as well as through more specific factors, as protein complexes which mediate discrete interactions between the DNA and other nuclear compartments or between different genomic regions.

Among the processes that determine the three-dimensional disposition of the genome inside the nucleus, one of the most important is the physical tethering of many genomic loci to the inner surface of the nuclear envelope<sup>39,40</sup>. This mechanism, called “nuclear tethering”, is thought to have important implications in different DNA metabolism transactions. For instance, nuclear tethered sequences have been described to be late-replicating DNA regions<sup>41,42</sup>.

Nuclear tethering has been mainly described as a process associated with transcriptional repression. In fact, early studies showed that the radial distribution of chromosome territories correlates with gene activity, associating proximity to the nuclear periphery with lower levels of gene expression<sup>41,43</sup>. An example is the inactive-X chromosome territory, which is located closer to the nuclear envelope respect to its active counterpart<sup>44</sup>. As a matter of fact, major silent heterochromatin domains are located at the nuclear periphery in different organisms<sup>45-47</sup>. However, the effect of the re-localization of genes toward the NE can lead either to their silencing or activation or it can have no effects on gene expression. In fact, the destiny of a certain genomic region localized at the nuclear periphery depends on different factors, such as its position towards other genes, the presence or the absence of transcriptional repressors or activators in a determined nuclear microenvironment, or the nature of its regulatory elements.

#### 3.1. NUCLEAR TETHERING AND GENOMIC STABILITY

Recent studies conducted in lower eukaryotes, suggest that nuclear tethering can influence



many other processes beyond chromatin silencing and transcription.

Indeed, the perinuclear positioning of certain genomic loci and the physical connection with the inner nuclear membrane are thought to be crucial for the maintenance of genomic stability, since they can influence processes such as DNA replication, repair and recombination<sup>12,48,49</sup>. Also, nuclear tethering has been related to the ability of restarting stalled replication forks that is pivotal to maintain genome stability upon endogenous or exogenous DNA replication stress sources<sup>50</sup>.

### 3.1.1. NUCLEAR ORGANIZATION AND DNA REPAIR

Several studies link nuclear organization to DNA repair mechanisms<sup>51-53</sup>. Recent experiments based on 3-C technique and fluorescence microscopy demonstrated that artificial induction of Double Strand Breaks (DSBs) at the level of internal chromosomic regions causes the re-localization of the damaged locus toward the nuclear periphery, associated with slow kinetics of repair<sup>54</sup>. Moreover, it has been demonstrated that such re-localization is dependent on Rad51, a factor involved in the Homologous Recombination (HR) pathway, which promotes the mobility of damaged DNA strands and the search for homologous sequences to use as templates<sup>55,56</sup>. The authors of this study hypothesized that such re-localization takes place when major repair pathways are inefficient or too slow in resolving the lesion. The damaged DNA would then be moved to another environment in which alternative pathways could operate in order to repair the broken chromosome.

The close correlation between DNA repair and nuclear periphery has been confirmed in other studies in which microarray analysis of immunoprecipitated chromatin showed that the DNA adjacent to DSBs is frequently bound by factors associated to the nuclear envelope, as NPC components and integral nuclear membrane proteins<sup>53,54</sup>.

Also, it has been demonstrated that, in yeast, persistent DSBs translocate from the nuclear interior toward the periphery and associate to nuclear pores. This association seems to be fundamental for DNA repair since mutations in some NPC components were shown to be

synthetic lethal with mutations in genes required for double strand break repair<sup>57</sup> and produced increased sensitivity to DNA damaging agents<sup>58</sup>.

Moreover, in *Drosophila*, it has been shown that heterochromatic DSBs are re-localized to the nuclear periphery, in order to accomplish efficient repair and prevent ectopic recombination, through a mechanism that involves NPC components and INM proteins<sup>59</sup>.

Studies conducted in mammalian cells did not give evidence of re-localization of lesions at the nuclear periphery<sup>60</sup>. However, it has been shown that depletion of nucleoporin Nup153 leads to a defective recruitment of DNA repair factor 53BP1 at damaged loci and to a hyper-activation of HR pathway<sup>61</sup>.

All the observations reported until now indicate that there is a great selectivity in the recruitment of damaged loci to the nuclear periphery, since not all the DSBs and stalled replication forks are localized at the nuclear envelope<sup>53,54,62</sup>. For this reason, it has been proposed that the nuclear tethering of damaged loci is required for the repair of lesion generated at the level of particular genomic regions, which need the action of specific repair pathways.

### 3.1.2. NUCLEAR TETHERING AND HOMOLOGY DIRECTED REPAIR

The proper repair of damaged chromosomes is mediated by different pathways, which are differentially regulated depending on the kind of lesion and the cell cycle phase in which the damage has occurred. The main mechanism of DNA DSBs repair is mediated by HR factors, through a mechanism that implies the exchange of nucleotidic sequences between sister chromatids. This mechanism is critical for different aspects of genome integrity maintenance and many types of cancers are related to genes involved in HR such as BRCA genes, which are often find mutated in prostate, ovary and breast cancer<sup>63</sup>.

In eukaryotes, the majority of HR events are induced by programmed DSB that occur mainly during meiosis through reciprocal exchange of entire chromosomal regions between homologous chromosomes, known as crossovers. Such process is critical both to ensure a

correct chromosome segregation and to promote the evolutionary divergence between species<sup>64</sup>.

During mitosis, despite some cases of programmed HR events, such as mating type switching in *S. cerevisiae* and immunoglobulin locus rearrangement in mammals, the events of HR are rarer and mainly occur to repair spontaneous DNA breaks<sup>65,66</sup>.

The exchange of genetic information preferentially takes place between sister chromatids, because they can provide an identical copy of the damaged sequence to be used as a template, allowing an error-free repair of the lesion. For this reason HR-mediated repair is favoured during S and G2 phases, when the DNA has been already replicated, while during G1, when this copy is not available yet, DNA breaks are mainly repaired through other mechanisms such as Non Homologous End Joining (NHEJ) and Single Strand Annealing (SSA), that are error-prone<sup>67-69</sup>.

An important aspect to take into account is that, differently from what happens during meiosis, during mitosis crossover events are strongly suppressed because they could have deleterious effects on genomic stability like loss of genetic material in diploid cells (Loss of Heterozygosity, LOH) or aberrant rearrangements between identical non-allelic sequences, (such as repetitive sequences)<sup>70,71</sup>.

The kind of damage that trigger homology directed repair includes a large variety of lesions such as DSBs, ssDNA gaps or structures generated by DNA metabolism (like stalled or collapsed replication forks)<sup>72</sup>. Moreover, HR can be stimulated by unconventional DNA structures. For example, it has been proposed that in regions containing redundant sequences, the denaturation of the DNA that occurs at the level of the replication fork can cause the alignment of repetitive sequences and the formation of hairpin or cruciform structures, which generate DSB and stimulate contraction or expansion of the repeats<sup>68,73,74</sup>.

The basic mechanism of HR initially includes a resection step, in which the broken DNA filaments are partially degraded at the 5' - ends. Therefore, the two protruding 3' - overhangs that are generated by resection are used as recruitment site for Rad51 recombinase, an

enzyme that can polymerize onto ssDNA forming a nucleoprotein complex called presynaptic filament<sup>75</sup>.

The presynaptic filament can bind another DNA molecule and “search” on it a sequence which is identical to its own one. Subsequently, the ssDNA invades the homologous region onto the “donor” DNA forming a three-stranded structure called Displacement-loop (D-loop)<sup>76</sup>. Formation of the D-loop allows the DNA polymerases to repair the lesion, using the 3'-overhangs as primers for the synthesis of a new DNA filament and the homologous sequence as template. After formation of the D-loop, there are two predominant models proposed for homology directed repair of DSBs<sup>77,78</sup>(Figure 3). The first one, called Synthesis-Dependent Strand Annealing (SDSA) pathway, is achieved through the extension and annealing of the invading strand to the broken molecule, leaving a small gap that is subsequently repaired by ligation of the broken ends. The second model, called Double Strand Break Repair (DSBR) pathway, involves the formation of a structure containing two four-filament cruciform junctions called double Holliday Junctions (dHJ)<sup>79</sup>. Processing of dHJs is mainly accomplished through two mechanisms. The first one is called “dissolution” and is achieved through the migration of the two cruciform junctions toward each other and resolution of the so formed “hemicatenane” by Type I topoisomerase, restoring the original layout of chromosomes. Alternatively, dHJ are processed through a second mechanism, called “resolution”, in which specific nucleases cut the DNA strands at the level of the junctions, generating either crossover or non-crossover products depending on the cut orientation<sup>80</sup> (Figure 3).

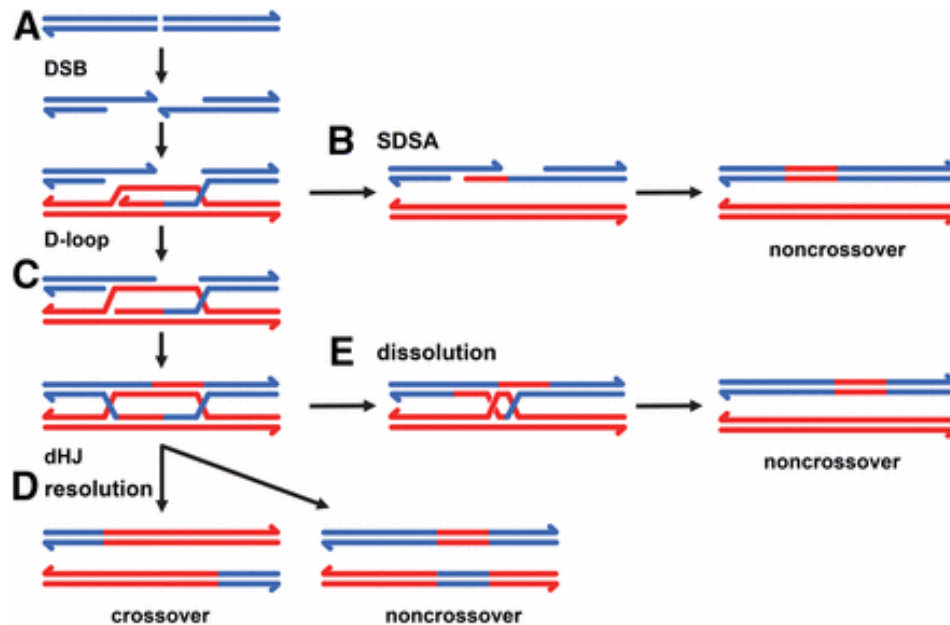


**Figure 3. Pathways of Homologous Recombination.**

Repair of DSBs begins with resection of the DNA broken ends, generating two ssDNA overhangs (A). One of these undergoes strand invasion in a homologous DNA molecule generating a D-loop. In SDSA pathway, the D-loop migrates causing the re-annealing of the newly-synthesized strand to the broken molecule, which will be further repaired by ligation, generating a non-crossover product (A).

Alternatively, additional synthesis of DNA leads to the formation of a double Holliday Junction (dHJ), which is further processed through resolution (D), generating either crossover or non-crossover products. Otherwise dHJs can be processed through dissolution (E), generating non crossover products. (Image taken from Zapotoczny et al<sup>78</sup>.)

As mentioned above, the effect of nuclear tethering on genome stability is particularly relevant for genomic loci containing redundant sequences, which are particularly abundant in eukaryotes<sup>81</sup>. Indeed, those sequences can undergo aberrant recombination events, which promote loss or gain of entire chromosomal regions. Such phenomenon, if not restrained, can ultimately lead to genomic instability, which in eukaryotes is one of the main hallmarks of cancer cells<sup>82,83</sup>. On the other side, the disposition of repetitive sequences at the same location, like ribosomal DNA (rDNA) or clustered centromeres and telomeres, allows the co-regulation of genes and could also facilitate the occurrence of faithful recombination events required to promote genetic diversity in a cell population under stress conditions<sup>84,85</sup>.

In the last years, numerous experimental data indicate how the connection of specific sequences or genomic regions to the nuclear envelope can be determinant for the maintenance of genomic stability. In fact, it is believed that the localization of the DNA to the nuclear periphery could limit aberrant recombination which can lead, if not properly carried out, to a variation in the nucleotide sequence of specific DNA segments resulting in loss or gain of genetic information. In particular, it has been proposed that the inhibition of recombination could be due to a poor concentration of recombination factors at the level of nuclear periphery and to the exclusion of specific chromosomal loci from the bulk of nuclear DNA<sup>86</sup>.

One important mechanism that leads to genomic instability is the loss of telomeres<sup>87,88</sup>. In fact, in the absence of such control, chromosomes become prone to undergo deleterious recombination events as chromosome ends fusion<sup>89</sup>. Moreover, another characteristic that make telomeres susceptible to aberrant recombination is the high content of repetitive sequences, that can reach up to several thousand units in the human telomeres<sup>90</sup>. For these reasons, cells have evolved a number of mechanisms to protect telomeres and maintain genome stability. One of these mechanisms is accomplished through the interaction of telomeres and sub-telomeric regions with NE components.

Nuclear positioning of telomeres is not random but it varies among organism, tissues and cell cycle stages. Despite this, they are often found connected to the nuclear envelope<sup>91</sup>, and during meiosis, the attachment of telomeres at the nuclear periphery is a widely conserved feature of all the cells<sup>92</sup>.

In yeast, telomeres are stably anchored to the NE through multiple redundant pathways that involve several INM and NPC components. It has been proposed that such perinuclear localization could be needed to limit unequal recombination at telomeres by keeping telomeric repeats away from recombination factors, to maintain proper alignment of sister chromatids during DNA replication and to promote efficient repair of DSBs<sup>86,93,94</sup>.

In mammals, although telomeres are mostly localized in the nuclear interior, it has been

found that several sub-telomeric regions are associated to the nuclear lamina<sup>95</sup> and that human telomeres contain a specific repeated sequence which acts as a perinuclear positioning element through physical interaction with type-A lamins<sup>45</sup>. Accordingly, it has been demonstrated that loss of type-A lamins in mouse cells is associated with changes in nuclear localization of telomeres, telomere shortening, alteration of telomere chromatin structure and, ultimately, genomic instability<sup>96</sup>.

### 3.1.3. NUCLEAR TETHERING AND DNA REPLICATION STRESS

The maintenance of genome integrity at “critical” chromosomal loci, like telomeres, is especially relevant during the S phase of the cell cycle, which is a time span of great vulnerability for the genome.

In eukaryotic organisms the presence of multiple origins of replication implies the possibility that during S phase, replication forks can encounter elements that block or slow down their progression, a condition known as “replication stress”<sup>97</sup>. Stalled replication forks are very fragile structures that must be stabilized and re-started in order to prevent breakage of the DNA double strand and aberrant recombination, ultimately leading to genomic instability. In the majority of the cases, the primary cellular response to replication stress aims to the protection of the stalled fork and replisome components for the time necessary to remove or overcome the obstacle. However, in case of a persistent obstruction or a collapse of the replicative fork due to replisome components detachment, the recombination apparatus is employed to restart DNA replication<sup>98,99</sup>. Usually, during S phase, recombination takes place between identical DNA sequences located on sister chromatids but it can also occur between allelic or ectopic regions, leading to deleterious events like loss of heterozygosity or Gross Chromosomal Rearrangements (GCRs)<sup>100,101</sup>.

Numerous observations suggest that defects in replication fork progression are associated to the presence of chromosome fragile sites, which are defined as sequences prone to show chromosomal breaks or gaps during mitosis<sup>102-104</sup>. The use of genome-wide approaches led

to the identification of conserved fragile sites, which were found to concentrate nearby elements such as telomeres, centromeres, replication origins, transposable elements, tRNA genes and G-quadruplexes<sup>105,106</sup>. Some studies correlated those particular regions to peculiar physical properties of the DNA, as high flexibility, elevated A/T content and tendency to adopt secondary conformations (cruciform or hairpin structures) promoted by nucleotide repeats, negative supercoiling given by purin-pyrimidine alternance or quadruplex conformation formed by planar pairing of four guanine residues (known as G-quadruplexes)<sup>102,106-109</sup>.

A huge amount of data suggests that the regulation of chromatin association to the nuclear periphery has a critical role in both the prevention and the repair of replication stress associated DNA lesions<sup>110,111</sup>.

Interestingly, recent published data obtained in mammalian cells show that fragile sites are moved toward the nuclear periphery and experience crossover recombination upon DSB<sup>112</sup>. Moreover, it has been demonstrated that, in yeast, the dissociation of actively transcribed genes from the nuclear pores during S phase is required to avoid collision between the replication fork and the transcription machinery, which otherwise could result in fork stalling and generation of DSBs<sup>50</sup>. Together with common fragile sites, transcribed genes are also associated with the pausing of the replication forks<sup>113</sup>. It has been hypothesized that the mechanism beyond this phenomenon cannot be attributed only to the physical collision of the replisome and the transcriptional machinery<sup>113</sup>. Instead it seems more appropriate to correlate the interference between DNA replication and transcription to the fact that transcribed genes may act as topological barriers, because they can limit the free rotation of the DNA molecule on its own axis. In fact, the unwinding of the DNA double helix that takes place during the replication generates some conformational variations of the DNA (such as catenation or supercoiling) that can lead to accumulation of torsional energy in the proximity of elements anchored to fixed structures, like the nuclear envelope<sup>114,115</sup>. Genes transcribed by RNA polymerase II belong to this group of elements, since complexes that couple



transcription with mRNA export create a physical continuity between the DNA and the nuclear pores. It has been proposed that, during the passage of the replication fork, the disassembly of the transcriptional apparatus and the alleviation of torsional stress are required to prevent deleterious events like fork collapse, formation of DNA-RNA hybrids (also known as R-loops), chromosome breakage and genomic instability.

For this reason, the control of DNA nuclear tethering could have crucial role in the maintenance of genomic stability in a context in which chromosomal replication has to face a deregulated transcription, as it occurs during oncogenesis.

### 3.2. CELL CYCLE AND CHROMATIN ORGANIZATION

Although highly organized, the structure of the nucleus is dynamic and nuclear structure and functions change as cells progress through the cell cycle and/or differentiate.

During G<sub>0</sub> and G<sub>1</sub> phases of the cell cycle, the organization of chromatin displays a bivalent status: at the centre of the nucleus, the chromatin is mainly found in a relaxed conformation (euchromatin), which is associated with active gene expression, while at the nuclear periphery it is preferentially arranged in a condensed and silent form (heterochromatin). This organization is completely remodelled when the cell cycle progress towards the cell division: during the DNA replication phase chromatin progressively condenses, reaching a compact heterochromatic status at the end of S phase. During G<sub>2</sub> phase, the chromosomes condense and undergo significant topological changes in order to be properly segregated during the next stage of cell division.

#### 3.2.1. EFFECT OF NUCLEAR TETHERING ON DNA REPLICATION

Accurate and complete duplication of eukaryotic genome is of crucial importance for the faithful inheritance of the genetic information required for cell survival and proliferation. This process, termed as DNA replication, takes place during the S phase of the cell cycle, and it starts at the level of specialized chromosomal regions called replication origins<sup>116</sup>.

In eukaryotes, replication origins are set by a three-step process: recognition of the origin, assembly of pre-Replication Complex (pre-RC), which contains DNA helicases, and activation of the pre-RC. The first factor that binds DNA is the Origin Recognition Complex (ORC), which is the only initiation factor thought to directly recognize replication origins. After ORC binds to the DNA, other two factors (Cdc6 and Cdt1) are recruited, promoting the loading of the MiniChromosome Maintenance (MCM) complex, which determines the licensing of the replication origin. The pre-RC is then activated by several other factors (such as Cdc45) which further enable the association of DNA polymerases machinery and the traveling of MCM complex ahead of the polymerases to open the double stranded DNA, allowing the synthesis of the complementary strand<sup>116</sup> (Figure 4).

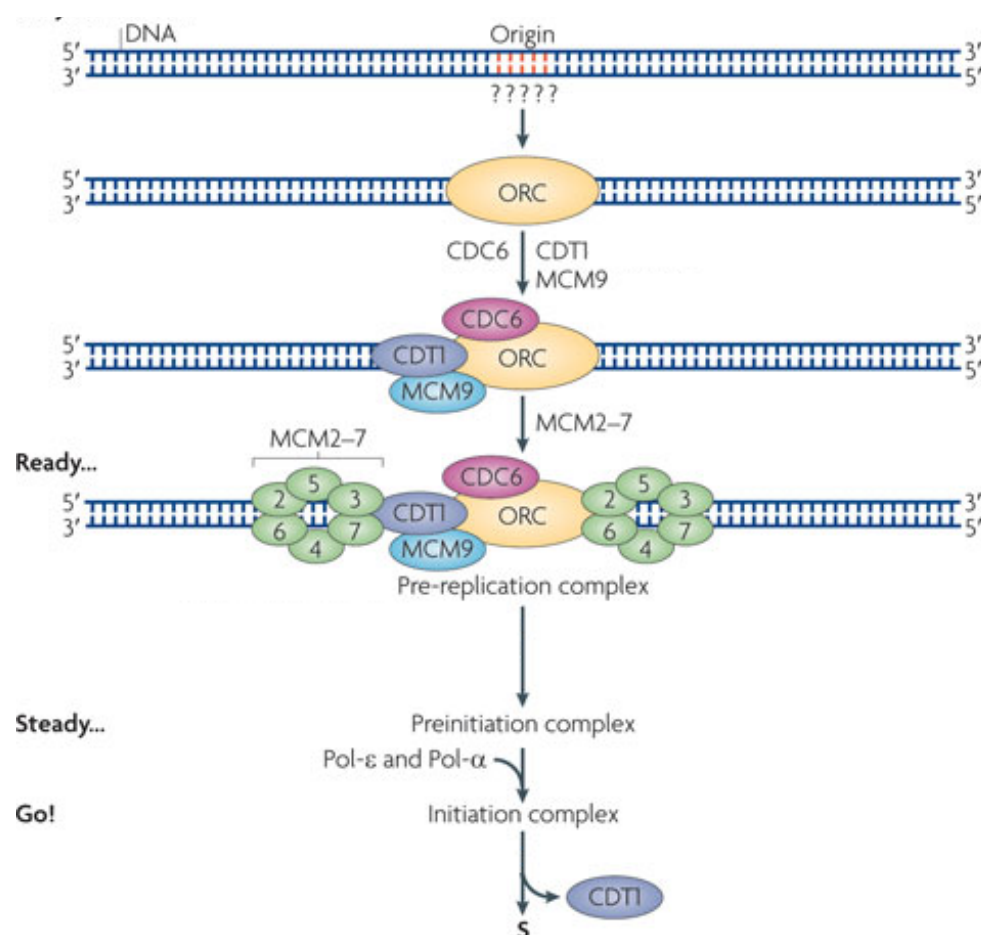


**Figure 4. Pre-Replication Complex (Pre-RC) assembly on DNA replication origin.**

After Origin of Replication Complex (ORC) binds to DNA, it recruits other two factors (Cdt1 and Cdc6) which have the role of loading the MiniChromosome Maintenance (MCM2-7)

*complex onto the replication origin, forming the Pre-RC. Conversion of the Pre-RC into an Initiation complex, through the recruitment of replicative polymerases, leads to the initiation of DNA synthesis. (Image adapted from Mechali<sup>117</sup>)*

Numerous studies have evidenced that genome organization and nuclear tethering take part in the regulation of DNA replication. A clear example of how genome architecture influences the origin recognition can be found during the early stages of embryo development, when nuclear structure is adapted to support rapid cell cycles and fast DNA replication. In fact, it has been proposed that the nuclei of fertilized eggs are organized into short loops of chromatin at S phase entry, allowing the recruitment of a large amount of ORC. This situation is in deep contrast to the temporal and spatial regulation of origin activation that takes place in differentiated cells, where a striking increase in loop size correlates with a decreased ability of the chromatin to bind ORC<sup>118,119</sup>.

Moreover, it has been demonstrated that genome organization plays an important role in defining the temporal order in which chromosomes are replicated, which is known as “replication timing”. In fact, it has been evidenced that different chromosomal regions that occupy the same discrete location (defined as TADs, described above), share the same DNA replication timing. Moreover, it has been demonstrated that regions associated to the nuclear lamina (known as Lamin Associated Domains, LADS) have a late replication timing<sup>120</sup>, underlining the role of the nuclear lamina in assisting DNA replication through the physical organization of the genome.

Accordingly, it has been shown that nuclei assembled in the absence of lamins fail to replicate their DNA<sup>121,122</sup>, while the expression of lamin mutants, which causes reorganization of endogenous lamins inhibits DNA replication in *Xenopus laevis* egg extracts<sup>123,124</sup>.

Apart from lamins, other structural nuclear proteins have been demonstrated to be involved in DNA replication. For example, nuclear *Xenopus laevis* cell-free extracts supplemented with a portion of lamin-binding protein Lap2 $\beta$  containing its chromatin-binding domain fail

to replicate the DNA<sup>125</sup>. Similarly, ectopic expression of recombinant Lap2 $\beta$  polypeptides deprived of transmembrane region has been shown to inhibit the progression into S-phase of mammalian cells<sup>126</sup>.

Recent evidences also suggest an active role for nuclear pore complexes in the regulation of DNA replication. Experiments performed in *Xenopus* egg extracts, showed a physical interaction of the NPC component Elys/Mel-28 with the MCM2–7 complex, the main component of the eukaryotic replicative helicase<sup>127</sup>. In addition, the authors showed that inhibition of MCM2-7 chromatin loading was able to delay nucleoporins chromatin association and nuclear size growth, highlighting a strict coordination between nuclear envelope assembly and DNA replication. This interaction appears conserved in vertebrates since it has been observed that mutation of ELYS gene can reduce Mcm2 levels on chromatin in *Zebrafish*<sup>128</sup> and inactivation of a conditional *elys* allele in mouse progenitor cells promote apoptosis under replication stress conditions<sup>129</sup>.

### 3.2.2. NUCLEAR ASSEMBLY AND DISASSEMBLY DURING MITOSIS

While lower eukaryotes engage “closed” or “semi-closed” mitosis, in which the nuclear envelope remains (completely or partially) intact during all the cell division, in vertebrates the disassembly of the NE marks the transition between the prophase and metaphase of the mitosis. During the “open” mitosis, the nuclear architecture is destroyed and the whole genome is partitioned before segregation of sister chromatids. Nuclear envelope breakdown involves lamina depolymerisation, cleavage and removal of nuclear membrane from the chromatin surface and disassembly of NPCs<sup>130</sup>. During this process, the chromosomes remain associated with the disassembling lamina, suggesting that the lamina could play an important role in chromosome segregation<sup>131,132</sup>.

After anaphase is completed, lamins, NPC components and ONM and INM proteins are recruited on the chromatin surface and nuclear reformation takes place.

The nuclear assembly process is very fast and relies on rapid sub-sequential steps<sup>133</sup>: first membrane vesicles are targeted to the chromatin, through a mechanism that requires both lamins and lamin associated proteins. As the membrane vesicles merge, NPCs are assembled at sites of intraluminal fusion between the INM and the ONM, in a process that does not seem to require lamins or chromatin. The first NPCs are assembled before nuclear envelope is sealed and, as soon as transport-competence is acquired, they accelerate nuclear assembly by locally concentrating nuclear envelope proteins next to the chromatin surface.

As soon as nuclear envelope assembly is complete, nuclear growth takes place. The mechanism of nuclear membrane expansion seems to be regulated by processes that depend on nuclear import, such as lamina assembly and chromatin decondensation.

All this process is critical, because nuclear structure reassembly has to proceed in a tightly coordinated manner during nuclei reformation, ensuring that the interphase organization of chromatin can be re-established in daughter cells<sup>134</sup>.

### 3.3. ROLE OF NUCLEAR TETHERING IN GENE REGULATION AND CELL DIFFERENTIATION

The radial disposition of the genome inside the nucleus correlates with cell type and differentiation status, suggesting that is either an outcome of the transcriptional state or it has a role in the regulation of gene expression<sup>135,136</sup>. In fact, the nuclear periphery is mostly occupied by silent heterochromatin, which is characterized by a low density of genes and low levels of transcription. During the differentiation process, which relies on a radical change in the gene expression profiles of the cell, the three-dimensional arrangement of the chromatin is reorganized and thousands of genes are moved towards or away from the nuclear periphery<sup>136</sup>.

High-resolution mapping of chromatin-nuclear lamina interactions allowed to describe the reorganization of chromosome architecture that happens during lineage commitment and differentiation of mouse embryonic stem cells (mESCs)<sup>137</sup>. Such remodelling involves both

single transcriptional units as well as entire genomic regions and to affect many genes involved in cellular identity. Similar changes in nuclear architecture were also observed during reprogramming and disease<sup>138-140</sup>.

Analysis of the genomic sequences lying close to the nuclear envelope has shown that interaction with the nuclear lamina was often associated to transcriptional repression<sup>141</sup>.

Moreover, it has been demonstrated that artificial tethering of endogenous or reporter genes to the nuclear envelope can induce their transcriptional downregulation in mouse and human somatic cells<sup>141,142</sup>.

Among the genes that are relocalized at the nuclear periphery during differentiation the most abundant class is represented by pluripotency genes and tissue-specific genes, which become repressed as cells differentiate. However, only 30% of those genes actually change their expression as they are bound by nuclear lamina, suggesting that the nuclear periphery does not necessarily induce transcriptional downregulation. Moreover, it was shown that many of the genes that were released from the nuclear lamina upon differentiation were not actually showing active transcription, suggesting that the relationship between association to the nuclear envelope and transcriptional repression is not fully univocal<sup>137</sup>.

Surprisingly, it seems that chromatin tethering to the nuclear periphery is not dependent on lamins in mouse embryonic stem cells, as silencing of both A and B-type lamins have no detectable effects on the genome-wide interaction pattern of chromatin with the nuclear envelope, suggesting that other components of the nuclear lamina may mediate these interactions<sup>143</sup>.

A wide number of studies showed that lamina components interact with signalling factors belonging to pathways which regulate cell proliferation and differentiation<sup>144-147</sup>. This interaction can have a role in transcription regulation, since it can be required for the recruitment of transcription factors or to mediate the activation of signalling molecules. For example, the interaction between Lamin A/C and INM proteins Lap2 $\alpha$  and Lap2 $\beta$  has been shown to be important for the stabilization of Retinoblastoma protein (pRb), a tumour

suppressor and cell proliferation regulator<sup>148,149</sup>.

Moreover, several lamin-associated proteins of the INM have been shown to negatively regulate transcription by blocking the action of signalling components which regulate stem cell differentiation<sup>150-153</sup>.

#### 4. THE NUCLEAR LAMINA

The nuclear lamina is present in all metazoans and it is composed by a group of intermediate filaments (called lamins) and lamin associated proteins<sup>154</sup>. The genes encoding for this factors are absent from plants and fungi, as it has been hypothesized that the first appearance of nuclear lamina during evolution has occurred during the transition from “open” to “closed” mitosis<sup>130</sup>.

Nuclear lamina forms a filamentous layer that is predominantly found close to the INM, providing structural support to the nuclear envelope and regulating nuclear size and shape. Moreover, the position of the lamina at the interface between the nuclear membrane and the chromatin suggests that it is involved in chromatin organization.

Interestingly, there is strong evidence that lamins and lamin-binding proteins are not restricted to the nuclear periphery but can localize also at the nuclear interior<sup>155</sup>. However, their molecular structure and functions are still poorly defined.

##### 4.1. LAMINS

Lamins represent the major structural component of the nucleus, as they contribute to its physical and mechanical properties.

In animal cells there are two types of lamins: type-A lamins (which include Lamin A and Lamin C) and type-B lamins (which include Lamin B1 and Lamin B2). Contrary to B-type lamins, lamin A has also been suggested to localize to the nuclear interior in some cell types<sup>155</sup>.

It has been observed that mutation or downregulation of either A- or B-type lamin genes lead to changes in nuclear shape, as formation of membrane invaginations or protrusions, in different organisms<sup>156-160</sup>.

In the past years, mutations in lamin and lamin-binding proteins were found to be linked to a large spectrum of diseases, called laminopathies or nuclear envelopathies<sup>19,161,162</sup>. Among laminopathies, the vast majority is associated to mutations of the Lamin A/C gene (LMNA), which give rise to multiple phenotypes including striated muscle dystrophy, lipodystrophy, peripheral neuropathy and accelerated ageing<sup>19,163</sup>.

The broad range of cellular phenotypes associated to laminopathies mostly arise by a combination of various effects, including structural abnormalities of the nuclear lamina and subsequent defects in chromatin organization and signalling pathways.

One of the most characterized LMNA mutations, associated with the premature aging disease Hutchinson Gilford Progeria Syndrome (HGPS)<sup>164,165</sup>, leads to the accumulation in the nuclear periphery of a defective dominant negative variant of Lamin A precursor that is called progerin<sup>163</sup>. Cells affected by progerin accumulation reveal dramatic defects in nuclear envelope structure, nuclear morphology and heterochromatin organization<sup>166,167</sup>. Moreover, they are characterized by genomic instability and replication stress as result of defective recruitment of DNA replication and repair factors<sup>168-170</sup>. For this reasons HPGS cells are ultimately characterized by a reduction in the proliferative capacity, induction of DNA damage and acceleration of senescence<sup>168</sup>.

Interestingly, progerin production has been also found in normal cells<sup>171</sup>, uncovering a possible relationship between normal aging and progerin production in “healthy” individuals.

#### 4.2. LAMIN-ASSOCIATED PROTEINS: LEM DOMAIN FAMILY

Among lamin-associated proteins, one of the most abundant class is represented by a large family of proteins, called LEM-Domain (LEM-D) proteins<sup>172,173</sup>, characterized by the



presence of a highly conserved ~40 aa domain called LEM (Lap2 $\beta$ -Emerin-Man1) that allows the attachment of chromatin to the nuclear periphery through a direct interaction with the chromatin remodelling complex BAF (Barrier-to-Autointegration-Factor)<sup>172,174-176</sup>. In addition to BAF, LEM-D proteins are also able to directly bind A and B-type lamins through a separate domain<sup>177</sup>.

Interestingly, INM proteins with LEM domain are conserved also in lower eukaryotes, like yeast, which lack both lamins and BAF<sup>174</sup>. This observation suggests that this protein family have evolved from an ancestral DNA binding protein involved in tethering the DNA to the nuclear envelope.

LEM-D proteins can be divided in three groups, based on their structure and subnuclear localization<sup>172</sup> (Figure 5). Group I, to which belong Emerin and Lap2 $\beta$ , include mostly integral membrane proteins that carry one amino-terminal LEM domain and one large nucleoplasmic domain. These proteins are mostly integral of the INM, but can also localize in the nucleoplasm. Group II proteins, which representatives are Man1 and Lem2, are characterized by the presence of one N-terminal LEM domain, two central transmembrane regions and one DNA-binding C-terminal domain and are only localized in the nuclear envelope. Finally, proteins belonging to Group III (like Ankle1 and Ankle2), carry one internal LEM domain and multiple ankyrin repeats, a feature that is shared by many signalling molecules. Group III proteins differ from the other LEM-D proteins because of their sub-nuclear localization, since they have been found also in the cytoplasm and in the endoplasmic reticulum<sup>172</sup>.

The great variability in structure and subcellular localization of the different LEM-D proteins underlies their functional diversity. In fact, several studies showed how this family of proteins is involved in different cellular processes including DNA replication, cell cycle control, chromatin organization, nuclear assembly and regulation of gene expression and signalling pathways<sup>125,126,178,179</sup>.

The principal function of LEM-D proteins is to provide a link between the chromatin and

the nuclear envelope. In yeast, which only has Group II proteins, it has been shown that LEM-D proteins are required to connect telomeres and rDNA repeats to the INM and their loss can cause genomic instability at the level of this particular regions<sup>180,181</sup>.

Similarly, in metazoans, which present at least one representative for each of the three groups, LEM-D proteins seem to have a role in the nuclear tethering of high repetitive regions and “gene poor” repressive loci<sup>182</sup>.

Because of their direct interaction to chromatin remodelling factors, such as histone deacetylases and BAF, it has been hypothesized that LEM-D proteins might have a role in the establishment of repressive heterochromatin at the nuclear periphery and, therefore, in the regulation of global genome organization<sup>183,184</sup>.

Most of the roles of LEM-D proteins rely on their interaction with their molecular partners, among which the most relevant is BAF (which will be described in the next paragraph).

Mutations in members of the LEM-D protein family have been linked to several tissue-restricted human laminopathies. Among them, the most characterized ones are Emery-Dreyfuss Muscular Dystrophy (EDMD), caused by mutation in Emerin gene, and bone disorder Bushke-Ollendorf Syndrome, caused by Man1 mutations. Altered tissue development and homeostasis in LEM-D associated diseases has been also attributed to misregulation of developmental signalling pathways, as several LEM-D proteins have a role in the regulation of nuclear envelope localization of transcription factors involved in tissue differentiation<sup>150,152,153,185</sup>.

The fact that loss of LEM-D proteins gives rise to similar tissue-specific defect suggests that these proteins may have overlapping functions. This hypothesis is also supported by the evidence that loss of two LEM-D proteins has more severe effects than loss of a single one<sup>186,187</sup>. For this reason, it is possible to believe that the impact of the loss of a single LEM-D protein will greatly depend on the ability of other members of the family to compensate, or not, the lost function in a specific tissue.

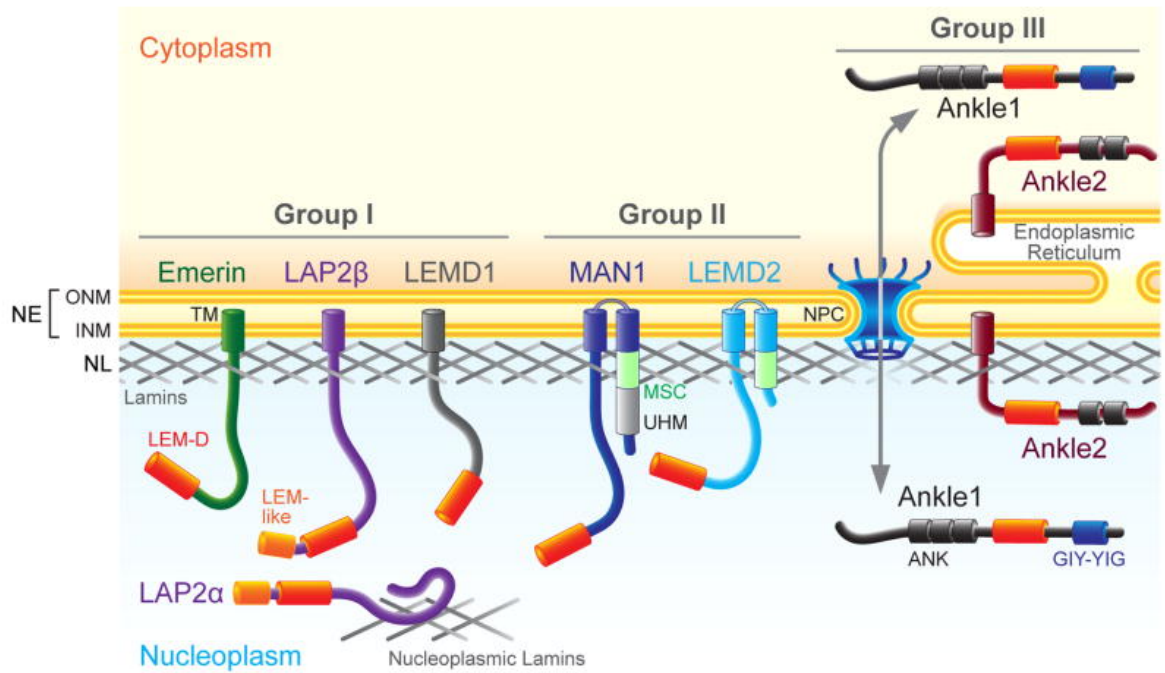


**Figure 5. LEM-domain protein family.**

The picture shows the features and subcellular localization of human LEM-D proteins which represent all the three family subgroups (I, II and III). Picture taken from Barton et al.<sup>172</sup>

#### 4.3. BARRIER TO AUTOINTEGRATION FACTOR (BAF)

BAF is a small protein of 10 kDa which is highly conserved in all metazoans<sup>188</sup>. *In vitro*, it has been demonstrated to form stable homodimers which can bind double stranded DNA without apparent sequence-specificity<sup>189</sup>. It has been proposed that one major role of BAF is in the regulation of nuclear assembly after mitosis by recruiting LEM-D proteins onto chromatin surface. In fact, experiments carried out in *Xenopus* cell-free extracts demonstrated that an excess of BAF can slow down membrane recruitment, block lamina assembly and cause hypercompaction of chromatin. Moreover, addition of BAF mutants unable to bind Emerin LEM-D protein causes physical detachment of the DNA from the nuclear envelope and condensation of the chromatin mass<sup>190</sup>.

*In vivo*, it has been shown that loss of BAF causes embryonic lethality, defects in chromosome segregation and abnormalities in interphase chromatin organization<sup>189,191,192</sup>.

In addition to its role in nuclear assembly in mitosis, several studies indicate that BAF is also important for gene regulation during interphase.

In fact, it has been shown that BAF depletion in *C. elegans* negatively interferes with the transcriptional silencing of heterochromatic loci<sup>193</sup>. Moreover, depletion of BAF in mouse embryonic stem cells causes a global downregulation of known stem cell markers (such as Sox2, Oct4 and Nanog) and, on the other hand, enhances the expression of differentiation factors<sup>146</sup>, suggesting that BAF could be required to maintain ESC pluripotency by influencing high-order chromatin structure.

Mutation of BAF in humans has also been linked to a rare premature aging disease called Nestor-Guillermo Progeria Syndrome (NGPS)<sup>194</sup>, which shares many clinical features with the lamin-associated disease HGPS.

#### 4.4. MAN1

Man1, also known as Lemd3, is a LEM-domain and an integral nuclear membrane protein which is conserved from lower to higher eukaryotes and it is ubiquitously expressed<sup>188</sup>. Its secondary structure displays a large amino-terminal domain which include the LEM domain as well as the binding sites for lamins and other LEM-D proteins and it is required for the INM targeting of Man1<sup>195</sup>. On the opposite side, the carboxy-terminal region exhibit two conserved domains called MSC (Man1-Src1p-C-terminal), required for direct DNA interaction<sup>196</sup>, and RRM (RNA-Recognition-Motif), which mediates interaction with Smads transcriptional regulators (described below)<sup>197,198</sup>.

While lamins and most of the LEM-D protein are present only in metazoan, orthologues of Man1 and its paralog Lem2 have also been found in yeast (*S. cerevisiae* Src1/Heh2 and *S. pombe* Man1/Lem2) and are characterized by the presence of a LEM-like domain and a conserved MSC, which both are thought to mediate the direct interaction with the DNA.

Data obtained by studying the yeast Man1 homolog Src1 underline the importance of this protein in different processes of the cell cycle. In fact, *src1Δ* mutants are characterized by

premature sister chromatids separation during mitosis<sup>181</sup> and genomic instability at rDNA and telomeric loci<sup>86,180</sup>. Moreover, gene expression misregulation<sup>180</sup>, deformation of chromatin mass<sup>199</sup> and alteration of NPCs distribution along the nuclear envelope<sup>200</sup> can be observed in the absence of Src1.

In the fission yeast *S. japonicus*, Man1 is required for the equal distribution of NPCs in daughter nuclei and for proper segregation of nucleoli<sup>201</sup>, whereas in *S. pombe* it is involved in nuclear tethering of heterochromatic and subtelomeric regions<sup>202</sup>.

In animal models, the function of Man1 has been the subject of developmental studies, for its role in antagonizing Smad-mediated signalling pathway during embryogenesis<sup>185</sup>.

Smad proteins are a family of signal transducing factors which are involved in the modulation of signalling by Transforming Growth Factor  $\beta$  (TGF $\beta$ ), a family of cytokines involved in several cellular processes such as proliferation and differentiation<sup>203</sup>. Upon activation by TGF $\beta$  receptors, Smads are translocated in the nucleus and associate with transcription factors to modulate the expression of target genes. Involvement of Man1 in TGF $\beta$  signalling has been evidenced in different organisms, where it has been shown that Man1 has a role in antagonizing the pathway of Bone Morphogenetic Protein (BMP), a subgroup of TGF $\beta$  cytokines involved in the dose-dependent regulation of embryonic patterning, by inhibiting Smads activity<sup>151,176,197,204</sup>. It has been proposed that the mechanism beyond such inhibition could be addressed to the sequestration of Smads proteins to the nuclear envelope by Man1, disrupting their association with target genes<sup>151,197</sup>.

Consistently, Man1 appeared to be important for neuroectoderm differentiation of *Xenopus* embryo<sup>185</sup> and its expression was shown to promote osteogenesis in human mesenchymal stem cells<sup>205</sup>. On the other hand, it was observed that Man1 depletion in *Drosophila* embryos reduced animal viability and led to sterility and neuromuscular defects in surviving adults<sup>206</sup>, while it appeared to cause lethality in early stage mouse embryos<sup>151</sup>.

In humans, heterozygous mutation in the Man1 gene has been found to be associated with genetic diseases related to tissue development such as Bushcke-Ollendorf syndrome,

osteopoikilosis and melorheostosis<sup>207,208</sup>. These diseases are characterised by increased bone density, probably due to hyperactivation of TGF $\beta$ /BMP pathway<sup>205</sup>.

However, despite the large amount of data that underlie the importance of Man1 in signalling pathways during animal development, still there are few informations about its role in the whole genome organization of the large and complex vertebrate nucleus. For this reason, further characterization of vertebrate Man1 could provide novel insight into the role of nuclear tethering mediated by Man1 in the maintenance and regulation of chromatin organization and its possible implications in different cell processes.

## 5. *XENOPUS* CELL-FREE EXTRACT AS MODEL SYSTEM TO STUDY NUCLEAR ASSEMBLY AND DNA METABOLISM

In this study the *Xenopus* cell-free extract system was used in order to investigate the function of Man1 in the nuclear organization and DNA metabolism.

This particular *in vitro* system can efficiently reproduce the key nuclear transitions taking place during the cell cycle with the same dynamics and under the same controls that occur *in vivo*<sup>209-211</sup>. The ability of *Xenopus* egg extracts to support cell cycle progression *in vitro* relies on the fact that most of the material required for nuclear assembly and DNA replication is already present inside the egg at high concentrations. In order to obtain cell-free extracts of good quality, unfertilized *Xenopus* eggs, which are arrested at the metaphase of second meiotic division, are activated by the addition of calcium ionophore, which mimics the calcium wave generated during the fertilization and promotes the entry into the first mitotic interphase<sup>212</sup>. The release of extracts from metaphase arrest activates the replication licensing system, enabling the replication of exogenous DNA. After the activation, eggs are crushed and the extracts are generated by a series of centrifugation steps in order to collect cytoplasmic and membrane fractions deprived of lipids and organelles. The incubation of interphase extract with DNA is sufficient to induce formation of functional structures corresponding to interphase nuclei competent for DNA replication. A great benefit of the

*Xenopus* cell-free system is the possibility to supplement the extract with recombinant proteins, drugs or antibodies in order to study the role of particular factors intervening in different processes. Moreover, it is also possible to generate extracts deprived of specific factors by immunodepletion of the target protein using specific antibodies. In a different strategy it is also possible to overload the extract with recombinant mutant proteins, which displace or outcompete the endogenous proteins in the molecular steps and complexes in which they are involved.

# MATERIALS AND METHODS

## 1. SOLUTIONS

PBS (Phosphate Buffered Saline)

0,13 M NaCl

7 mM Na<sub>2</sub>HPO<sub>4</sub>

3 mM NaH<sub>2</sub>PO<sub>4</sub>

pH adjusted to 7.5

TBS (Tris Buffered Saline) and TBST

10 mM Tris-base

150 mM NaCl

0,05 % Tween-20 (only for TBST)

pH adjusted to 7.5 with HCl

TAE (Tris Acetate EDTA)

0,04 M Tris-Acetate

0,01M EDTA

pH 8

SDS-page running buffer

25 mM Tris base

192 mM Glycine

0,1 % SDS

RIPA Buffer:

50 mM Tris-HCl pH 7.5



150 mM NaCl  
1 % NP-40  
1 mM EDTA  
0,5% Na-deoxycholate  
0,1 mM NaOVan  
10 mM NaF  
20 mM  $\beta$ -Glycerophosphate

#### LAEMMLI BUFFER 2X

100 mM Tris pH 6.8  
4 % SDS  
30 % Glycerol  
0,2 % Bromophenol Blue  
10 %  $\beta$ -Mercaptoethanol

## 2. GROWTH MEDIA

### 2.1. *ESCHERICHIA COLI* GROWTH MEDIA

#### LURIA-BERTANI BROTH (LB)

1 % w/v bacto-tryptone (DIFCO)  
0,5 % w/v yeast extract (DIFCO)  
0,1 M NaCl  
pH adjusted to  $\sim 7$

#### LB AGAR

LB broth + 2 % (w/v) Bacto agar

## 2.2 MOUSE EMBRYONIC STEM CELL MEDIA

### ESC PROLIFERATION MEDIUM

Knockout DMEM (Invitrogen)

10 % FBS ES-tested (Invitrogen)

1 mM Na-Pyruvate

0,1 mM Non-essential aminoacids

0,1 mM  $\beta$ -Mercaptoethanol

2 mM L-Glutamine

2 U/ml LIF

3  $\mu$ M PD0325901 (Sigma Aldrich)

1  $\mu$ M CHIR99021 (Sigma Aldrich)

### ESC DIFFERENTIATION MEDIUM

High glucose DMEM w/o Hepes (Lonza)

20 % FBS, US origin (Gibco)

2 mM L-Glutamine

1 mM Na-Pyruvate

0,1 mM Non-essential aminoacids

50 U/ml Penicillin–Streptomycin mix (Microtech)

0,01 mM  $\beta$ -Mercaptoethanol

## 3. MOLECULAR BIOLOGY TECHNIQUES

### 3.1 AGAROSE GEL ELECTROPHORESIS

Horizontal agarose gels were routinely used for the separation of DNA fragments. All agarose gels were 0,8 % w/v agarose in 1xTAE. The samples were loaded in 1x loading dye (6x stock: 0,25 % bromophenol blue; 0,25 xylene cyanol; 30 % v/v glycerol). Gels also

contained 1 µg/ml ethidium bromide to allow visualisation of the DNA under UV light. 1Kb ladder (New England Biolabs) was used for fragment size determination.

### 3.2 TRANSFORMATION OF *E. COLI*

Plasmid transformation into *E. coli* 100 µl of competent cells were mixed with transformation DNA and incubated on ice for 30 minutes. The cells were then heat-shocked at 42 °C for 30 seconds, and cooled on ice. 1ml of warm LB was then added and the tubes were incubated at 37 °C with shaking for 1 hour. Lastly, the cells were spun down and plated onto selective plates.

### 3.3. CLONING OF *XENOPUS* MAN1

Total RNA was extracted from *Xenopus* leavis eggs with RNaeasy kit (Qiagen) according to manufacturer's protocol.

cDNA inserts coding for either residues 1-45 (LEM domain), 1-345 (N-terminal) and 520-782 (C-terminal) of *Xenopus* Man1 were obtained by reverse transcription and PCR amplification from total *Xenopus* mRNA using specific primers (Table 1).

Name	Sequence (5'-3')
xMan1_1-345_Forward	CGCGAACAGATTGGAGGTGCGGCCGCTCAGTTAACGGAT
xMan1_1-345_Reverse	GTGGCGGCCGCTCTATTAGAATCTCCCTGCAGCAGACAC
xMan1_520-782_Forward	CGCGAACAGATTGGAGGTTGGCGATACATAAAATATCGT
xMan1_520-782_Reverse	GTGGCGGCCGCTCTATTAAGAGCATGACTGAGAATTTGA
xMan1_1-45_Forward	CGCGAACAGATTGGAGGTGCGGCCGCTCAGTTAACGGAT
xMan1_1-45_Reverse	GTGGCGGCCGCTCTATTATCTTTGCTCTTCCCTCAACTT

**Table 1. List of PCR primers used for *Xenopus* Man1 cloning.**

Inserts were then cloned in pETite N-His SUMO vector (Lucigen) according to manufacturer's protocol and transformed into HiControl 10G competent cells (Lucigen) to obtain stable clones and into HiControl BL21(DE3) competent cells (Lucigen) to induce protein expression.

#### 3.4. PREPARATION OF RECOMBINANT XMAN1 PROTEINS

Expression of the protein was induced with 1 mM IPTG for 3 hours at 37 °C (for recombinant LEM domain) or overnight at 16 °C (for N- and C-terminal fragments). Proteins were affinity-purified with Ni-NTA resin (Quiagen) and further cleaned by gel filtration (Superdex S200, GE Healthcare). Finally, proteins were concentrated and stored at -80°C in 50 mM Tris-HCl pH 8, 300 mM KCl, 10 % glycerol, 2 mM  $\beta$ mercaptoethanol.

#### 3.5. SDS-PAGE

Proteins were separated according to their molecular weight by reducing sodium dodecyl sulfate polyacrylamide gel electrophoresis (SDS-PAGE) using CRITERION TGX precast gels (BioRad). Gels were run in SDS-PAGE running buffer 1X at 150V until the desired molecular weight marker exit from the gel. Precision Plus dual colour protein markers (BioRad) or Broad range (175.7 kDa) prestained protein marker (New England Biolabs) were used as molecular weight standards.

#### 3.6. WESTERN BLOT ANALYSIS

Proteins run on SDS-PAGE gels were transferred to Protran PVDF membranes (Whatman) for 2 hours at 200 mA in cold transfer buffer. Membranes were then washed with deionised water and quickly stained with Ponceau S solution in order to assess transfer efficiency. Membranes were washed in TBST and incubated for 1 hour in 5% (w/v) non-fat powder milk in TBST at room temperature to allow saturation (blocking). Primary antibodies were prepared at dilutions indicated in Table 2 in 5% milk in TBST. Membranes were incubated

2-3 hours at room temperature or overnight at 4 °C. After three washes in TBST, 10 minutes each, primary antibodies were detected using HRP-conjugated secondary antibodies (Dako) in 5% milk in TBST. Membranes were washed again for three times and antibody complexes were detected using ECL substrate (GE Healthcare) or WesternBright™ ECL (Advansta), and visualised on Carestream Kodak BioMax MR film (Sigma Aldrich).

### 3.6.1. ANTIBODIES

The following antibodies were used in this study (Table 2):

Antigen/Name	Provider	Concentration
<i>Xenopus</i> Cdc45	J. Gannon (Clare Hall laboratories)	1:1000
<i>Xenopus</i> Cyclin B2	J. Gannon (Clare Hall laboratories)	1:5000
Mcm7 (sc9966)	Santa Cruz	1:5000
Orc1 (sc53391)	Santa Cruz	1:3000
PCNA (PC10)	BioRad	1:1000
H2B (07-371)	Millipore	1:1000
Pol Alpha p180 (ab31777)	Abcam	1:1000
Man1 (A305-251A)	Bethyl	1:2000
GAPDH (G8795)	Sigma Aldrich	1:5000
Alpha-Tubulin (ab6160)	Abcam	1:1000

**Table 2. List of primary antibodies used for Western Blot analysis**

## 4. XENOPUS TECHNIQUES

### 4.1. XENOPUS SPERM AND EGG EXTRACTS

Mature *X. laevis* females were primed about 1 week in advance with 50 U of pregnant mare serum gonadotropin per animal. To induce ovulation, 400 U of human chorionic gonadotropin per animal was used.

All steps were carried out at room temperature (approximately 22 °C); all centrifugations were carried out at 4 °C and all steps after crushing of the eggs were carried out on ice. During all wash steps care was taken not to pour solutions onto the eggs directly, but on the side of the beaker. Eggs with spontaneous necrosis or pigment variegation were removed using a 1.5 ml Pasteur pipette during all wash steps as and when necessary.

#### 4.1.1. INTERPHASE EXTRACTS

S-phase extracts was prepared as described<sup>213</sup>. Briefly, freshly laid *Xenopus* eggs were collected in 90 mM NaCl. Eggs were incubated for 5 minutes in dejellying buffer (10 mM Tris pH 8.5, 110 mM NaCl, 5 mM DTT), washed with Marc's Modified Ringer (MMR; 100 mM HEPES-KOH, pH 7.5, 2 M NaCl, 10 mM KCl, 5 mM MgSO<sub>4</sub>, 10 mM CaCl<sub>2</sub>, 0,5 mM EDTA) and activated with 1 µg/ml calcium ionophore A23187 (Sigma Aldrich) for 5 min. The activated eggs were washed with MMR and then washed three times with ice-cold S-buffer (50 mM HEPES-KOH pH 7.5, 250 mM sucrose, 50 mM KCl, 2,5 mM MgCl<sub>2</sub>, 2 mM β-mercaptoethanol, 15 µg/ml leupeptin). The eggs were packed by spinning and then crushed at 13000 rpm for 15 min. The cytoplasmic fraction between lipid cap and pellet was collected, supplemented with cytochalasin B (40 µg/ml) and centrifuged at 70000 rpm for 15 minutes to remove residual debris. The cytosolic and membrane fractions were collected and supplemented with 30 mM Creatine Phosphate (CP) and 150 mg/ml Creatine Phosphokinase (CPK). Extracts were then snap-frozen with 3% glycerol in beads of 20 µl.

#### 4.1.2. MITOTIC (CSF-ARRESTED) EXTRACTS

Mitotic extracts were prepared as described<sup>214</sup>. Briefly, *Xenopus laevis* eggs were laid and collected in 1X MMR solution (0,1 M NaCl, 2 mM KCl, 1 mM MgCl<sub>2</sub>, 2 mM CaCl<sub>2</sub>, 0,1 mM EDTA, 5 mM HEPES, pH 7.8) and extract was prepared in the absence of calcium ions in order to maintain the cytostatic factor (CSF) mediated arrest in metaphase of meiosis II. The jelly coat of eggs was removed by incubation in 2% cysteine in salt solution (2%

cysteine, 2 M KCl, 100 mM EGTA, 40 mM MgCl<sub>2</sub>, 1N NaOH) for not longer than 10 min. The dejellied eggs were then washed 3 times with XB wash buffer (100 mM HEPES, pH 7.8, 500 mM sucrose). XB wash buffer was then poured off and 14 µl of 10 mg/ml cytochalasin B (in DMSO) and LPC protease inhibitors (10 µg/ml Leupeptin, 10 µg/ml Pepstatin, 10 µg/ml Chymostatin). The eggs were poured into a 15 ml polypropylene round-bottomed tube (Falcon 2059) and packed by centrifuging for 1 minute at 300 x g in a swing bucket rotor (rotor 4250, Beckman Allegra X-22R). Excess liquid on top of the packed eggs was removed and the eggs were crushed by centrifugation in a swing rotor at 22500 x g for 20 minutes (Beckman; rotor JS 13.1 12000 rpm). The resulting cytoplasmic extract (middle golden yellow layer) was removed by puncturing the side of the tube with a 19-gauge needle and slowly removing the cytoplasmic layer with a 2 ml syringe. This extract was placed in a 5 ml polypropylene round-bottomed tube (Falcon 2063). Energy mix (375 mM CP, 50 mM ATP, 10 mM EGTA, 50 mM MgCl<sub>2</sub>) (1:50 dilution), LPC protease inhibitors (30 mg/ml each of leupeptin, pepstatin and chymostatin in DMSO) and cytochalasin B (10 mg/ml) were added (1:1000 dilution). The extract was then mixed gently using a 1.5 ml Pasteur pipette and then centrifuged at the same conditions for a further 15 min. In order to fit the 5 ml tubes in the JS 13.1 rotor, they were placed inside a 15 ml Falcon tube with 1 ml water to act as a cushion. The resulting extract was also removed by needle and syringe as above, and the extract placed in a fresh tube ready for use. Extract was kept on ice until use and was incubated at 23 °C during assays. For long term storage the extract was mixed with 2 M sucrose (10% in the extract) and frozen in liquid nitrogen in 20 µl aliquots, which form small balls when added to the liquid nitrogen. CSF egg extracts were induced to enter interphase by a final concentration of 0,4 mM CaCl<sub>2</sub> and supplemented further with 0,2 mg/ml Cycloheximide (Calbiochem).

After extract preparation, 20 µl aliquots were snap-frozen and stored in liquid nitrogen. Just before use, aliquots were thawed in ice and supplemented with 30 mM CP and 0,15 mg/ml CPK as energy regenerator system and with 0,1 mg/ml Cycloheximide (Calbiochem).

#### 4.1.3. CYCLING EXTRACTS

Mitotic extracts were prepared as described<sup>214</sup>. *Xenopus laevis* eggs were laid and collected in 1X MMR solution (0,1 M NaCl, 2 mM KCl, 1 mM MgCl<sub>2</sub>, 2 mM CaCl<sub>2</sub>, 0,1 mM EDTA, 5 mM HEPES, pH 7.8). Eggs were first rinsed in MilliQ water for 10 minutes to improve further activation step. After that, the jelly coat of eggs was removed by incubation in 2% cysteine in salt solution (2% cysteine, 2 M KCl, 100 mM EGTA, 40 mM MgCl<sub>2</sub>, 1N NaOH) for not longer than 10 min. The dejellied eggs were then washed two times with 0,2X MMR and activated with 1 µg/ml calcium ionophore A23187 for 5 min. MMR buffer was then poured off and eggs were washed 4 times with XB buffer (0,1 M KCl, 5 mM Hepes-KOH pH 7.7, 2,5 mM sucrose) and two times with XB plus 10 µg/ml LPC protease inhibitors. Eggs were poured into a 15 ml polypropylene round-bottomed tube (Falcon 2059) and packed by centrifuging for 1 minute at 150 x g and then 30 seconds at 600 x g in a swing bucket rotor (rotor 4250, Beckman Allegra X-22R) at 16 °C. Excess liquid on top of the packed eggs was removed and eggs were incubated in ice for 15 minutes. After that, eggs were crushed by centrifugation in a swing rotor at 10000 x g for 15 minutes (Beckman; rotor JS 13.1 12000 rpm) at 15 °C. The resulting cytoplasmic extract (middle golden yellow layer) was removed by puncturing the side of the tube with a 19-gauge needle and slowly removing the cytoplasmic layer with a 2 ml syringe. This extract was placed in a 5 ml polypropylene round-bottomed tube (Falcon 2063) and supplemented with 1:50 Energy mix and cytochalasin B (10 µg/ml). Extract was kept on ice until use and was incubated at 23 °C during assays.

#### 4.1.4. DEMEMBRANATED SPERM PREPARATION

*Xenopus laevis* demembrated sperm was prepared as described<sup>213</sup>. *Xenopus* male frogs were primed with 50 U Folligon seven days in advance. Testes were extracted and rinsed three times in cold 1x MMR buffer (0,1 M NaCl, 2 mM KCl, 1 mM MgCl<sub>2</sub>, 2 mM CaCl<sub>2</sub>, 0,1 mM EDTA, 5 mM HEPES, pH 7.8), twice in cold NPB buffer (250 mM sucrose, 15 mM



HEPES pH 7.4, 1 mM EDTA, 0,5 mM spermidine trichloride, 0,2 mM spermidine tetrachloride, 1 mM DTT) and finely chopped with a razor. The obtained material was homogenized in a homogenizer, filtered through 25 µm Nylon membrane and centrifuged at 3000 rpm for 10 minutes at 4 °C in HB-4 swing-out rotor. The pellet was resuspended in 1 ml of NPB buffer at room temperature and 50 µl of 10 mg/ml lysolecithin was added. The samples were incubated at room temperature for 5 min. Sperm demembration was tested by mixing 1 µl of sample with 1 µl of Hoechst stain (1µl/ml). Following demembration greater than 95%, 10 ml of cold NPB buffer supplemented with 3% BSA was added to 1 ml sample and centrifuged at 3000 rpm for 10 minutes at 4 °C in HB-4 swing –out rotor. Obtained pellet was resuspended in 500µl of cold NPB buffer supplemented with 0.3% BSA and 30% glycerol. The sperm density was then counted and aliquots were quickly frozen in liquid nitrogen.

#### 4.2. NUCLEAR ASSEMBLY IN INTERPHASE EXTRACTS

Demembrated sperm nuclei (3000 nuclei/µl) were added to interphase egg extract supplemented with 1 µM Cy3-dCTP (GE Healthcare) and the desired amount of recombinant protein and incubated in 1.5 ml tubes at 23 °C. At the desired time-point, 3 µl samples were taken from the tube and fixed with 3 µl of fixing solution (10 % formalin, 15 mM PIPES pH 7.2, 15 mM NaCl, 80 mM KCl, 50 % glycerol, 2 µg/ml Hoechst 33258 (Sigma-Aldrich), 2 µg/ml DHCC (3,3'-Dihexyloxycarbocyanine iodide, Sigma- Aldrich)). Samples were mounted on glass slides and visualized with a fluorescence microscope (Axioplan).

#### 4.3. ASSAY FOR THE NUCLEAR ENVELOPE INTEGRITY

Nuclear assembly reactions were incubated at 23 °C in the presence of recombinant Man1 N-terminal fragment or BSA. After 1 hour, reactions were supplemented with 2,5 µg of Rhodamine-Dextran (Sigma-Aldrich), incubated for other 30 minutes at 23 °C and then

stopped on ice for 15 minutes. Samples were fixed with fixing solution and visualized using a fluorescence microscope.

#### 4.4. NUCLEAR PORE ASSEMBLY ASSAY

Pore-free nuclear intermediates were reconstituted by incubation of demembrated sperm nuclei (3000 nuclei/ $\mu$ l) in interphase egg extract in the presence of 5 mM BAPTA (Sigma-Aldrich) and 1  $\mu$ M Cy3-dCTP (GE Healthcare) at 23 °C. After 60 minutes, reactions were diluted in 10 volumes of fresh interphase egg extract in the presence of 1  $\mu$ M Cy3-dCTP and either BSA or Man1 N-terminal fragment.

#### 4.5. IMMUNOFLUORESCENCE ON ISOLATED *XENOPUS* NUCLEI

Nuclear assembly reactions were incubated for 1 hour at 23 °C in the presence of recombinant Man1 N-terminal fragment or BSA. Reactions were stopped by dilution in ten volumes of dilution buffer (10 mM HEPES-KOH, 100 mM KCl, 2 mM MgCl<sub>2</sub>, 0,1 mM CaCl<sub>2</sub>, 5 mM EGTA) and fixed for 10 minutes at room temperature in presence of 1 % formaldehyde. Samples were gently laid on a 30 % glycerol cushion in tubes containing round coverslips at the bottom. Isolated nuclei were attached to the coverslips by centrifuging the samples at 5500 rpm for 20 minutes at 18 °C in a swinging-bucket rotor. Coverslips were then washed with TBST, blocked for 30 minutes with 3 % BSA and incubated overnight with primary antibody (listed in Table 3). After two 5-minutes washes with TBST, samples were incubated with fluorescent secondary antibodies for 1 hour, washed again with TBS-T and finally incubated for 5 minutes with TBST containing 1  $\mu$ g/ml Hoechst. Coverslips were mounted on glass slides with mounting medium (Vectashield, Vectorlabs) and visualized at the fluorescence microscope.

Antigen/Name	Provider	Concentration
Nup153 (sc292438)	Santa Cruz	1:1000
PhosphoH2A.X (Ser139) (05636)	Millipore	1:1000

**Table 3. List of primary antibodies used for immunofluorescence on *Xenopus* nuclei**

#### 4.6. REPLICATION ASSAY

Demembrated sperm nuclei (3000 nuclei/ $\mu$ l) were added to interphase egg extract supplemented with 50 nCi/ $\mu$ l [ $\alpha$ -<sup>32</sup>P]-dCTP and incubated at 23 °C. For agarose gel replication assay, aliquots were stopped in Stop buffer (8 mM EDTA, 80 mM Tris HCl pH 8.0, 0,13 % Phosphoric Acid, 10 % Ficoll, 5 % SDS, 0,2 % bromophenol blue, 1 mg/ml Proteinase K (Roche)) and incubated at 50 °C for 2 hours. The obtained mixtures were then resolved by electrophoresis on agarose gel (0,8% in TAE buffer) and analysed by autoradiography (Typhoon scanner). The acquired signals were then quantified using ImageJ. For replication efficiency quantification, replication reactions were stopped in Stop-C buffer (5 mM EGTA, 20 mM Tris HCl pH 7.5, 0,5 % SDS) supplemented with 0,2 mg/ml Proteinase K and incubated at 37 °C for 30 minutes. Nucleic acids were precipitated with 5 % Trichloroacetic Acid (TCA), 2 % Sodium Pyrophosphate and spotted on 25 mM Glass microfiber filter discs (Whatman). Filters were washed once with 5 % TCA, 0,5 % Sodium Pyrophosphate and twice with 100 % ethanol on a vacuum manifold and dried. The incorporated radioactivity was counted in a scintillation counter and the amount of replicated DNA was evaluated as described<sup>211</sup>.

#### 4.7. VISUALIZATION OF NASCENT SINGLE STRANDED DNA ON ALKALINE AGAROSE GEL

Replication reactions were prepared as described in section 4.6. and incubated at 23 °C for 30 minutes. At that point, each 20  $\mu$ l reaction was supplemented with 0,5  $\mu$ l of [ $\alpha$ -<sup>32</sup>P]-dCTP

(3000 Ci/mmol) and after 2 minutes they were chased with 2,5 mM of unlabelled dCTP plus 0,5 mM roscovitine (Sigma-Aldrich). Reactions were then incubated again at 23 °C and stopped at the desired time-points with 10 volumes of stop buffer (2% SDS, 80 mM EDTA, 600 mM NaCl). After adding 0,2 mg/ml Proteinase K (Roche), samples were digested at 37 °C for 1 hour. The DNA was precipitated by adding to each sample 7,5 µl of NaAc 5M and purified by performing two rounds of phenol/chloroform/isoamylalcol extraction followed by ethanol precipitation. Finally, the DNA pellets were resuspended in 20 µl of 1x alkaline gel running buffer (50 mM NaOH, 1 mM EDTA pH 8.0) and then mixed with 4 µl of 6x alkaline loading buffer (300 mM NaOH, 6 mM EDTA, 18% ficoll, 0,15 % bromophenol blue, 0,25 % xylene cyanol).

To prepare the alkaline agarose gel, 1,2 g of agarose were dissolved in 135 ml of bidistilled water. Melted agarose was cooled down at 55 °C and then mixed with 15 ml of 10x alkaline gel running buffer (500 mM NaOH, 10 mM EDTA pH 8.0).

The samples were first separated at 45 V until complete migration outside of the gel wells, then the voltage of the electric field was lowered at 32 V and applied for 16 hours at 4 °C.

After that, the gel was submerged in neutralizing solution (1 M Tris-HCl pH 7.6, 1,5 M NaCl) for 45 minutes and precipitation of nucleic acids was performed by immersing the gel into TCA 30%. Finally, the agarose gel was dried and subjected to autoradiography.

#### 4.8. CHROMATIN BINDING EXPERIMENT

To isolate chromatin fractions, demembrated sperm nuclei (4000 nuclei/µl) were added to interphase extract together with BSA or Man1 N-terminal fragment and incubated at 23 °C. Samples were stopped on ice at the indicated times and diluted in ten volumes of EB (100 mM KCl, 2,5 mM MgCl<sub>2</sub>, 50 mM Hepes-KOH pH 7.5) containing 0,25 % NP-40 (Nonidet-40). The diluted extract was carefully layered onto an equal volume of EB-NP-40 -30 % sucrose cushion. Chromatin and chromatin-bound proteins were subsequently spun through the sucrose cushion for 5 minutes at 8,300 x g at 4 °C in a swinging-bucket rotor. Chromatin

pellets were washed once in EB and resuspended in Laemmli loading buffer. Proteins were resolved by SDS-Page on a 4-15 % acrylamide gel and analyzed by Western Blotting.

#### 4.9. HALO ASSAY

Nuclear assembly reactions were incubated for 1 hour at 23 °C in the presence of recombinant Man1 N-terminal fragment or BSA. Reactions were stopped by dilution in ten volumes of EB-NP40 and kept in ice for 5 minutes. Isolated nuclei were attached to round coverslips by centrifuging the samples through a sucrose cushion in a 16-well plate with coverslips placed at the bottom. Nuclei were stabilized for 10 minutes at 4 °C with stabilization solution (1 mM CuCl<sub>2</sub>, 10 mM MgCl<sub>2</sub>, 0,5 mM CaCl<sub>2</sub>, 25 mM Tris-HCl pH 8, 1 mM PMSF) and then they were sequentially dipped for 30 seconds in a solution containing 0,2 mM MgCl<sub>2</sub>, 25 mM Tris-HCl pH 8, 1 mM PMSF with 0,5 M, 1 M, 1,5 M and 2 M NaCl. The last solution was also supplemented with 50 µg/ml Ethidium Bromide. After that, coverslips were exposed for 2 minutes to short-wave UV light (UV Stratalinker, Stratagene) to induce release of the chromatin loops and then mounted on glass slides with mounting medium (Vectashield, Vectorlabs) before observation at the fluorescence microscope. Images were analysed with ImageJ and halo size was calculated taking into account that the chromatin loop size is twice the maximum distance between the margins of the fluorescent halo and of the nuclear matrix (Maximum Fluorescence Halo Radius, MFHR). The length of linear DNA was calculated using the correspondence of 1 µm to 2,3 Kbp<sup>118</sup>.

#### 4.10. NUCLEAR ASSEMBLY IN CSF EXTRACTS

Demembrated sperm nuclei (3000 nuclei/µl) were added to CSF extract supplemented with the desired amount of recombinant protein and incubated at 23 °C. After 20 minutes, extract activation was induced by adding 0,2-0,8 mM CaCl<sub>2</sub> (depending on the extract). At the desired time-points, 3 µl of the samples were fixed with an equal amount of fixing solution and observed at the fluorescence microscope.

#### 4.11. ANALYSIS OF THE CELL CYCLE USING *XENOPUS* CYCLING EXTRACTS

Demembrated sperm nuclei (500 nuclei/ $\mu$ l) were added to cycling extract supplemented with the desired amount of recombinant protein and 50  $\mu$ g/ml of porcine Tubulin HiLyte 488 (Tebu-Bio) and incubated at 23 °C. At the desired time-points, 3  $\mu$ l of the samples were fixed with an equal amount of fixing solution and observed at the fluorescence microscope. For monitoring Cyclin B2 levels, 1  $\mu$ l of the samples were taken from the reaction at different time-points, diluted 1:10 in 2x Laemmli loading buffer and resolved by SDS-Page on a 10 % acrylamide gel followed by Western Blotting.

### 5. CELL CULTURE TECHNIQUES

#### 5.1 ESC CELL LINES

The following mESC cell lines were used in this study:

Name	Source
D1	<i>Mus musculus</i> embryonic stem cells derived from embryo inner cell mass of Rosa26-Cas9 knockin mice Gt(ROSA)26Sor <sup>tm1.1(CAG-cas9*, -EGFP)Fezh/J</sup> (The Jackson Laboratory) Cells were produced and provided by IFOM transgenic facility
E14	<i>Mus musculus</i> embryonic stem cells derived from embryo inner cell mass of 12910la strain (Austin Smith's laboratory). Cells were provided by IFOM transgenic facility

**Table 4. List of ESC cell lines used in this study**

#### 5.2. GENERATION OF CRISPR-CAS9 MAN1 KO CLONES

To obtain stable mES Man1-knockout cell lines, CrispR/Cas9 genome editing tool was used. This system is based on a bacterial CRISPR-associated protein-nuclease 9 (Cas9) and two

RNAs: the CRISPR RNA (crRNA) and trans-acting CRISPR RNA (tracrRNA), which can anneal together forming a duplex called guide RNA (gRNA). These two RNAs can both bind to the Cas9 nuclease, which is guided to the sequence complementary to the crRNA and cleaves the DNA, inducing a DSB. The DSB generated by CRISPR/Cas9 leads to the activation of endogenous cellular DNA repair mechanisms, including Non-Homologous End Joining (NHEJ)-mediated error-prone DNA repair and Homologous Recombination (HR)-mediated error-free DNA repair. Insertion and deletion mutations generated either by NHEJ and HR allow the disruption or the abolishment of the functions of the target gene.

To knockout mouse *Man1*, three crRNAs (Table 5) were designed using Target Finder software (Zhang Lab).

Name	Sequence (5'-3')	Targeted <i>Man1</i> exon
crMan1_1	TAACGAATCTAGAGTCCGTACGG	9
crMan1_2	CCGCCGTTACGGCTTATCTCCGG	1
crMan1_3	GCTTGCCGTAGGCGGTTTTTCAGG	1

**Table 5. List of crRNA oligos used to knockout *Man1* by CRISPR/Cas9**

To produce *Man1* gRNAs, annealing of crRNAs and tracrRNAs was performed as described: for each annealing reaction, 10  $\mu$ l of each 50  $\mu$ M gRNA were mixed with 10  $\mu$ l of 25  $\mu$ M ATTO<sup>550</sup>-tracrRNA (IDT) and 80  $\mu$ l of nuclease-free duplex buffer (IDT). The reactions were incubated at 100 °C for 2 minutes and let cool down at room temperature.

Transient transfection of the gRNAs was first performed on D1 mESCs, which are constitutively expressing the Cas9 nuclease.

The day before transfection, cells were seeded on gelatin-coated 100 mm dishes at a concentration of  $5 \times 10^4$  cells for each plate. Next day, lipofectamine complexes were prepared as described: for the transfection of single guides 16,5  $\mu$ l of annealing reactions were mixed with 500  $\mu$ l of Optimem (Thermofisher) and, separately, 15  $\mu$ l of Lipofectamine

RNAiMAX reagent (Thermofisher) were added to 500  $\mu$ l of Optimem. The two solutions were then mixed together and incubated at room temperature for 15 minutes.

For the transfection of the three guides, 16,5  $\mu$ l of the three annealing reactions were pooled together and mixed with 1,5 ml of Optimem. Separately, 45  $\mu$ l of Lipofectamine RNAiMAX reagent were added to other 1,5 ml of Optimem. The two solutions were then mixed together and incubated at room temperature for 15 minutes.

After the incubation of the complexes, fresh medium was added (to reach a final volume of 10 ml for each reaction) and everything was added to the plated cells. After 24 hours, transfection efficiency was evaluated at the microscope by visualization of ATTO<sup>550</sup> fluorescent signal. After 48 hours from the transfection, cells were harvested to perform RT-qPCR and Western blot analysis.

To perform Man1 KO on E14 mESCs, cells were transfected with the Cas9. For each 100 mm dish, 24  $\mu$ g of plasmid pSpCas9(BB)-2A-Puro (Addgene) were mixed with 500  $\mu$ l of Optimem and, separately, 60  $\mu$ l of Lipofectamine 2000 reagent (Thermofisher) were added to other 500  $\mu$ l of Optimem. The two solution were mixed and incubated for 15 minutes at room temperature. The reaction was added to 100 mm dishes together with  $8 \times 10^6$  cells in a total volume of 10 ml of medium. After one day, the medium was changed and puromycin was added at a concentration of 2  $\mu$ g/ml.

For the transfection of the three gRNAs, lipofectamine complexes were prepared as described above. The complexes were plated together with cells in suspension ( $10 \times 10^3$  cells for each 100 mm dish) in a total volume of 10 ml of medium supplemented with puromycin. After few days, puromycin selection was removed to allow better growth of the colonies.

One week after, isolated colonies were picked and transferred in 96-well plates.

### 5.3. PCR SCREENING OF CRISPR-CAS9 CLONES

To extract genomic DNA, 100  $\mu$ l of 0,25 M NaOH were added to each well of the 96-well plate and incubated at 100  $^{\circ}$ C for 10 minutes.



PCR mix was prepared as following:

Buffer Go-Taq Flexi (Promega)	5 $\mu$ l
100 $\mu$ M dNTPs	0,5 $\mu$ l
100 $\mu$ M Forward primer	0,1 $\mu$ l
100 $\mu$ M Reverse primer	0,1 $\mu$ l
GoTaq Hot Start (Promega)	0,2 $\mu$ l
Genomic DNA	5 $\mu$ l
25 mM MgCl <sub>2</sub>	1,5 $\mu$ l
ddH <sub>2</sub> O	Up to 20 $\mu$ l

The following primers were used:

36B4 Forward: 5'-ACTGGTCTAGGACCCGAGAAG-3'

36B4 Reverse: 5'-TCAATGGTGCCTCTGGAGATT-3'

Man1 Forward: 5'-GGAGAGCACCCCGGCCCGTCT-3'

Man1 Reverse: 5'-GCCTCCTGCCACGGGGCTCT-3'

PCR was performed with the following program:

98 °C	5'	}	35
98 °C	15''		
59 °C	20''		
72 °C	30''		
72 °C	5'		
4 °C	$\infty$		

#### 5.4. PREPARATION OF WHOLE CELL EXTRACTS FOR WESTERN BLOTTING

Cell pellets were washed twice in ice-cold PBS 1x, harvested and resuspended in 10 volumes of RIPA buffer supplemented with Protease Inhibitor Cocktail (Roche). After incubation on ice for 10 minutes, samples were sonicated using a Bioruptor® Standard sonication device (Diagenode) for 8 minutes (30 seconds high intensity pulse-30 seconds wait) in cold water supplemented with small amounts of crushed ice. Insoluble material was collected by centrifugation at 16,000 x g for 15 minutes. Protein concentrations were determined using

Bradford method<sup>215</sup>. Required amount was mixed with loading buffer and incubated for 4 minutes at 100 °C before loading.

## 5.5. TOTAL RNA EXTRACTION

Total RNA extraction was performed by mechanical rupture of cell pellets with an insulin syringe with 1 ml of Trizol (Thermofisher), according to manufacturer's protocol. Briefly, homogenates were incubated at 30 °C for 5 minutes and, after that, 200 µl of Chlorophorm were added. Tubes were vortexed and incubated at 30 °C for 2 minutes. Tubes were centrifuged at 12000 xg for 15 minutes at 4 °C to allow separation of aqueous and organic phase. The upper aqueous phase was collected and mixed with 0,5 ml of isopropanol to allow RNA precipitation. Tubes were incubated at 30 °C for 10 minutes and then centrifuged 12000 xg for 10 minutes at 4 °C. The supernatant was removed and the pellets were washed with 1 ml of 75% ethanol. The tubes were centrifuged again at 7500 x g for 5 minutes at 4 °C and the pellets were air-dried on ice. Finally, the RNA pellets were resuspended in MilliQ water and quantified at the Nanodrop.

## 5.6. REVERSE-TRANSCRIPTASE QUANTITATIVE PCR (RT-QPCR)

One microgram of total RNA was first reverse-transcribed into first-strand cDNA in the presence of random primers using SuperScript™ III Reverse Transcriptase (Invitrogen) according to manufacturer's protocol. Then real time-PCRs were performed in triplicate in LigthCycler® 480 Semi skirted 96-well plates (Roche) using LightCycler 96 Real time system (Roche). A master mix was prepared adding the following reagents to each reaction:

ddH <sub>2</sub> O	10 µl
100 µM Forward primer	0,1 µl
100 µM Reverse primer	0,1 µl
LightCycler 480 SYBR Green I Master	10 µl

Each well was filled with 19  $\mu$ l of Master mix and 1  $\mu$ l of 1:4 cDNA dilution in water were added to each well. Plates were then sealed using Microseal® B Adhesive Sealer (BIO-RAD) and centrifuged for 5 minutes at 4000 rpm before program starting.

The cycle parameters used were:

Preincubation	95 °C	300''		
2-step amplification	95 °C	10''	}	x 45
	60° C	30''		
	95 °C	10''		
Melting	65 °C	60''		
	97 °C	1''		

Fluorescence was measured at the end of the annealing period of each cycle to monitor the amplification. Immediately after the amplification, melting curves were recorded in order to verify that a single product was amplified in all reactions.

Expression levels of target genes were determined by comparison with the housekeeping gene GAPDH. For each PCR run, the relative mRNA level was determined by the expression:

$$\text{Fold change} = 2^{-\Delta\Delta\text{Ct}}$$

$$\Delta\Delta\text{Ct} = \Delta\text{Ct}_{\text{Control or treated}} - \Delta\text{Ct}_{\text{control}}$$

$$\Delta\text{Ct} = \text{Ct}_{\text{target gene}} - \text{Ct}_{\text{GAPDH}}$$

Ct=Cycle Threshold

The RT-qPCR experiments were conducted 3 times and averaged. Primers used are listed below (Table 6):

Gene	Forward primer (5'-3')	Reverse primer (5'-3')
Man1	CGGAATATGCTGGGAAGGCT	AGGGAGTGTGCAAGTGAGG
Nanog	CAGGTGTTTGAGGGTAGCTC	CGGTTCATCATGGTACAGTC
Oct4	CCGTGTGAGGTGGAGTCTGAGA	GCGATGTGAGTGATCTGCTGTAGG
Sox2	TAGAGCTAGACTCCGGGCGATGA	TTGCCTTAAACAAGACCACGAAA
Rex1	ACGAGTGGCAGTTTCTTCTTGGGA	TATGACTCACTTCCAGGGGGCACT
GAPDH	ACCCAGAAGACTGTGGATG	CACATTGGGGGTAGGAACAC
PcRNA	TGGCGAGAAACTGAAAATCACG	TCTTGCCATATTCCACGTCTTAC
TERRA	CGGTTTGTTTGGGTTTGGGTTTGG- -GTTTGGGTTTGGGTT	GGCTTGCCTTACCCTTACCCTTACCC- -TTACCCTTACCCT

**Table 6. List of primers used for Reverse-Transcription quantitative PCR (RT-qPCR)**

#### 5.7. ALKALINE PHOSPHATASE STAINING

Alkaline phosphatase staining was performed with Leukocyte Alkaline Phosphatase Kit (Sigma Aldrich) according to manufacturer's protocol. Cells were seeded on gelatin-coated 6-well plates at a concentration of  $3 \times 10^5$  cells/well.

#### 5.8. EMBRYOID BODIES FORMATION

When cultured in suspension and in absence of LIF, mES cells differentiate spontaneously, forming spherical aggregates called Embryoid Bodies (EBs), which can differentiate giving rise to cells of all three germ layers.

For EB formation,  $5 \times 10^4$  cells were harvested and transferred in single-cell suspension into a low-attachment culture dishes. EBs were cultured ESC differentiation medium. After 5-7 days in floating culture, EBs were collected by sedimentation and transferred onto gelatin-coated 6-well plates and cultured with fresh medium for other three days to induce further differentiation in all the cell types.

## RESULTS

### 1. MAN1 CHARACTERIZATION USING THE *XENOPUS* CELL-FREE EXTRACT SYSTEM

To investigate the function of Man1 in nuclear assembly and DNA replication, recombinant mutant proteins derived from *Xenopus* Man1 were added to the extracts.

Studying *Xenopus* Man1 function using immunodepletion was excluded as a strategy for the following reasons: first, removing integral membrane proteins from eggs membranes is technically challenging, as this procedure includes membranes solubilisation and a final reconstitution of the depleted membranes, besides the specific immunodepletion. A second complication arises from the functional redundancy of LEM proteins and other nuclear envelope factors, which could compensate the loss of Man1.

To overcome these problems a “dominant negative strategy” was chosen, as a similar experimental setup has been already used to study the effect of nuclear envelope protein Lap2 $\beta$  on nuclear architecture<sup>125</sup>. Truncated mutants of Man1 were generated to compete with the endogenous wild-type protein and interfere with the tethering of the chromatin to the nuclear envelope.

#### 1.2. ANALYSIS OF *X. LAEVIS* MAN1 SEQUENCE AND STRUCTURE

*X. laevis* Man1 (xMan1) cDNA sequence was obtained from *Xenopus* IMAGE cDNA library (clone name: IMAGE:9093697). The translated sequence was aligned to human Man1 (NCBI Reference Sequence: NP\_055134) using Geneious Software in order to identify conserved functional domains.

Full length *X. laevis* Man1 protein sequence is composed by 782 aminoacids and shares around 50% overall similarity with the human ortholog. The most conserved regions are the

LEM domain (>80% similarity) located in the N-terminal extremity and the C-terminal RRM motif (87% similarity), whereas other regions are less conserved (Figure 6).

Structurally, xMan1 is composed by a N-terminal and a C-terminal regions separated by two transmembrane domains. The entire N-terminal region (residues 1-345) contains, beyond the LEM domain (residues 4-33), other putative polypeptide binding sites. In fact, even if the entire N-terminal region shares only 30% of homology with the human counterpart, it was possible to identify some highly conserved sites which most likely represent binding consensus sequences for lamins and other nuclear envelope proteins. The first transmembrane domain is predicted to be located in the region between residues 352 and 372 and it is highly conserved between human and *Xenopus* (90% of identity) whereas the second transmembrane region is predicted to be located at residues 498-518 with a lower degree of conservation (38 % of identity). The residues between the two transmembrane domains constitute the luminal domain, which is still uncharacterized in vertebrates, but is known to contain in the yeast ortholog protein Src1 some interaction sites with NPC components<sup>200</sup>.

The C-terminal region (residues 520-782) contains other two main functional domains. The first one is the MSC domain (residues 392-622), which shares 20% of sequence homology with the yeast protein Src1 and is predicted to adopt a secondary conformation capable of directly bind DNA. The second domain is called RRM (residues 657-736) and is shared with many RNA interacting factors. In fact, it contains an DNA/RNA binding site (residues 704-706) and a polypeptide binding site (residues 734-736). These residues are likely to mediate the interaction with Smads transcription factors, even if the identification of a specific consensus motif on the *Xenopus* sequence was not successful.

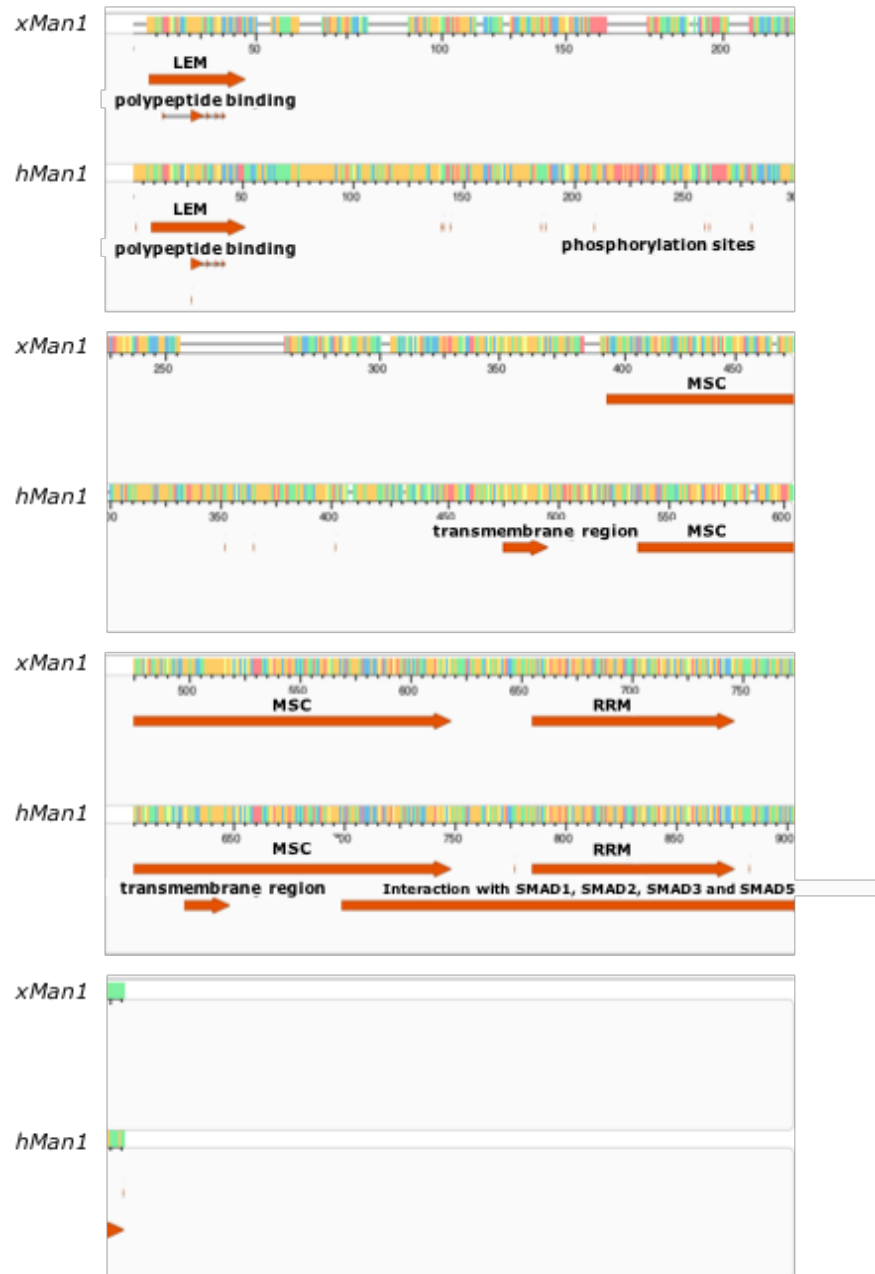


**Figure 6. Sequence alignment between *X. laevis* (top) and human (bottom) *Man1* proteins.** The alignment analysis was performed using MegAlign software. Red arrows represent conserved domains. A detailed description of *Man1* sequence is available in the text.

### 1.3. GENERATION OF MAN1 DERIVATIVE MUTANTS

As previously described, wild-type *Man1* spans twice the inner nuclear membrane, exposing to the nucleoplasm two putative DNA-interaction sites, located in the amino and carboxy-terminal extremities (Figure 7A). Two truncated mutants of *Man1*, corresponding to the entire N-terminal and C-terminal regions deprived of the transmembrane domains, were

generated (Figure 7B). The N-terminal fragment (corresponding to residues 1-345) is predicted to have lamin-binding properties and, more importantly, it contains the LEM domain, which mediates the interaction with the chromatin. On the other hand the C-terminal fragment (corresponding residues 520-782) includes the RRM domain, essential for the regulation of transcription factor activity during embryo development<sup>150,185</sup>, and a putative DNA binding domain called MSC, which function is still uncharacterized.

Such mutants are predicted to compete with the binding of the endogenous wild-type protein with its targets (in particular, DNA and chromatin).

Man1 truncated mutants were generated by cloning Man1 cDNA into a bacterial expression vector carrying a SUMO-histidine tag. Recombinant proteins were obtained by affinity purification from induced *E. coli* cultures (Figure 7C). Due to the intrinsic instability of the free N-terminal fragment it was not possible to remove the His-SUMO tag without causing precipitation of the recombinant protein. Anyway it is possible to exclude that the phenotypes observed in this study was given by the SUMO-tag since it wasn't either removed from the C-terminal fragment which seemed to have no phenotype (as shown in the next section).



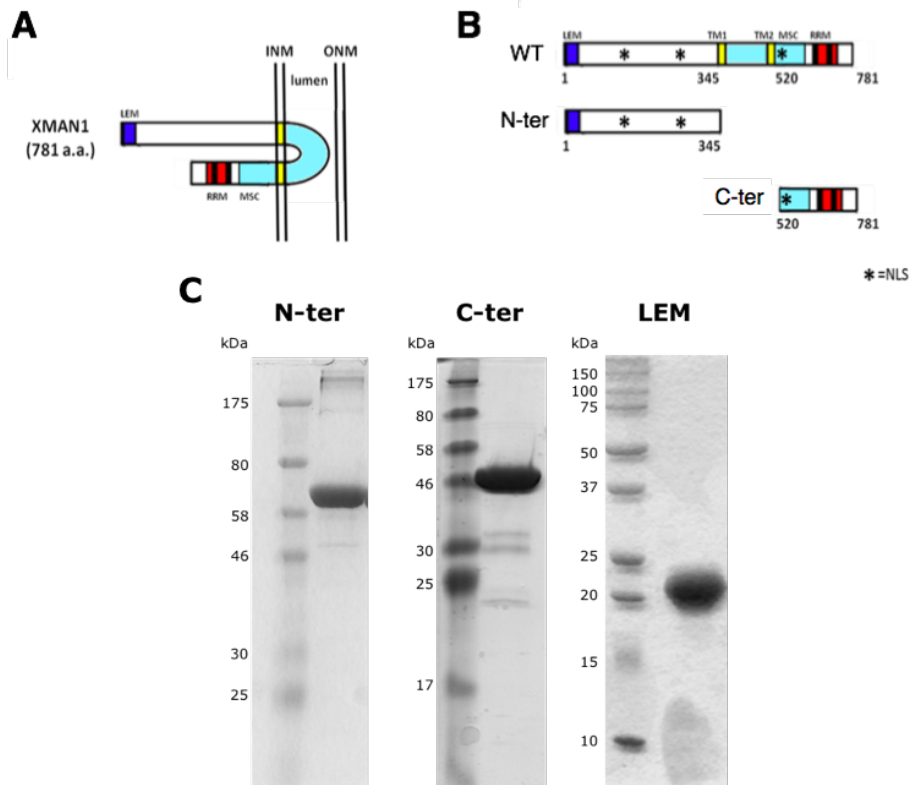


**Figure 7. Structure and functional domains of *Xenopus Man1* and its recombinant derivatives.**

A) Endogenous *Xenopus Man1* spans the inner nuclear membrane twice, exposing to the nucleoplasm functional domains of interaction: the LEM domain (in blue), the two transmembrane domains (in yellow), the MSC domain (light blue) and the RRM domain (in black and red). Black asterisks indicated the position of Nuclear Localization Signals. B) Recombinant *Xenopus Man1* mutants used in this project. C) Coomassie staining of purified recombinant proteins (5 µg of each protein were loaded on the gel). Prestained protein marker, Broad range (New England Biolabs) and Precision plus dual color marker (BioRad) were used as protein standards.

The image was adapted from Osada et al<sup>185</sup>.

#### 1.4. THE N-TERMINAL FRAGMENT OF MAN1 IMPAIRS NUCLEAR ASSEMBLY AND CHROMATIN DECONDENSATION

To characterize Man1 function in nuclear assembly dynamics, SUMO-HIS tagged versions of both the N-terminal and C-terminal domains from *Xenopus laevis* Man1 protein were produced in bacterial cells and purified to homogeneity. In order to compete with the activity

of the endogenous Man1 factor, these recombinant protein mutants were added to *Xenopus* nuclear assembly at a concentration of 3  $\mu$ M.

To exclude any possible non-specific effect given by simple addition of proteins into the extract, control reactions were prepared by adding an equal molar amount of Bovine Serum Albumin (BSA).

As shown in the middle panel of Figure 8A, nuclei assembled in the presence of the C-terminal fragment appeared similar to the control ones, with no detectable defects in envelope expansion and chromatin decondensation, monitored by fluorescent staining with, respectively, a lipophilic fluorescent dye DHCC and Hoechst.

Moreover, they appeared to be competent for DNA replication, as indicated by efficient incorporation of a fluorescence-labelled nucleotide (Cy3-dCTP).

On the other hand, extract supplemented with the N-terminal fragment were unable to assemble normal shaped nuclei (Figure 8A and B, bottom panels). In particular, addition of purified N-terminal fragment to the extract determined an evident delay in nuclear expansion at 3  $\mu$ M protein concentration while at higher concentrations (12  $\mu$ M) almost completely arrested nuclear formation (Figure 9).

This result is consistent with the effect of Lap2 $\beta$ -truncated mutants on nuclear assembly in *Xenopus* extracts reported in a study in which a similar dominant negative strategy was used<sup>125</sup>.

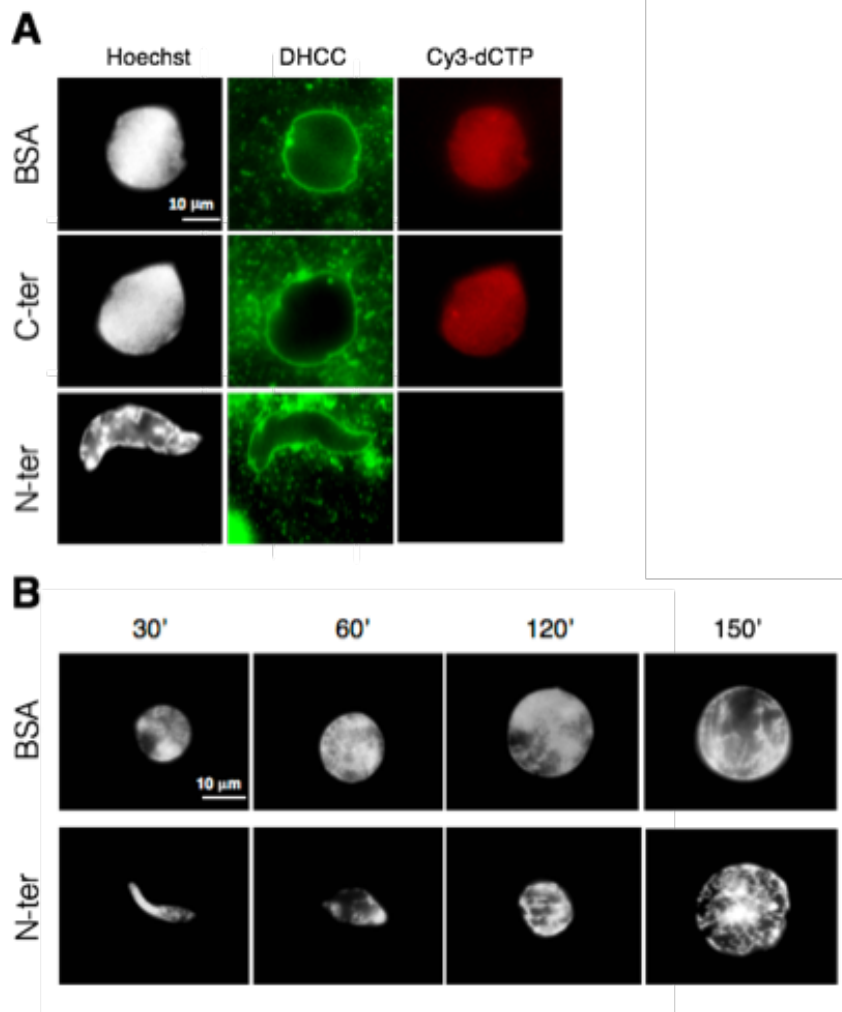


**Figure 8. Effect of *Man1* mutants on nuclear assembly and nucleotide incorporation.**

*A) Demembrated sperm nuclei assembled for 1 hour in Xenopus interphase extract containing the same molar amount (3  $\mu$ M) of BSA, C-terminal or N-terminal fragment were fixed on coverslips and observed by fluorescence microscopy. Left panels show DNA staining (Hoechst), central panels show membrane staining (DHCC) and right panels show nucleotide incorporation (Cy3-dCTP). B) Representative time-course of the effect of N-terminal fragment on nuclear formation (Hoechst staining). Images are representative of at least 10 independent experiments.*

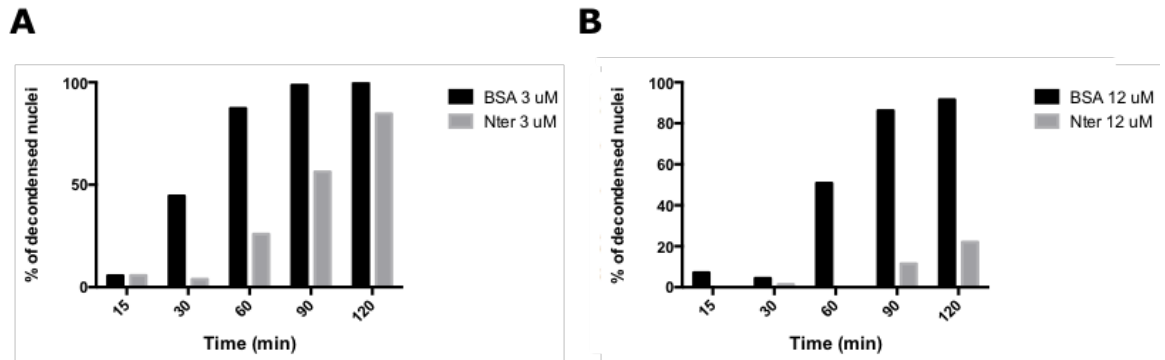


**Figure 9. Dose-dependent effect of Man1 N-terminal fragment on nuclear assembly over time.**

The histograms show the percentage of decondensed nuclei assembled in presence of BSA or N-terminal fragment either at 3 (A) or 12 (B)  $\mu\text{M}$  concentration over time. At least 100 nuclei were counted for each experimental point.

These results indicate that the addition of the N-terminal fragment, containing the putative chromatin-binding domain of Man1 but lacking connection with the nuclear membrane might interfere with envelope expansion and chromatin decondensation.

The same effect was obtained also by using a shorter 45 aa peptide corresponding to the sequence of the LEM domain of Man1 alone (Figure 10), suggesting that the observed impairment in nuclear assembly could be mediated by this specific domain.

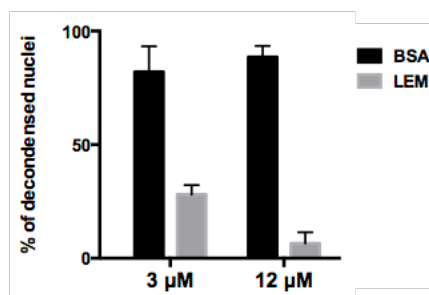


**Figure 10. Effect of recombinant LEM domain on nuclear assembly.**

Percentage of decondensed nuclei assembled for 1 hour in presence of BSA or recombinant LEM domain, either at 3 or 12  $\mu\text{M}$  concentration. The histogram shows mean values  $\pm$  standard deviation (error bars) of three independent experiments. At least 100 nuclei were counted for each experimental point.

## 1.5. MAN1 N-TERMINAL FRAGMENT DOES NOT IMPAIR NUCLEAR ENVELOPE INTEGRITY BUT IT AFFECTS NUCLEAR PORE FORMATION

Given the results mentioned above, it is possible to think that the truncated N-terminal mutant of Man1 could interfere with nuclear envelope assembly. For this reason, the functional properties of the NE were assayed with different methods upon treatment with the N-terminal fragment. A possible reason for the observed defects in nuclei formation could be that the N-terminal fragment can interfere with membrane fusion. In order to assess whether addition of the N-terminal domain could disrupt the integrity of the nuclear envelope, the ability of nuclei to exclude large 70 kDa dextran molecules was tested.

Since the size of such molecule is above the limit for diffusion through nuclear pores (that is considered to be around 60 kDa)<sup>216</sup>, it can enter into nuclei only if there are gaps in the nuclear envelope or if nuclear membrane assembly process is incomplete.

In these assays rhodamine-labelled dextran was added to the extract containing either control (BSA) or the N-terminal and nuclei were let assemble for 1 hour. After 30 minutes, samples were fixed in presence of Hoechst and DHCC and observed by fluorescence microscopy. As shown in Figure 11, the results of these analyses demonstrated that the large majority of control nuclei and N-terminal treated nuclei were efficient in excluding 70 kDa dextran molecules, indicating that they were both able to assemble intact nuclear membranes.

Such result indicates that Man1 N-terminal fragment is not interfering with the fusion of nuclear membrane vesicles.

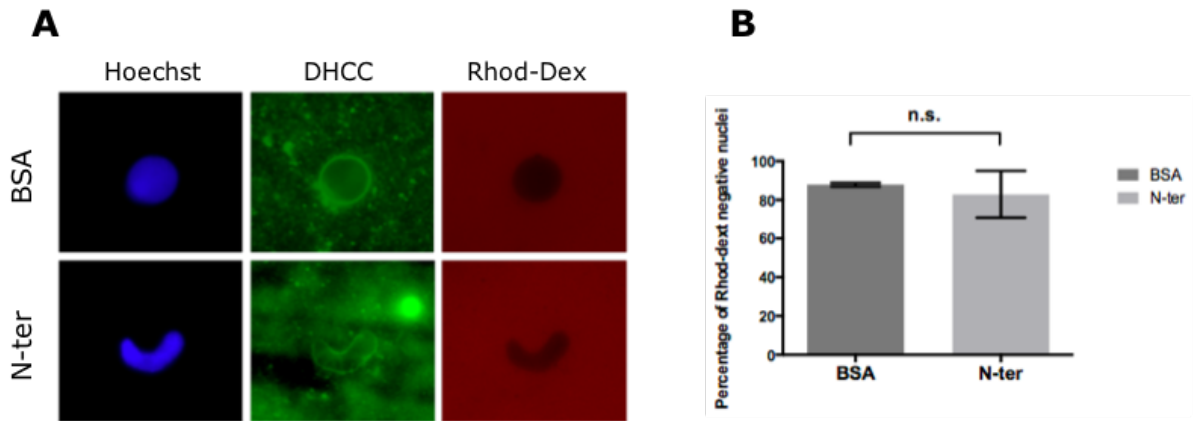


**Figure 11. Effect of Man1 N-terminal mutant on nuclear envelope integrity.**

A) Nuclei were assembled for 1 hour in the presence of BSA or N-terminal fragment and then incubated for 30 minutes in presence of rhodamine-labelled 70 KDa Dextran. The histogram shows percentage of nuclei able to exclude 70 KDa Dextran from the lumen. The histogram shows mean values (bar)  $\pm$  standard deviation (error bars) of three independent experiments. At least 100 nuclei were counted for each experimental point.

Given this observation, the effect of the N-terminal fragment on nuclear assembly and expansion could be also explained by defects in active nuclear import, since nucleocytoplasmic transport mediated by NPCs is required for NE expansion and nuclear growth<sup>121,217</sup>. For this reason, nuclei assembled in presence of N-terminal domain were tested for the ability to actively import a Nuclear Localization Signal (NLS)-tagged fluorescent substrate (NLS-GFP). As shown in Figure 12, it was not possible to detect any significant difference in the import ability between control and N-terminal treated nuclei, suggesting that the observed phenotype was not caused by defects in bulk import of proteins inside the nuclei.

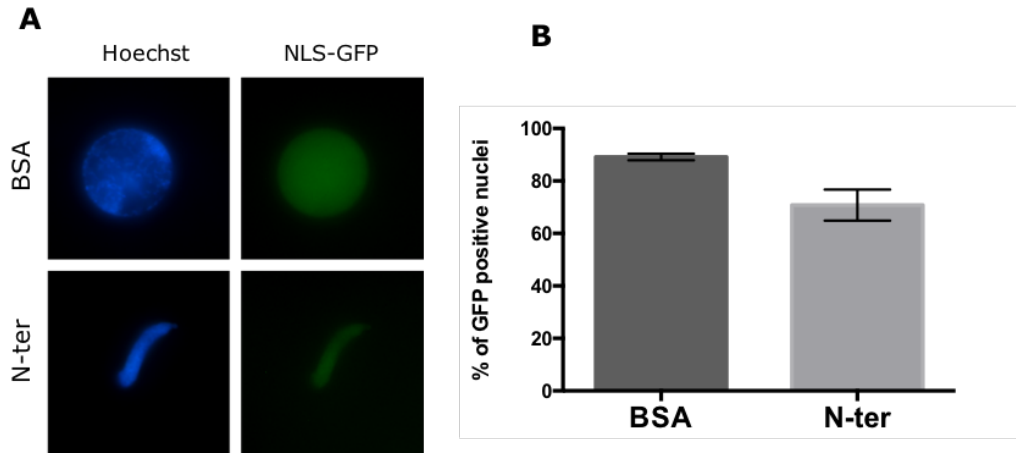


**Figure 12. Effect of Man1 N-terminal mutant on nuclear import.**

A) Nuclei were assembled for 1 hour in the presence of BSA or N-terminal fragment and then incubated for 30 minutes in presence of recombinant NLS-GFP. B) The histogram shows percentage of nuclei able to actively import NLS-GFP. The histogram shows mean values  $\pm$  standard deviation (error bars) of three independent experiments. To obtain percentages, at least 100 nuclei were counted for each experimental point.

Another possible explanation of the observed impairment in nuclear assembly could be that Man1 N-terminal fragment impairs NPC assembly without affecting dramatically the bulk nuclear import of proteins. In order to answer to this question, the effect of Man1 N-terminal fragment on NPC assembly was tested, by adding it to pore-free nuclear intermediate structures, that were previously assembled in *Xenopus* extracts by using the calcium chelator BAPTA (Figure 13A and 13B). In fact the addition of BAPTA in nuclear assembly reactions is able to inhibit the assembly of mature NPCs, resulting in the formation of nuclei with fully sealed nuclear membranes deprived of nuclear pores<sup>217</sup> (Figure 13A).

As shown in Figure 13, addition of BAPTA in the egg extract led to the formation of small condensed nuclei with a continuous DHCC staining and unable to incorporate Cy3-dCTP, indicating impaired DNA replication. The rescue of NPC assembly and proper nuclear functions could be achieved by subsequent dilution of BAPTA intermediates in fresh egg extract, leading to the maturation of NPCs, chromatin decondensation and DNA replication (Figure 13B, BSA panel). However, incubation of BAPTA intermediates in fresh extract

containing N-terminal Man1 fragment was not able to completely restore nuclear functions. In fact, the resulting nuclei were not able to recover complete chromatin decondensation and nuclear growth, while they were still able to incorporate labelled nucleotides (Figure 13, N-ter panel).

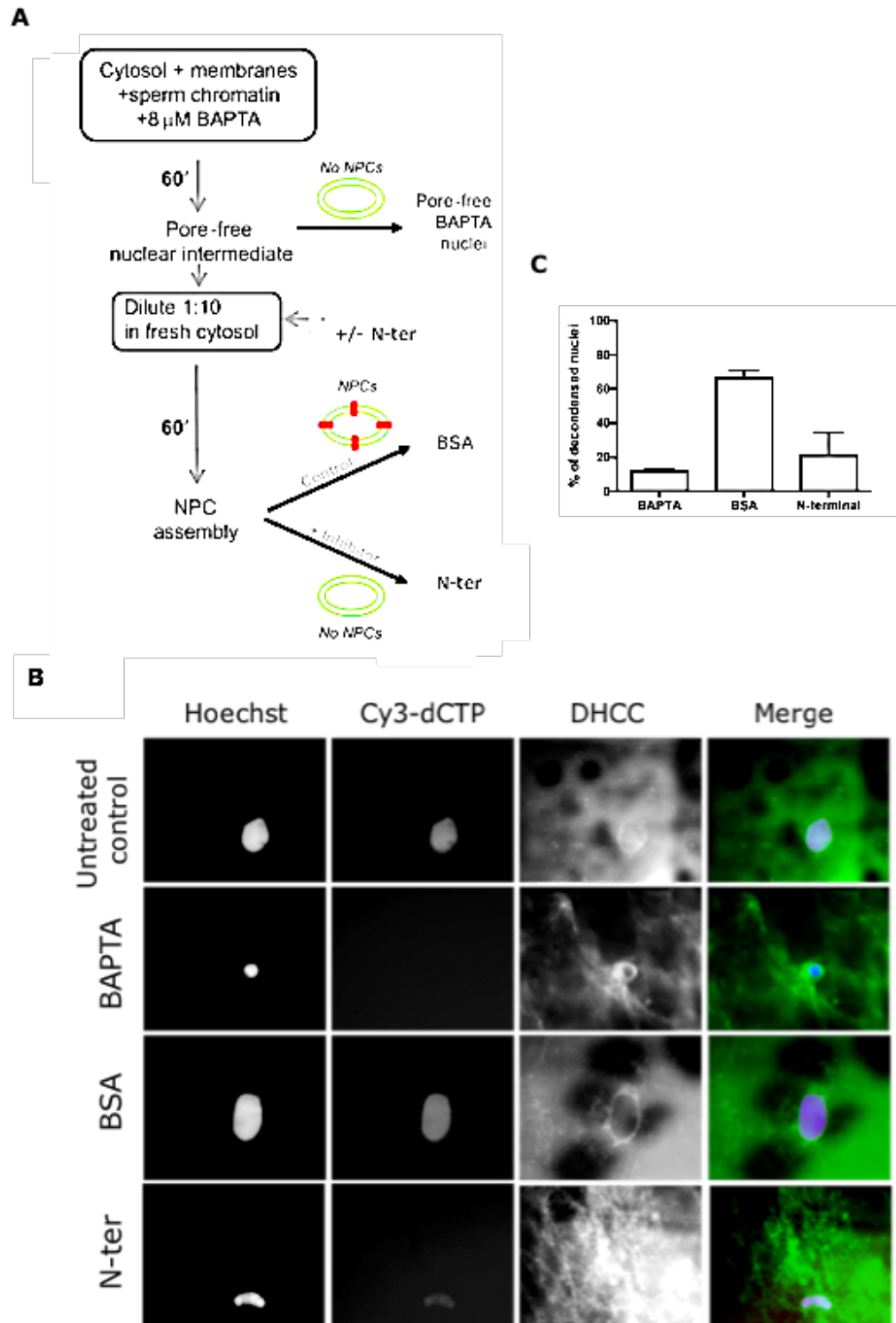


**Figure 13. Nuclear pore assembly assay.**



A) Schematic representation of the experiment (Adapted from Bernis et al.<sup>218</sup>). To assemble pore-free nuclear intermediates, sperm nuclei (3000 nuclei/ $\mu$ l) were incubated in interphase extract in the presence of 8 mM BAPTA and Cy3-dCTP for 60 min. Pore-free nuclei were subsequently diluted in 10 volumes of fresh extract containing either BSA or N-terminal fragment and incubated for further 60 minutes. B) Representative pictures of assembled nuclei fixed and visualized at the fluorescence microscope. C) The graph shows the percentage of fully decondensed nuclei. The histogram shows mean values (bar)  $\pm$  standard deviation (error bars) of three independent experiments. At least 100 nuclei were counted for each experimental point.

In parallel, immunofluorescence staining of nucleoporins performed on nuclei assembled in the presence of Man1 N-terminal fragment showed an abnormal pattern of NPCs on the surface of the NE (Figure 14). This data is also supported by a study in which specific defects in nucleoporin distribution were associated to deletion of gene encoding for yeast Man1 hortholog Scr1<sup>200,219</sup>.

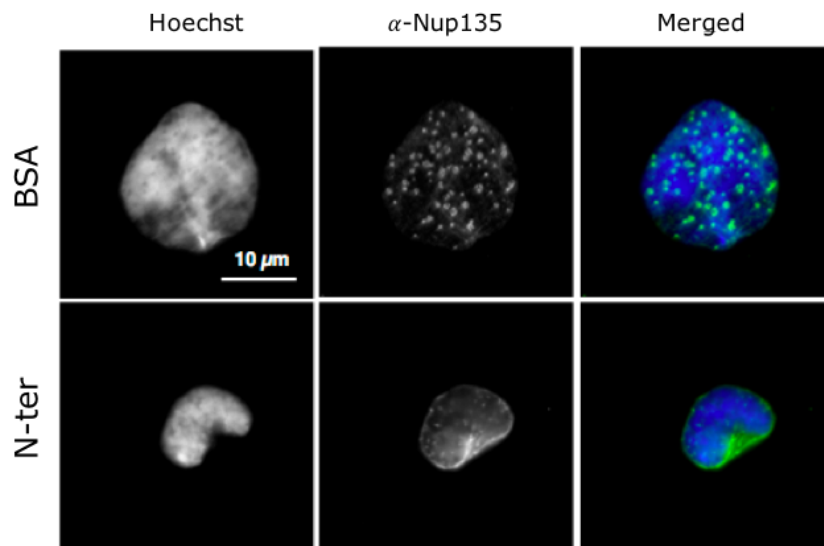


**Figure 14. Nup-153 immunostaining of assembled nuclei.**

Sperm nuclei were assembled for 1 hour in interphase extract in presence of either BSA or N-terminal fragment. Isolated nuclei were attached to glass coverslips and stained with anti-Nup153 mouse primary antibody followed by anti-mouse alexa488-conjugated secondary

*antibody. DNA staining was performed with Hoechst. Images are representative of 3 independent experiments.*

#### 1.6. MAN1 N-TERMINAL DOMAIN INHIBITS DNA REPLICATION AND CAUSES ACCUMULATION OF DNA DAMAGE

Rate and kinetics of DNA replication in *Xenopus* extracts are absolutely dependant on the efficiency of nuclear assembly<sup>220</sup>. The length of S phase, as well as the time of nuclear assembly, vary from extract to extract and can be affected by high concentrations of DNA or dilution of the extract. In a typical replication assay, with DNA concentrations of around 3000 nuclei/ $\mu$ l, *Xenopus* sperm nuclei enter S phase approximately 30 minutes after addition to the extract and complete DNA replication within 1 or 2 hours.

As previously shown, nuclei assembled in the presence of Man1 N-terminal fragment appeared to be deficient for DNA replication, as they failed to incorporate Cy3-dCTP. To better confirm the effect of the two Man1 mutants on DNA replication, sperm nuclei were assembled in presence of [ $\alpha$ -<sup>32</sup>P]-dCTP, with or without the C- and N- terminal fragments of Man1 and the replicated DNA was quantified both by agarose gel electrophoresis followed by autoradiography and by precipitation of nucleic acids followed by scintillation counting.

As shown in Figure 15, nuclei assembled in the presence of Man1 C-terminal domain replicated at levels as high as control nuclei. On the opposite side, the addition of the N-terminal fragment caused a strong decrease in the replication efficiency, with more than a 60 % reduction of [ $\alpha$ -<sup>32</sup>P]-dCTP incorporation after 2 hours compared to the control.

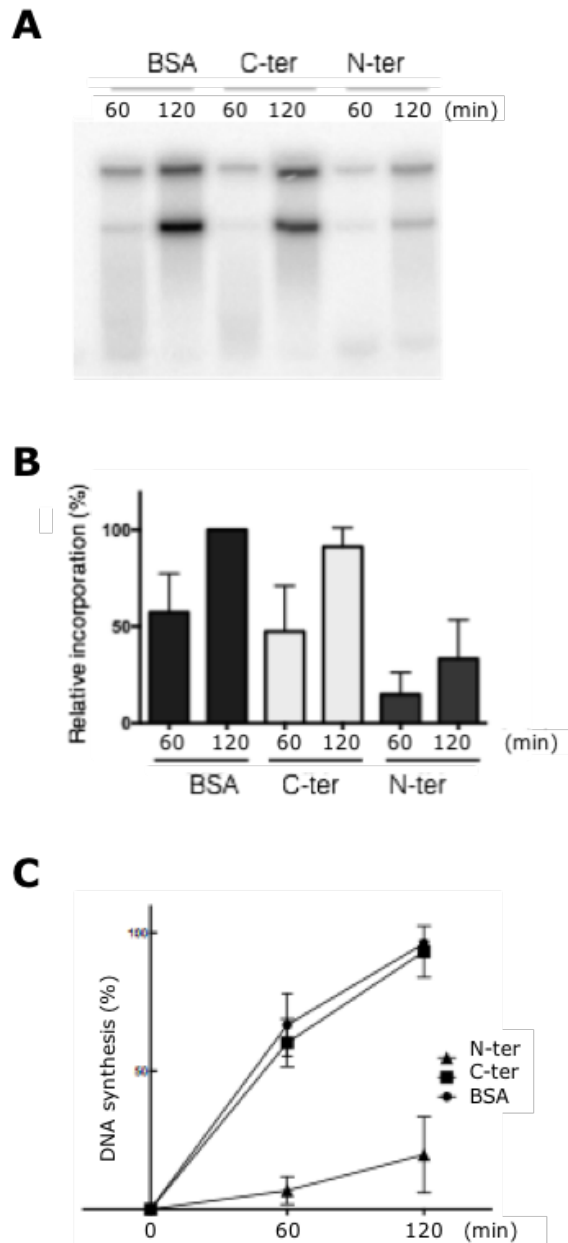


**Figure 15. Effect of Man1 mutants on DNA replication.**

A) Nuclei were assembled for 60 or 120 minutes with BSA, C-terminal or N-terminal domain of Man1, in the presence [ $\alpha$ - $^{32}$ P]-dCTP. Reactions were digested with proteinase K, resolved on agarose gel and the incorporation of radiolabelled dCTP was visualized by autoradiography. B) Signal intensities of 5 independent experiments as in panel A were quantified using ImageJ and relative incorporation rates were expressed as a percentage relative to control sample at 120 minutes. The histogram shows mean values  $\pm$  standard deviation (error bars) of 5 independent experiments. C) For replication efficiency quantification, nucleic acids were precipitated with trichloroacetic acid and the exact amount of newly synthesized DNA was calculated by scintillation counting. Results are the mean of 3 independent experiments. Error bars represent the standard deviation.

Replication dynamics were also monitored through the analysis of nascent DNA elongation by alkaline electrophoresis of replicating chromatin. To do so, replication reactions were constituted in presence of Man1 N-terminal fragment or BSA and the replicating DNA was pulse-labelled with [ $\alpha$ - $^{32}$ P]-dCTP at different time-points and resolved on agarose gel in denaturing conditions. In order to prevent further initiation of replication, 0,5 mM of Cyclin Dependent Kinases (CDK) inhibitor roscovitine<sup>221</sup> was added after 5 minutes from the [ $\alpha$ - $^{32}$ P]-dCTP pulses.

As shown in Figure 16, rates of growth of labelled ssDNA fragments are comparable between control and treated nuclei, indicating that the N-terminal fragment does not inhibit the elongation of newly synthesized DNA. On the other hand, the overall amount of [ $\alpha$ - $^{32}$ P]-dCTP was strongly reduced in N-terminal inhibited nuclei compared to the control, possibly correlating with a lower number of ongoing replication forks.

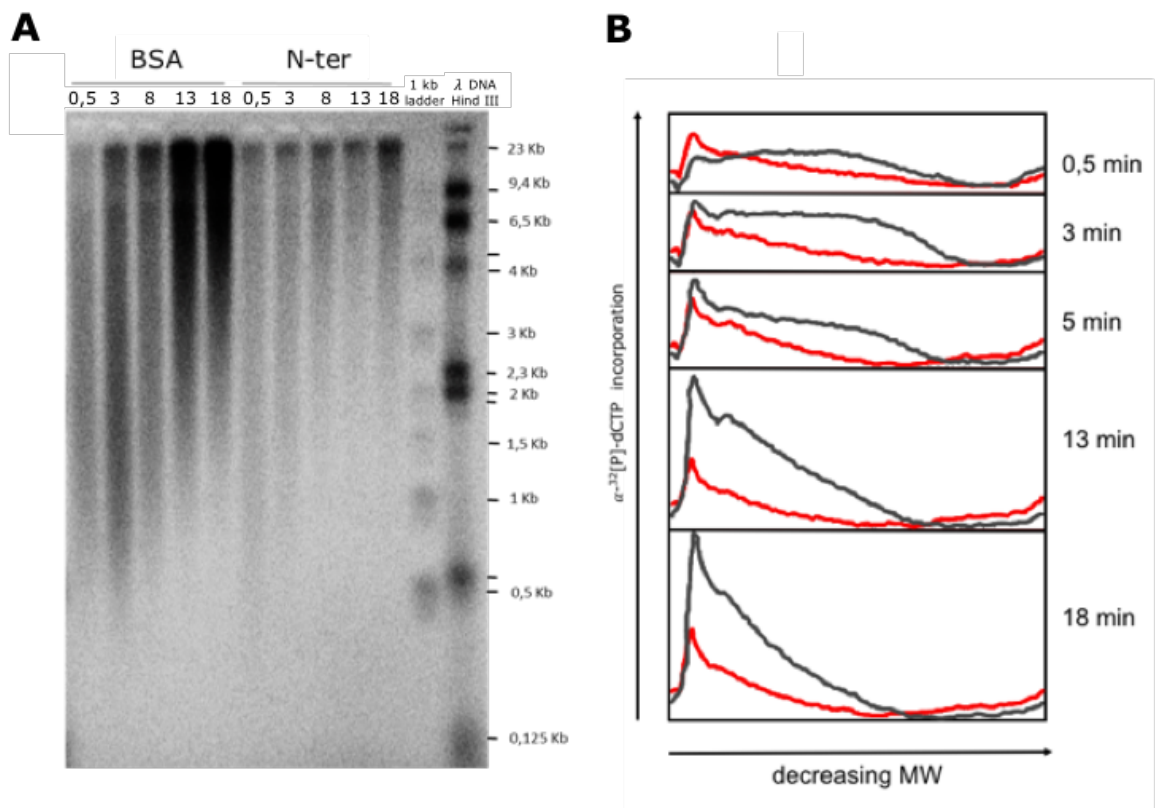


**Figure 16.** Visualization of nascent ssDNA strands by alkaline gel electrophoresis.

A) Sperm nuclei were incubated at 1000 nuclei/ $\mu$  in interphase extract. At 30 minutes, replication reactions were supplemented with [ $\alpha$ - $^{32}$ P]-dCTP plus 0,5 mM roscovitine<sup>221</sup>. At the indicated times, samples were chased with unlabelled dCTP. The DNA was isolated and analysed by alkaline electrophoresis followed by autoradiography. B) The signals were acquired with Typhoon scanner and analysed with ImageJ. The graph shows a comparison between the signals profiles of control (grey) and the N-terminal treated reactions (red).

Given the previous observations about the effect of Man1 N-terminal fragment on nuclear assembly, it was speculated that the lower detected replication rates could be dependent on the chromatin architecture inside the nucleus. In order to test this hypothesis, the ability of N-terminal treated extract to inhibit the replication of a small circular template (M13mp18 ssDNA), which does not require the formation of nuclear structures<sup>222</sup>, was tested. As expected, the replication efficiency of M13 ssDNA in the presence of Man1 N-terminal fragment was similar to the control, in deep contrast to the strong inhibition that occurred when using sperm DNA as template (Figure 17). These results confirmed that the basic replication machineries are not interfered by the presence of Man1 N-terminal domain and that the low chromatin replication efficiency previously observed only relies on an aberrant chromatin architecture.

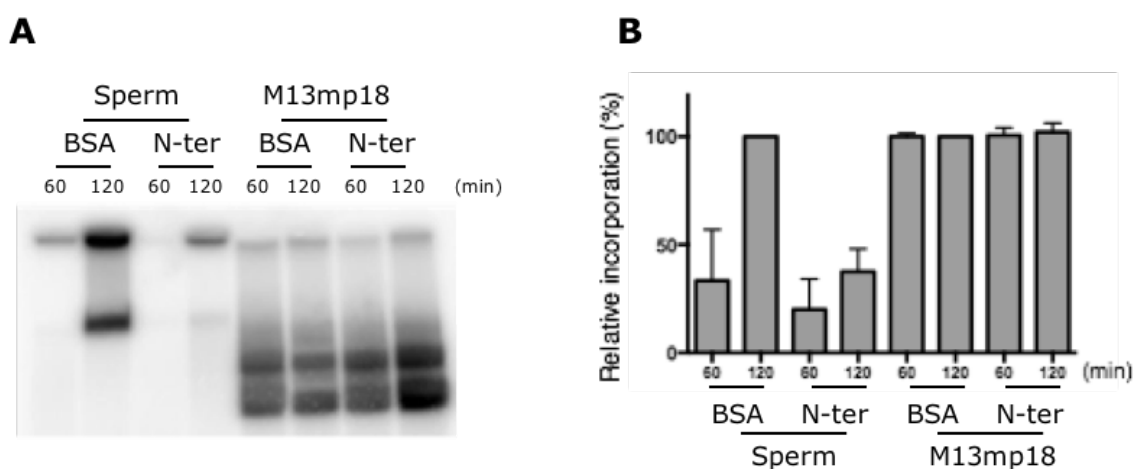


**Figure 17. Effect of Man1 N-terminal fragment on M13ssDNA replication.**

A) *Xenopus* interphase extracts containing BSA or Man1 N-terminal fragment were incubated in presence of [ $\alpha$ - $^{32}$ P]-dCTP and sperm nuclei or an equal amount of M13mp18

*ssDNA. Reactions stopped at 60 or 120 minutes were digested with proteinase K, resolved on agarose gel and visualized by autoradiography. B) Signal intensities were acquired using ImageJ analysis software and relative incorporation rates were calculated considering the signal of sperm control sample at 120 minutes as absolute value. The histogram shows mean values (bar)  $\pm$  standard deviation (error bars) of three independent experiments.*

In order to completely monitor the DNA replication dynamics in nuclei assembled in the presence of Man1 N-terminal fragment, the binding of major DNA replication factors to the chromatin was analysed by chromatin isolation followed by SDS-page and immunoblotting. The result of this analysis (Figure 18) confirmed a general reduction of replication factors involved in the establishment of replication origins, known as the pre-replication complex. This data suggests that addition of Man1 N-terminal fragment at the beginning of nuclear assembly process strongly impairs the formation of the pre-RC, causing a subsequent perturbation of the overall DNA replication mechanism.

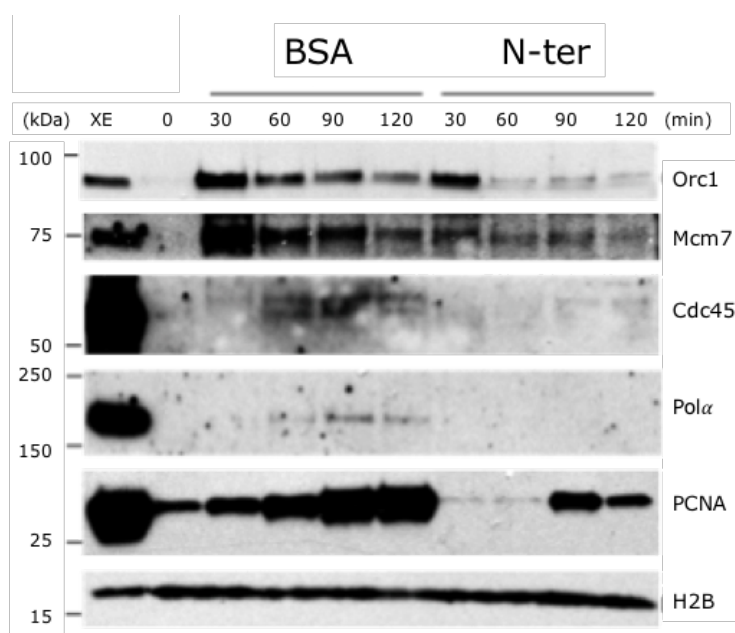


**Figure 18. Chromatin binding of DNA replication factors on nuclei assembled in the presence of Man1 N-terminal fragment.**

*Sperm nuclei were assembled in presence of BSA or Man1 N-terminal fragment and aliquots of the reaction were stopped at different time-points in order to monitor the loading of*

*replication factors on chromatin. Chromatin-bound proteins isolated from replicating nuclei were separated on SDS-PAGE and immunoblotted with antibodies against the indicated replication factors. Lower portion of the filter was blotted with anti-histone H2B antibody as loading control. First lane of the gel shows total Xenopus extract (XE) used as positive control for the antibody detection. The figure shows one representative result among 3 independent experiments.*

Since defects in DNA replication are often associated with generation of lesions and activation of the DNA damage response<sup>223</sup>, replicating nuclei were stained with an antibody raised against phosphorylated histone H2A.X ( $\gamma$ H2A.X), in order to understand if the observed reduction in replication efficiency was also associated with accumulation of DNA damage. In fact, such chromatin modification, conserved in all eukaryotes, occurs after spontaneous DSBs or replication stress-associated lesions, in a mechanism dependent on apical checkpoint kinases ATR and ATM<sup>224,225</sup>.

As expected, the addition of Man1 N-terminal fragment in the replication reaction led to a dramatic increase of  $\gamma$ H2A.X foci on the chromatin, which also appeared to increase over the time (Figure 19). This result indicates that nuclei assembled in the presence of N-terminal fragment accumulate DNA damage during the progression of DNA replication.

It is possible to speculate that the observed accumulation of lesions could be either due to an increase in DSBs generation during DNA replication or to a reduced ability in the repair of breaks that are spontaneously generated during S phase, likely due to defects in recruiting repair factors on the chromatin.

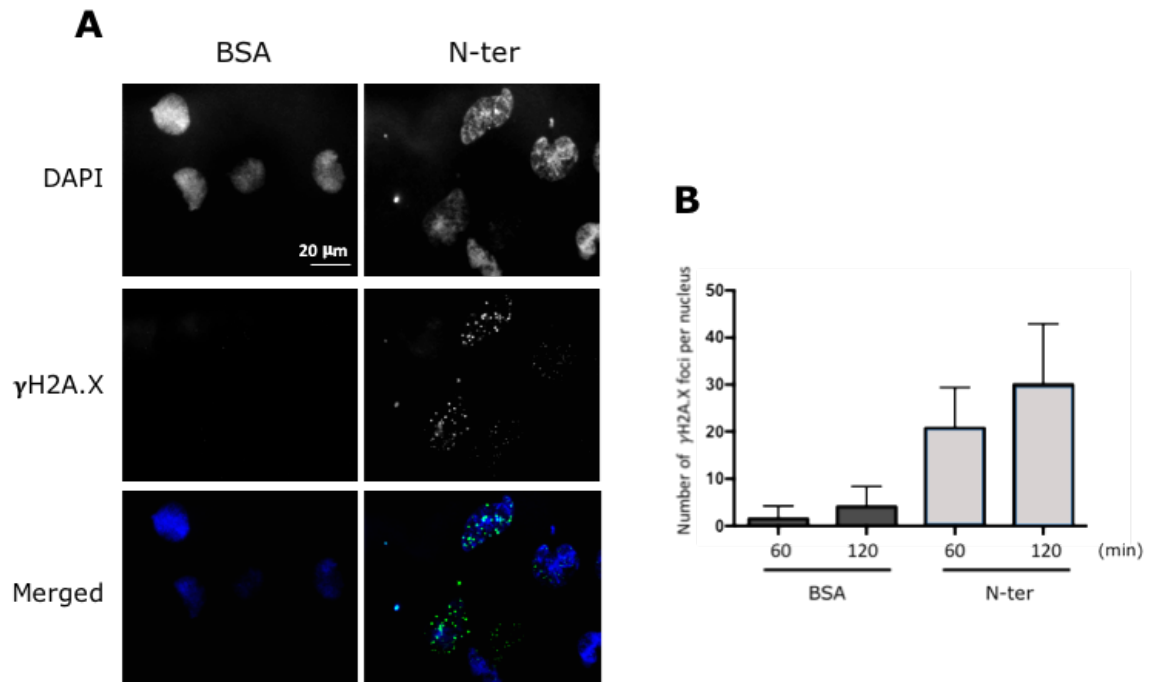


**Figure 19.  $\gamma$ H2A.X immunostaining of replicating nuclei.**

A) Sperm nuclei were assembled for 1 or 2 hours in interphase extract in presence of either BSA or N-terminal fragment. Isolated nuclei were attached to glass coverslips and stained with anti- $\gamma$ H2A.X mouse primary antibody followed by anti-mouse alexa488-conjugated secondary antibody. DNA staining was performed with DAPI. B) The histogram shows the average number of alexa-488 positive foci that was detected in each nucleus. The histogram shows mean values  $\pm$  standard deviation (error bars) of three independent experiments. At least 100 nuclei were counted for each experimental point.

### 1.7. MAN1 N-TERMINAL FRAGMENT ALTERS THE CHROMATIN ORGANIZATION INSIDE THE NUCLEUS

The association of DNA with the nuclear envelope is necessary to maintain the spatial arrangement of the chromatin inside interphase nucleus. Such “high order organization”, typical of eukaryotic organisms, depends on the fact that the chromatin is arranged in radial DNA loops with periodical attachments to the nuclear matrix<sup>226</sup>.

It is possible to reveal this organization using the “maximum fluorescence halo assay”, in which nuclei are extracted with high salt concentration, in order to remove the outer layer of histones and most of the other nuclear and chromatin proteins, and stained with ethidium



bromide, which introduces positive supercoils that relax the DNA loops<sup>227</sup>. These loops can be further visualized at the microscope as a fluorescent halo around the residual nuclear structure, which radius length (Maximum Fluorescence Halo Radius, MFHR) directly correlates with the loop size. The measurement of loop sizes in control nuclei and nuclei assembled in presence of the Man1 N-terminal fragment, revealed a substantial difference in chromatin organization between the two conditions (Figure 20A). In fact, while control nuclei showed a typical symmetric distribution of MFHR values, nuclei assembled in the presence of Man1 N-terminal fragment showed a more random one. Moreover, measuring the minimum and the maximum halo radius lengths for each nucleus, a significant difference between these values was observed in N-terminal treated nuclei respect to the control, meaning that in those nuclei there was a more variable distribution of loop sizes (Figure 20B).

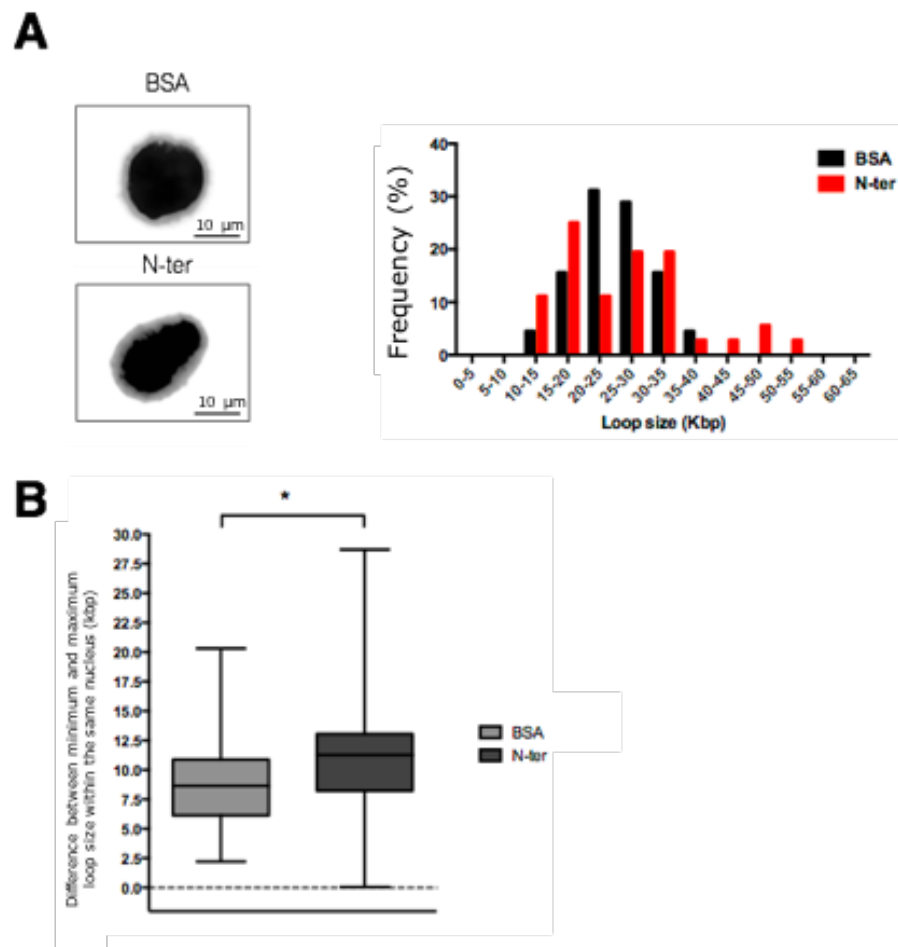


**Figure 20. High order chromatin organization in nuclei assembled in presence of Man1 N-terminal fragment.**

*A) Isolated nuclei were recovered on coverslips and processed with the Maximum Fluorescence Halo Radius technique. Histograms show distribution of individual loop size measurements. Image shows one representative experiment. B) Difference between the minimum and maximum loop size measurement for each single nucleus. The box plot represents first and third quartiles separated by the median (central horizontal line) ± maximum and minimum values (error bars) of 2 independent experiments. For each sample, at least 200 halos were counted.*

## 1.8. MAN1 N-TERMINAL FRAGMENT ALTERS CELL CYCLE PROGRESSION BY INHIBITING THE EXIT FROM MITOSIS

Since LEM-D proteins are also involved in the control of cell cycle progression<sup>172,173</sup>, Man1 truncation mutants were added to CSF-arrested *Xenopus* extract, which allows to follow both the exit of nuclei from mitosis and the subsequent progression into interphase<sup>214</sup>. Such extracts are naturally synchronized in metaphase and can be driven into interphase by addition of free Ca<sup>++</sup>, which mimics egg fertilization.

As showed in Figure 21, incubation of sperm DNA with Man1 N-terminal fragment in CSF extract completely inhibited nuclear formation after extract activation (middle panel), while control reaction showed efficient formation of interphase nuclei (top panel). In fact, sperm nuclei failed to fully decondense the chromatin and to assemble enclosed nuclear envelopes when assembled in the presence of Man1 N-terminal fragment. Remarkably, 2 hours after extract activation, they still shown shapes typical of mitotic chromosomes. The same phenotype was observed when recombinant LEM domain fragment alone was added instead of the full N-terminus.

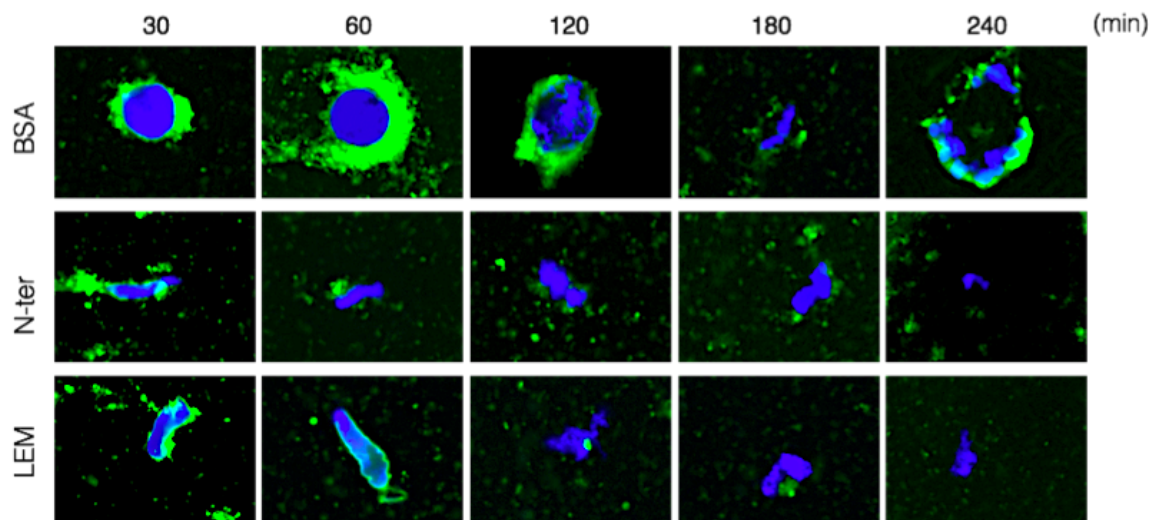


**Figure 21. Effect of Man1 N-terminal recombinant fragment and LEM domain on nuclear reformation after mitosis.**

Demembranated sperm nuclei were incubated for 20 minutes in CSF extract together with BSA (top), N-terminal fragment (middle) or LEM domain (bottom) and then driven into interphase by activation with  $\text{CaCl}_2$  ( $t=0'$ ). Samples were fixed on coverslips and analysed by fluorescence microscopy. Pictures represent merged signals acquired with blue filter (Hoechst) and green filter (DHCC). Image shows one representative result out of 3 independent experiments.

In order to have a wider view on the role of Man1 during cell cycle, the effect of N-terminal fragment was also tested using *Xenopus* “cycling” extract. This kind of extracts have the ability to perform multiple rounds of DNA replication in a short range of time, allowing to monitor all the phases of the cell cycle progression<sup>214</sup>.

Since the efficiency of this particular extracts is very sensitive to any kind of stress, such as extract dilution, it was chosen to test first the effect of recombinant LEM domain, which was more stable and less difficult to produce in more concentrated stock solution. The effect of the entire N-terminal fragment still remains to be tested.

Hence, recombinant LEM domain was added to cycling extract at interphase, together with sperm DNA, Cy3-dCTP and 488-tubulin, in order to visualize mitotic spindles. Aliquots from the reactions were sampled at short intervals and monitored by fluorescence microscopy. As shown in Figure 22, while control nuclei were able to perform multiple

cycles, nuclei assembled in the presence of recombinant LEM domain failed to progress through the first mitosis and arrested at metaphase.

The cell cycle progression of extracts containing Man1 LEM domain was also assessed by immunoblotting of the mitotic-specific protein Cyclin B2 which disruption and synthesis mark, respectively, exit and entry into mitosis. As shown in Figure 23, at time-points in which control sample displayed complete degradation of Cyclin B2, corresponding to efficient exit from mitosis, extracts containing recombinant LEM domain showed only partial degradation followed by accumulation of Cyclin B2 over the time, possibly correlating a persistence of the nuclei in a mitotic-arrested state.

All the observed defects in cell cycle progression could be explained by several mechanisms, not mutually exclusive respect to each other. On one hand, it is possible to think that the phenotype observed in CSF-arrested extracts was due to an inability of reforming the nuclear envelope after mitosis. This hypothesis is supported by a published study in which a delay in NE reformation after mitosis was observed after silencing of Man1 gene in mammalian cells<sup>228</sup>. On the other hand, results obtained using cycling extracts suggest that interference with Man1 could also affect other pathways that occur prior to mitotic exit and that can cause arrest into mitosis. Such hypothesis is also supported by a study in which ablation of Man1 function was found to be associated with blocked cytokinesis and accumulation of anaphase-bridged chromatin in *C. elegans*<sup>186</sup>.

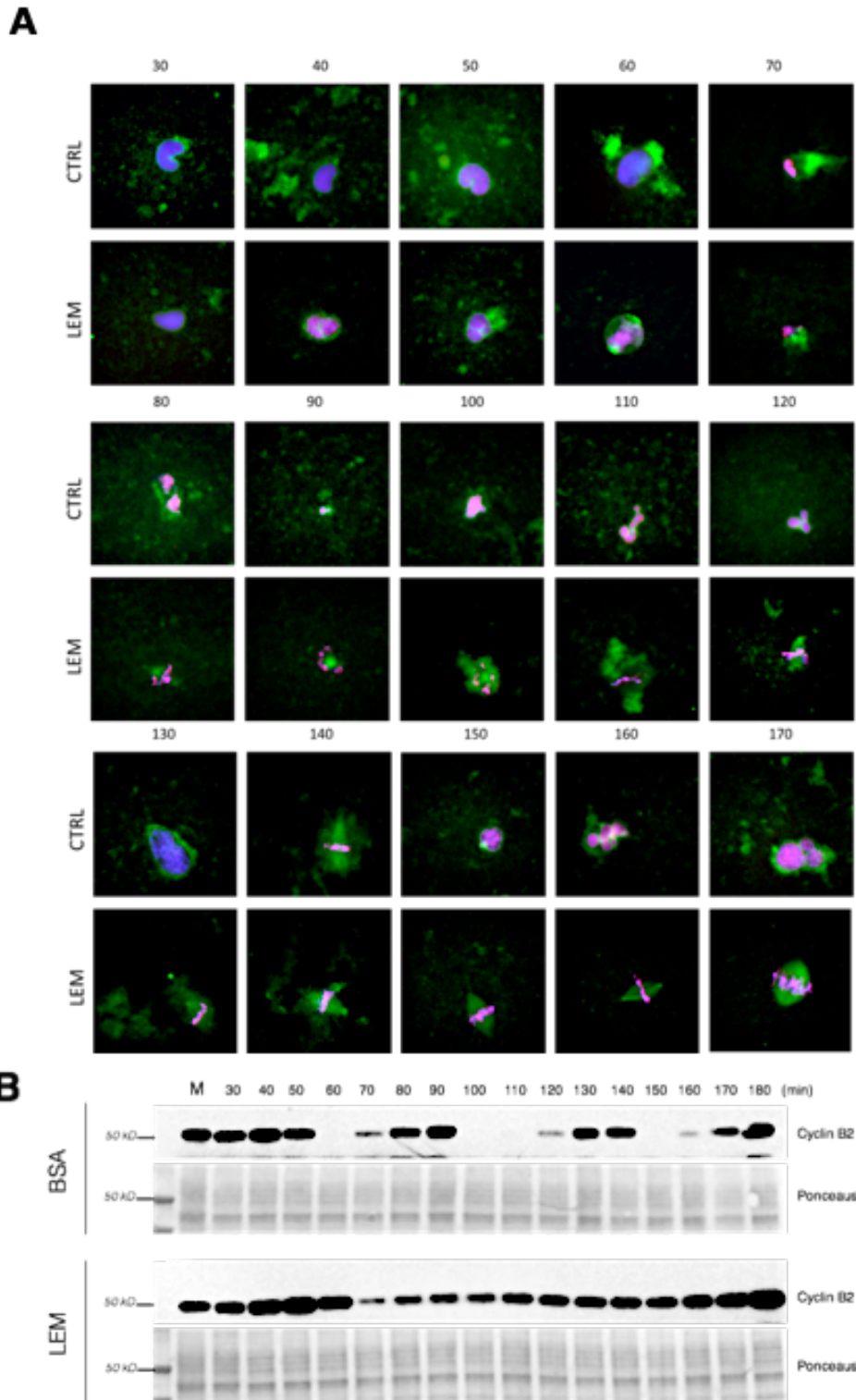


**Figure 22. Effect of recombinant LEM domain on cell cycle progression.**

Demembranated sperm nuclei were incubated in freshly prepared cycling extracts supplemented either with BSA or LEM domain, in the presence of Cy3-dCTP and 488-tubulin. The figure shows one representative result out of 3 independent experiments. A) A fraction of the samples was fixed on coverslips and observed by fluorescence microscopy. Pictures represent merged signals acquired with blue (Hoechst), green (DHCC and 488-

*tubulin) and red (Cy3-dCTP) filters. B) The other fraction of the samples was mixed with Laemmli loading buffer and processed for SDS-page and Western Blotting with antibody against Cyclin B2.*

## 2. CHARACTERIZATION OF MAN1 IN MOUSE EMBRYONIC STEM CELLS

To extend the characterization of Man1 function in mammalian cells, knockout of MAN1 gene was performed in mouse Embryonic Stem Cells (mESCs). One of the main reasons behind the choice of this particular model system is that embryonic stem cells behave in a similar way to the *Xenopus* cell-free extract, as both system recapitulate the cellular mechanisms that occur during the first zygotic divisions.

mESCs are stem cells derived from the inner mass of the mouse embryo that can be maintained in culture in an undifferentiated state in the presence of Leukaemia Inhibitory Factor (LIF), a differentiation-inhibiting cytokine. An important feature of these cells is their peculiar cell cycle organization which provide them a high proliferative capacity. In fact, mESCs spend most of their time in S phase, thanks to the fact that their G1 phase is strikingly shorter compared to differentiated cells<sup>229,230</sup>. This feature is shared by the *Xenopus* cell-free extract, which can sustain rapid and multiple cycles of transition between S phase and mitosis<sup>231</sup>.

Moreover, ESCs have the distinctive property to be pluripotent, meaning that they have the ability to differentiate into all somatic cell types found in the adult organism. Therefore, their pluripotency and their ability to replicate indefinitely renders them a very powerful tool for research. Interestingly, few years ago it was discovered that differentiated mammalian cells incubated in *Xenopus* extract are efficiently reprogrammed into an embryonic state and reactivate expression of pluripotency genes<sup>232</sup>, underlining the similarity between *Xenopus* oocyte extract and embryonic stem cells.

### 2.1. GENERATION OF STABLE MAN1-KNOCKOUT CELL LINES

The disruption of Man1 gene was achieved using CRISPR-Cas9 system, a genome editing tool<sup>233</sup> that takes advantage of the RNA-guided bacterial endonuclease Cas9 which can cleave double stranded DNA in a site-specific manner, leading to the disruption of the locus

of interest. In order to target Man1, three guide RNAs (gRNAs) were designed, directed to the 1<sup>st</sup> and the 9<sup>th</sup> exon of the mouse gene.

A first attempt to generate Man1-KO cells was made using ESCs derived from Cas9 knock-in mice (Rosa26-Cas9 knockin). The three guides were used both for single transfections and used in combination, in order to determine the most efficient way to delete the gene. As shown in Figure 23, single gRNAs were not sufficient to downregulate Man1 gene in a significant way, while the combination of the three guides was able to cause a decrease in Man1 expression of about 50%, as revealed by Reverse Transcriptase quantitative PCR (RT-qPCR). This result was also confirmed by western blot analysis (Figure 24).

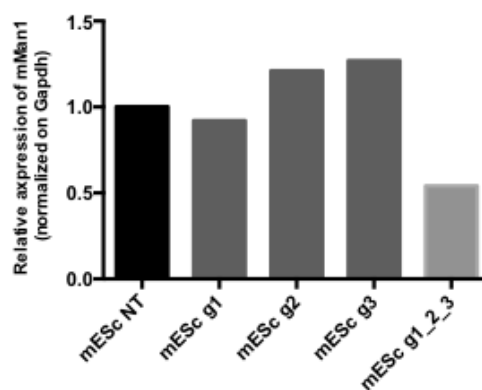


**Figure 23. Expression levels of Man1 in D1 Man1-Knockout mESCs.** The image shows the levels of expression of mouse Man1 (mMan1) in control (not transfected, NT) and cells transfected with different combinations of gRNAs against Man1. Total mRNA was extracted from control and transfected cells and analyzed by RT-qPCR. The histogram shows the relative expression levels of Man1 normalized to GAPDH levels.



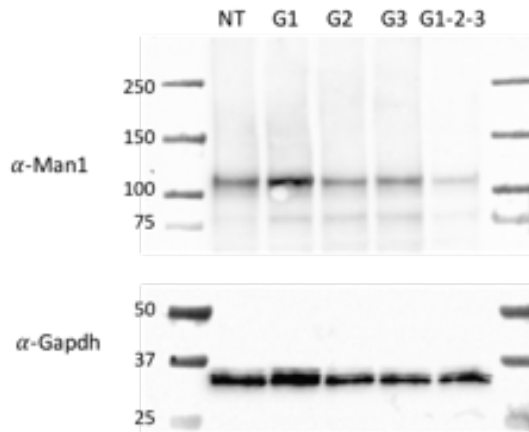


**Figure 24. Western blot analysis of D1 Man1-KO cells.**

*The western blot analysis was performed on total cell lysates (30 µg of lysate was loaded for each lane). GAPDH levels are shown as loading control.*

However, since it has been shown that constitutive expression of Cas9 can increase the number of off-target mutations<sup>234</sup>, it was chosen to perform the transfection of the three gRNAs together with Cas9 gene transient transfection in mESCs..

In order to obtain homogeneous clones, E14 mESCs were first transfected with a Cas9 expressing construct carrying a puromycin resistance. Cells were then transfected at a single-cell state with the combination of the three gRNAs. After that, puromycin selection was removed.

Isolated colonies were screened by PCR (Figure 25). Three positive clones were selected and the absence of the proteic product of the deleted gene was assessed by western blot analysis (Figure 26).

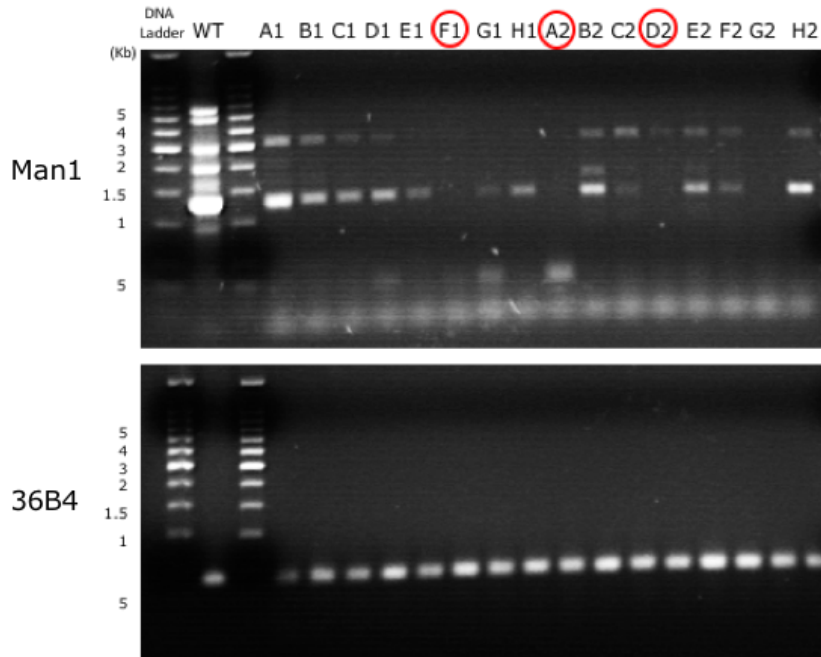


**Figure 25. PCR screening for E14 *Man1*-KO positive clones.** After CRISPR transfection, colonies were isolated and expanded. For each colony, a sample of genomic DNA was extracted and amplified by PCR with *mMan1* specific primers to check the deletion of the gene (top panel). As control, primers specific for an unrelated housekeeping gene (36B4) were also used in parallel (bottom panel).

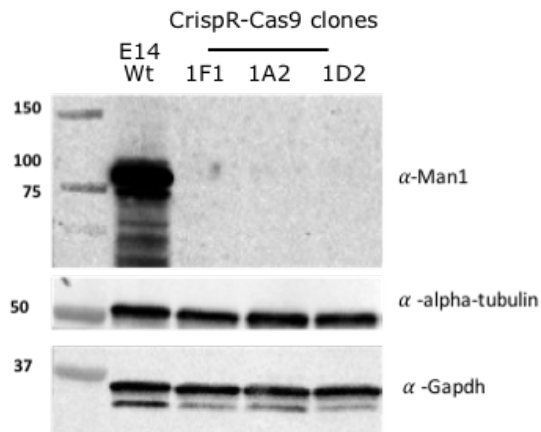


**Figure 26. Western blot analysis of E14 *Man1*-KO clones.**

Western blot analysis of *mMan1* of clones 1F1, 1A2 and 1D2 was performed on total cell lysates (30  $\mu$ g of lysate was loaded for each lane). Wild type *mESCs* with the same genetic background (E14 wt) were used as control. GAPDH and alpha-tubulin were used as loading control.

## 2.2. MAN1-KNOCKOUT MESCS DISPLAY FEATURES OF DIFFERENTIATING CELLS

mESCs colony appearance is explanatory of their health status. Typical mESC colonies are characterized by smooth and translucent borders and a compact and three-dimensional round shape, as sign of fast growth rate and undifferentiated status<sup>235</sup>. In contrast to this standard, colonies derived by Man1-KO clones appeared flat and with uneven and sharp borders, which are common features of differentiation (Figure 27). Moreover, all the three clones showed slower growth rates compared to the wild type cells (data not shown), another characteristic typical of differentiating cells.

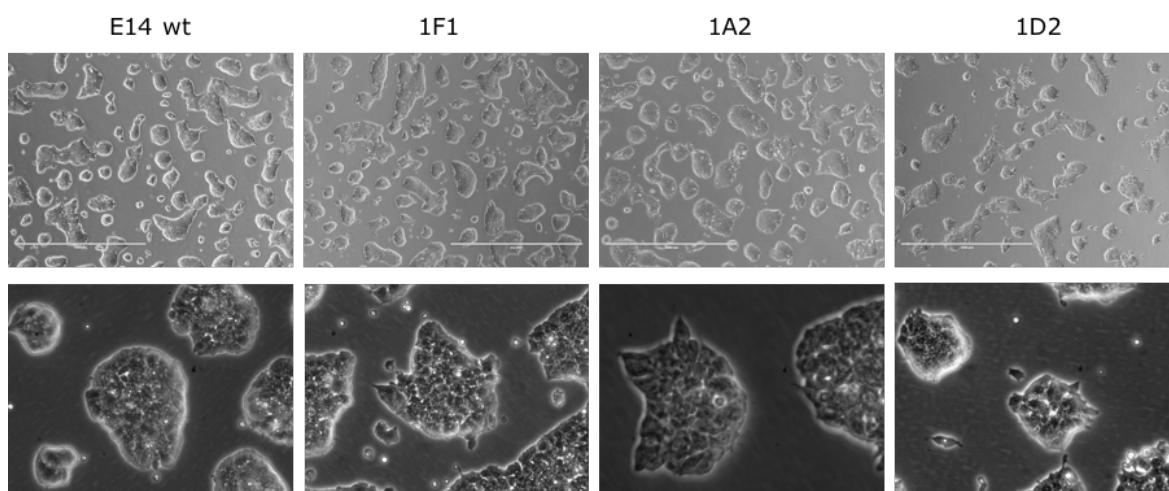


**Figure 27. Phase-contrast microscopic analysis of E14 Man1-KO colonies morphology.** Cells were cultured on gelatin-coated plates to reach 50% confluency. Images were taken at the inverted microscope with two different magnifications, 4x (top) and 20x (bottom).

To confirm that Man1 KO cells have a defect in the maintenance of stem cells status, colonies were subjected to Alkaline Phosphatase (AP) staining, a common marker of undifferentiated ESCs. As shown in Figure 28, wild type colonies appeared round and uniformly stained. On the opposite side, Man1-KO clones showed several cells emerging from the colonies with variable loss of staining, which likely represented differentiating cells.

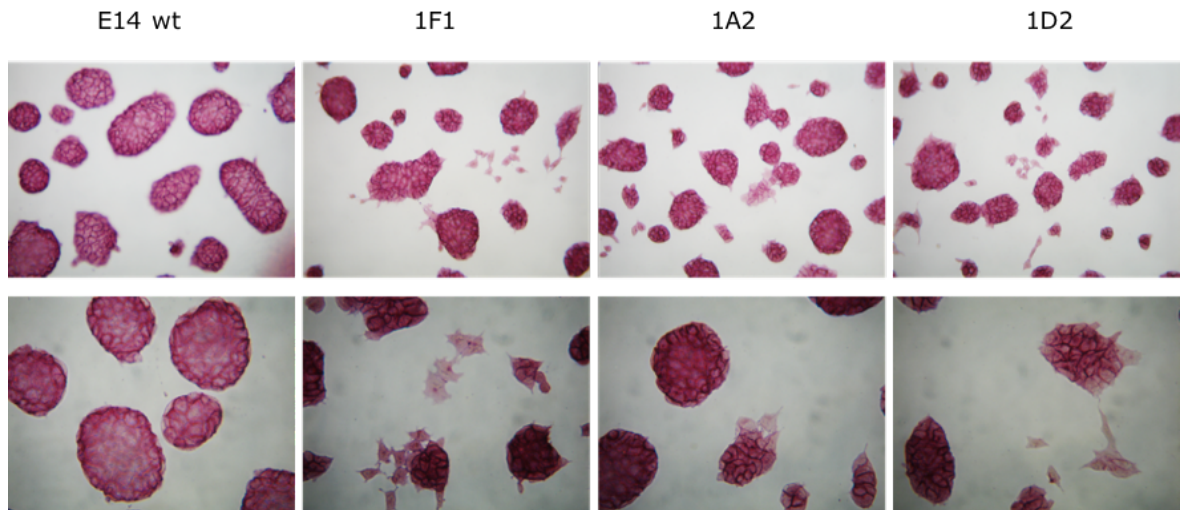


**Figure 28. Alkaline Phosphatase staining of E14 *Man1* KO colonies.**

*Cells were cultured on gelatin-coated 6-well plates until 50% confluency. Colonies were then fixed and stained for AP.*

The phenotype of *Man1*-KO mESCs was further confirmed by measuring the expression of common pluripotency markers by RT-qPCR. As shown in Figure 29, all the three clones showed a downregulation of genes involved in stem cell pluripotency and self-renewal as *Sox2*, *Oct4*, *Nanog* and *Rex1*.

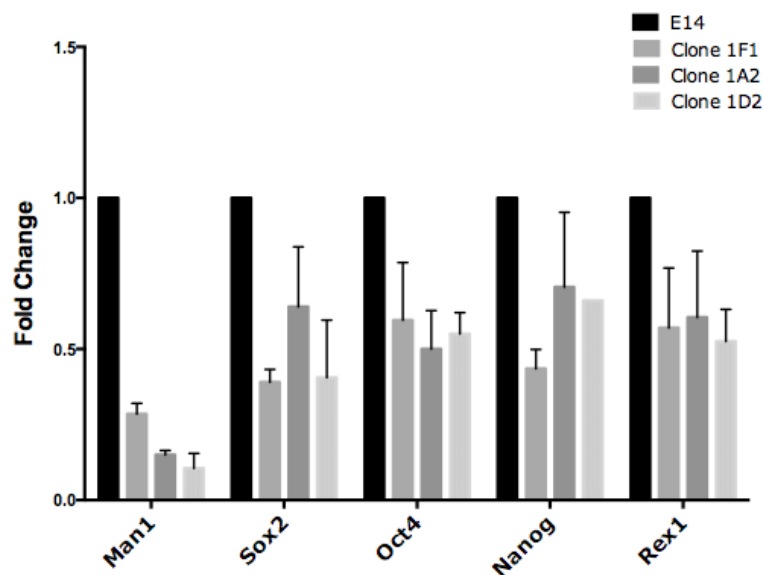


**Figure 29. Expression of common stem cell markers in E14 *Man1*-KO clones.**

*Total mRNA was extracted from wild type and *Man1*-KO clones and analysed by RT-qPCR. The expression fold change of the analysed genes is expressed as double delta Ct ( $\Delta\Delta Ct$ )*

calculated considering *GAPDH* as housekeeping gene. The histogram shows mean values  $\pm$  standard deviation (error bars) of two independent experiments.

To extend the characterization of Man1-KO clones, ES cells were tested for the *in vitro* differentiation capacity. To do that, dissociated cells were cultured in suspension in a medium lacking LIF and other anti-differentiation factors. In these conditions, mESCs spontaneously aggregated into spherical Embryoid Bodies (EB), which are structures that recapitulate the early stages of embryonal cells differentiation into the three germ lineages (endoderm ectoderm and mesoderm). The EBs were then attached to a gelatin-coated surface to induce further differentiation into various cell types.

As shown in Figure 30, Man1-KO clones did not show any evident defect in EB formation or differentiation, suggesting that even if Man1 downregulation seems to affect self-renewal of ESC promoting differentiation, it does not seem to interfere with their pluripotency features.

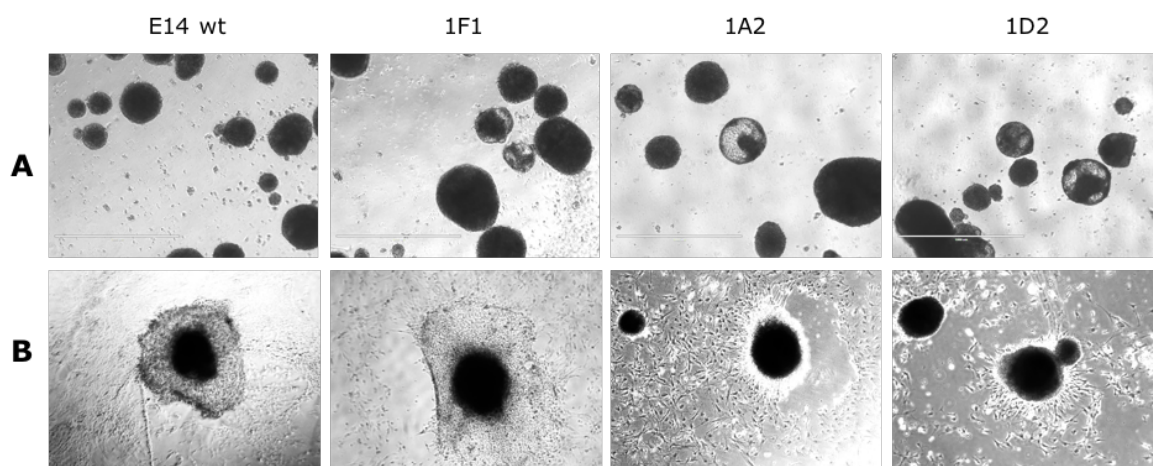


**Figure 30. Embryoid Bodies formation.**

*Phase contrast microscopy micrographs at day 6 (A) of EB cultured in suspension and subsequently attached to a gelatin-coated surface at day 9 (B).*

Furthermore, other preliminary results obtained so far show that Man1-KO mESCs have an altered proliferation rate (data not shown) and a tendency to differentiate, but have the capability to form EBs. These results may be explained by the described role of Man1 in downregulating the BMP4 pathway. In fact, as already mentioned, Man1 takes part to the

signal transduction pathway of BMP4 cytokine by inhibiting the action of its mediator factors, Smads<sup>150,185,197</sup>. A possible link between Man1 and the BMP4/Smads pathway will be discussed in the next section.

### 2.3. MAN1-KNOCKOUT MESCS SHOW AN ALTERATION OF PERICENTROMERIC AND TELOMERIC RNA EXPRESSION

Finally, some preliminary data obtained from gene expression analysis by RT-qPCR indicate that Man1-KO cells have a deregulated expression of pericentromeric and telomeric non-coding transcripts (Figure 31). In particular, Man1-KO cells showed a downregulation of pericentromeric satellite-repeat transcript while, on the other side, an increase in the expression of telomeric repeat-containing RNA TERRA. Since both of these elements are known to be located in heterochromatic loci<sup>236,237</sup>, the observed alteration in the transcriptional status could be due to an alteration of chromatin organization at those specific regions.

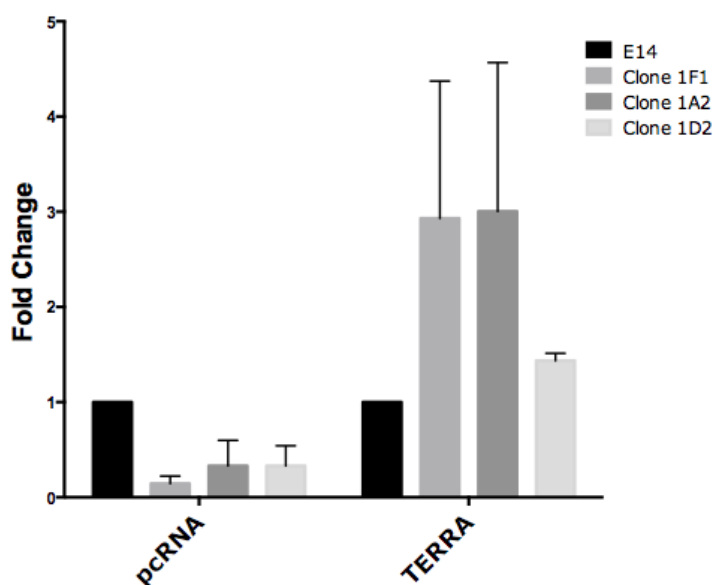


**Figure 31. Expression of pericentromeric and telomeric transcripts.**

Total mRNA was extracted from wild type and Man1-KO clones and analysed by RT-qPCR using primer pairs corresponding to pericentromeric satellite-repeats transcript (pcRNA) and telomeric repeat-containing RNA (TERRA). The expression fold change of pcRNA and

*TERRA is expressed as double delta Ct ( $\Delta\Delta Ct$ ) calculated considering Gapdh as housekeeping transcript. The histogram shows mean values  $\pm$  standard deviation (error bars) of two independent experiments.*

## DISCUSSION

Man1 is an integral nuclear membrane protein involved in the spatial organization of the chromatin inside the nucleus. *Xenopus* cell-free extracts supplemented with a fragment of Man1 corresponding to its entire N-terminal region fail to assemble normal nuclei, with evident defects in nuclear envelope expansion, NPCs assembly, chromatin decondensation, nuclear growth and DNA replication. Man1 N-terminal fragment contains a domain responsible for the tethering to chromatin through the chromatin remodelling factor BAF (known as LEM domain<sup>172</sup>), but it lacks the transmembrane regions, which are necessary for Man1 anchoring to the nuclear envelope. For this reason, it is hypothesized that an excess of recombinant Man1 N-terminal fragment during the nuclear assembly reaction may interfere with the binding of the endogenous protein to the chromatin and, therefore, with the physical attachment of the DNA to the nuclear envelope (Figure 32).

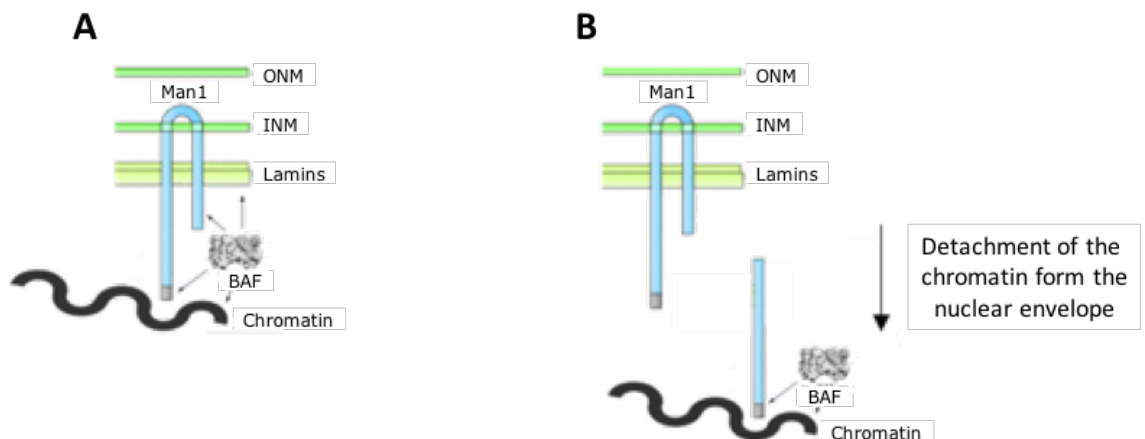


**Figure 32. Schematic representation of the proposed mechanism of action of *Xenopus* Man1 N-terminal fragment.**

A) In normal conditions, Man1 anchors the chromatin to the nuclear envelope, through the interaction with BAF. B) In the presence of an excessive concentration of the N-terminal fragment, the latter could saturate the binding sites of endogenous Man1 to BAF and the chromatin, causing a physical detachment of the DNA from the nuclear envelope. (Image adapted from Segura-Totten et al.<sup>174</sup>).



Addition of Man1 N-terminal fragment to *Xenopus* interphase extract leads to a delay in nuclear growth and interferes with the assembly of nuclear envelope. The same effect was reproduced by adding to the extract the recombinant LEM domain alone, which, is essential to bind the chromatin remodelling factor BAF and BAF-DNA complexes<sup>188</sup>. These experiments suggested that the physical interaction between Man1, BAF and the DNA is required to regulate the assembly of functional nuclei. This hypothesis is consistent with a previous study in which it has been demonstrated that misregulation of BAF concentration can alter membrane recruitment and chromatin decondensation during nuclear assembly in *X. laevis* egg extract<sup>190</sup>.

Addition of Man1 N-terminal domain into *Xenopus* extracts seemed to interfere also with the assembly of nuclear pore complexes. In fact, nuclei assembled in the presence of Man1 N-terminal fragment show defects in NPCs assembly and distribution along the nuclear envelope. This result is in concordance with published data that linked LEM-D proteins to the early steps of nuclear pore assembly regulation. Data obtained with Man1 *S. cerevisiae* orthologs Src1/Heh1 and Heh2 addressed for them a role in NPC assembly surveillance<sup>200,219</sup>. In particular, it has been proposed that such LEM-D proteins may be required to recruit factors of the endosomal sorting complex ESCRT to defective NPCs in order to remove them from the nuclear envelope. For these reasons, it is possible to speculate that an impairment in Man1 function could promote the accumulation of malformed NPC intermediates, lowering the overall distribution of complete and functioning NPCs. Consequently, the observed impairment in chromatin decondensation and nuclear growth can be addressed to the mislocalization of nuclear pores, since it has already been demonstrated that several NPC components can influence chromatin architecture inside the nucleus<sup>127,238</sup>. Accordingly, nuclei assembled in the presence of Man1 N-terminal fragment show an abnormal pattern of chromatin organization, as revealed by measurement of chromatin loops size distribution by Halo assay.

Man1 function impairment also seems to have an impact on DNA replication, consistently with the notion that efficient and complete nuclear envelope assembly is essential for the initiation of replication in *Xenopus* extracts<sup>239</sup>. In fact, the data reported in this study show that the presence of Man1 N-terminal fragment causes a dramatic inhibition of DNA replication in a nuclear-assembly dependent manner, correlating with a failure in pre-Replication Complex assembly onto the chromatin. This result is consistent with numerous evidences that link other factors of the nuclear lamina to DNA replication regulation. For example, it has been shown that nuclei assembled in the absence of lamins fail to replicate their DNA<sup>121,122</sup> and the expression of lamin mutants, that cause a reorganization of the endogenous lamin network, inhibits DNA replication<sup>123,124</sup>. Moreover, it has been shown that *Xenopus* extracts supplemented with a portion of LEM-D protein Lap2 $\beta$  containing the chromatin-binding domain fail to replicate the DNA<sup>125</sup> and that ectopic expression of recombinant Lap2 $\beta$  polypeptides deprived of the transmembrane region inhibits the progression into S-phase of mammalian cells<sup>126</sup>. To test whether the decrease in replication efficiency was associated to increase of DNA damage, nuclei assembled in the presence of Man1 N-terminal fragment were subjected to immunofluorescence analysis, monitoring the expression of  $\gamma$ H2A.X, a known DNA damage marker<sup>224</sup>. The result of this analysis showed that *Xenopus* nuclei assembled in presence of Man1 N-terminal fragment showed an accumulation of  $\gamma$ H2A.X foci, indicating either an increase of DNA lesions during the replication process or an inefficient DNA damage repair. The first hypothesis is supported by the observation that inhibition of DNA replication initiation can result in DNA damage that bypasses the intra S-phase checkpoint<sup>240</sup>, while, the second hypothesis is consistent with the observation that disruption of nuclear lamina architecture in progeria cells leads to a defective recruitment of repair proteins onto the chromatin, resulting in accumulation of persistent  $\gamma$ H2A.X foci inside the nucleus<sup>241</sup>.

At this point, to further assess the potential role of Man1 in cell cycle progression, the N-terminal fragment was added, together with demembrated sperm DNA, to *Xenopus* cycling extracts.

From this experiment it was shown that nuclei assembled in the presence of the recombinant LEM fragment of Man1 fail to progress into mitosis and arrest at the metaphase stage while control nuclei performed several cell cycles. Taken together, all this data support the idea that the dramatic inhibition of DNA replication that was previously described may lead to the entry into mitosis with under-replicated DNA, ultimately causing a block in mitotic progression. In fact, it has been proposed that the separation of intertwined chromosomes that arise after unfinished replication or unresolved DNA repair generates an increasing mechanical tension, which can induce the activation of mitotic checkpoint and a prolonged metaphase arrest<sup>242</sup>.

Moreover, using *Xenopus* mitotic extracts, it was shown that Man1 N-terminal fragment inhibits the nuclear envelope reassembly after mitosis. In fact, it was shown that addition of N-terminal fragment to mitotic extract before activation with calcium, impaired the nuclear reassembly, with subsequent degradation of the partially reformed nuclear envelope and return of the nuclei to a mitotic-like state. One possible explanation of this phenomenon could be that the presence of the Man1 N-terminal fragment causes a residual activation of the Spindle Assembly Checkpoint (SAC), which results in inefficient degradation of mitotic cyclins and reversion of mitotic exit<sup>243</sup>. Otherwise, it is possible to hypothesize that the N-terminal fragment inhibits the reformation of nuclear envelope in a similar way to what has been observed using interphase extracts, while, independently, residual levels of mitotic cyclins promote the reversion into mitosis.

The investigation of the role of Man1 using the *Xenopus* cell-free extract system shows that inhibition of Man1 function by its own N-terminal fragment has a pleiotropic effect, since it influences different nuclear dynamics which normally rely on the proper spatial arrangement of the chromatin inside the nucleus. The data presented here show that nuclear membrane

tethering of chromatin mediated by Man1 is important for nuclear envelope assembly as well as for DNA replication dynamics and faithful progression of the cell cycle (Figure 33).

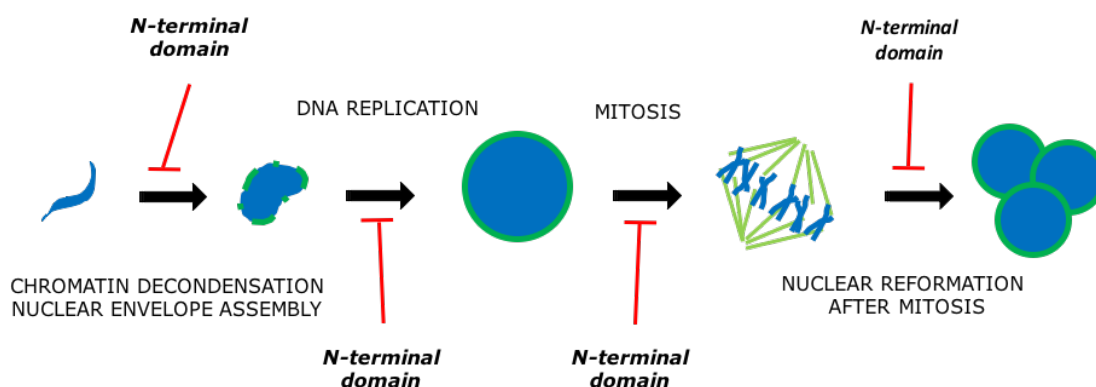


**Figure 33. Schematic representation of the role of Man1 in *Xenopus* nuclear assembly, DNA replication and mitosis.**

*The function of Man1 is required to regulate different cellular processes that rely on the physical organization of the chromatin inside the nucleus, such as nuclear assembly, chromatin decondensation, DNA replication, chromosome segregation and nuclear reformation after mitosis. See text for details.*

In order to extend the observations obtained in *Xenopus* to a mammalian system, knockout of mouse Man1 gene was performed in mESCs by CRISPR-Cas9. Preliminary data obtained with this system show that Man1-knockout cells have typical features of differentiating cells, indicating a decrease in stem cell self-renewal potential. As anticipated in the previous section, this phenotype can be addressed to the already described role of Man1 in antagonizing BMP4 pathway<sup>150,185</sup>. Interestingly, it has recently been shown that BMP4 collaborate with LIF in controlling the fate of ESCs. In fact, it has been found that these two factors are important for the suppression of, respectively, neural and mesodermal/endodermal differentiation and therefore, a perfect balance between these two signalling pathways is critical for the maintenance of ESCs pluripotency state<sup>244-246</sup>. For this reason, it can be speculated that loss of Man1 would cause an upregulation of BMP4 pathway and a subsequent perturbation of LIF-BMP equilibrium, which would result in a loss of stability of ES self-renewal state.

On the other side, no evident defects in nuclear shape and cell viability were observed in Man1 KO cells, indicating that loss of Man1 has no dramatic impact on the overall nuclear organization. However, preliminary RT-PCR data show that loss of Man1 could causes an alteration in the expression levels of pericentromeric and telomeric transcripts. This result suggests that Man1 could be important for the chromatin organization of particular regions, as centromeres and telomeres. Given the repetitive nature of the DNA sequences composing these particular regions, it is possible to speculate that Man1 could be necessary to prevent aberrant recombination at the level of these loci, which would result in chromatin disorganization and genomic instability. This hypothesis is consistent with the role of Man1 *S. cerevisiae* ortholog Src1 and its *C. elegans* paralog Lem2 in the stability of telomeres, centromeres and rDNA<sup>180,181,247</sup>.

Given the impact of centromeres, telomeres and rDNA instability in detrimental clinical conditions such as aging and cancer<sup>28,30,248</sup>, it could be of great interest to investigate the potential role of Man1 in the maintenance of genomic stability at the level of these, and possible other, particularly unstable genomic regions.

## REFERENCES

- 1 Embley, T. M. & Williams, T. A. *Evolution: Steps on the road to eukaryotes. Nature* **521**, 169-170, doi:10.1038/nature14522 (2015).
- 2 Rout, M. P. & Field, M. C. *The Evolution of Organellar Coat Complexes and Organization of the Eukaryotic Cell. Annu Rev Biochem* **86**, 637-657, doi:10.1146/annurev-biochem-061516-044643 (2017).
- 3 Li, C., Goryaynov, A. & Yang, W. *The selective permeability barrier in the nuclear pore complex. Nucleus*, 1-17, doi:10.1080/19491034.2016.1238997 (2016).
- 4 Fricker, M., Hollinshead, M., White, N. & Vaux, D. *Interphase nuclei of many mammalian cell types contain deep, dynamic, tubular membrane-bound invaginations of the nuclear envelope. J Cell Biol* **136**, 531-544 (1997).
- 5 Malhas, A., Goulbourne, C. & Vaux, D. J. *The nucleoplasmic reticulum: form and function. Trends Cell Biol* **21**, 362-373, doi:10.1016/j.tcb.2011.03.008 (2011).
- 6 Khadija, S. G., Chen, F., Hadden, T., Commissaris, R. L. & Kowluru, A. *Biology and Regulatory Roles of Nuclear Lamins in Cellular Function and Dysfunction. Recent Pat Endocr Metab Immune Drug Discov* **9**, 111-120 (2015).
- 7 Kubben, N., Voncken, J. W. & Misteli, T. *Mapping of protein- and chromatin-interactions at the nuclear lamina. Nucleus* **1**, 460-471, doi:10.4161/nucl.1.6.13513 (2010).
- 8 Butin-Israeli, V. et al. *Role of lamin b1 in chromatin instability. Mol Cell Biol* **35**, 884-898, doi:10.1128/MCB.01145-14 (2015).
- 9 Xie, W., Horn, H. F. & Wright, G. D. *Superresolution Microscopy of the Nuclear Envelope and Associated Proteins. Methods Mol Biol* **1411**, 83-97, doi:10.1007/978-1-4939-3530-7\_4 (2016).
- 10 Mans, B. J., Anantharaman, V., Aravind, L. & Koonin, E. V. *Comparative genomics, evolution and origins of the nuclear envelope and nuclear pore complex. Cell Cycle* **3**, 1612-1637, doi:10.4161/cc.3.12.1345 (2004).
- 11 Taddei, A., Hediger, F., Neumann, F. R. & Gasser, S. M. *The function of nuclear architecture: a genetic approach. Annu Rev Genet* **38**, 305-345, doi:10.1146/annurev.genet.37.110801.142705 (2004).
- 12 Lemaître, C. & Bickmore, W. A. *Chromatin at the nuclear periphery and the regulation of genome functions. Histochem Cell Biol* **144**, 111-122, doi:10.1007/s00418-015-1346-y (2015).
- 13 Urry, L. A. et al. (ed Pearson Education) *Ch. A tour of the cell*, (2006).

- 14 Davidson, S., Macpherson, N. & Mitchell, J. A. Nuclear organization of RNA polymerase II transcription. *Biochem Cell Biol* **91**, 22-30, doi:10.1139/bcb-2012-0059 (2013).
- 15 Ira, G. & Hastings, P. J. DNA breakage drives nuclear search. *Nat Cell Biol* **14**, 448-450, doi:10.1038/ncb2494 (2012).
- 16 Marks, A. B., Smith, O. K. & Aladjem, M. I. Replication origins: determinants or consequences of nuclear organization? *Curr Opin Genet Dev* **37**, 67-75, doi:10.1016/j.gde.2015.11.008 (2016).
- 17 Miné-Hattab, J. & Rothstein, R. Increased chromosome mobility facilitates homology search during recombination. *Nat Cell Biol* **14**, 510-517, doi:10.1038/ncb2472 (2012).
- 18 Aparicio, O. M. Location, location, location: it's all in the timing for replication origins. *Genes Dev* **27**, 117-128, doi:10.1101/gad.209999.112 (2013).
- 19 Worman, H. J., Ostlund, C. & Wang, Y. Diseases of the nuclear envelope. *Cold Spring Harb Perspect Biol* **2**, a000760, doi:10.1101/cshperspect.a000760 (2010).
- 20 Bonne, G. Nuclear envelope proteins in health and diseases. *Semin Cell Dev Biol* **29**, 93-94, doi:10.1016/j.semcdb.2014.04.023 (2014).
- 21 Meaburn, K. J. & Misteli, T. Cell biology: chromosome territories. *Nature* **445**, 379-781, doi:10.1038/445379a (2007).
- 22 Fritz, A. J. et al. Chromosomes at Work: Organization of Chromosome Territories in the Interphase Nucleus. *J Cell Biochem* **117**, 9-19, doi:10.1002/jcb.25280 (2016).
- 23 Parada, L. A., McQueen, P. G. & Misteli, T. Tissue-specific spatial organization of genomes. *Genome Biol* **5**, R44, doi:10.1186/gb-2004-5-7-r44 (2004).
- 24 Parada, L. A., McQueen, P. G., Munson, P. J. & Misteli, T. Conservation of relative chromosome positioning in normal and cancer cells. *Curr Biol* **12**, 1692-1697 (2002).
- 25 Rabl, C. Vol. 10 214-330 (*Morphologische Jahrbuch*, 1885).
- 26 Cowan, C. R., Carlton, P. M. & Cande, W. Z. The polar arrangement of telomeres in interphase and meiosis. Rabl organization and the bouquet. *Plant Physiol* **125**, 532-538 (2001).
- 27 Bass, H. W., Marshall, W. F., Sedat, J. W., Agard, D. A. & Cande, W. Z. Telomeres cluster de novo before the initiation of synapsis: a three-dimensional spatial analysis of telomere positions before and during meiotic prophase. *J Cell Biol* **137**, 5-18 (1997).

- 28 Ohshima, S. & Seyama, A. Cellular aging and centrosome aberrations. *Ann N Y Acad Sci* **1197**, 108-117, doi:10.1111/j.1749-6632.2009.05396.x (2010).
- 29 Zivković, L. et al. DNA damage in Alzheimer disease lymphocytes and its relation to premature centromere division. *Neurodegener Dis* **12**, 156-163, doi:10.1159/000346114 (2013).
- 30 Rizvi, S., Raza, S. T. & Mahdi, F. Telomere length variations in aging and age-related diseases. *Curr Aging Sci* **7**, 161-167 (2014).
- 31 Xu, L., Li, S. & Stohr, B. A. The role of telomere biology in cancer. *Annu Rev Pathol* **8**, 49-78, doi:10.1146/annurev-pathol-020712-164030 (2013).
- 32 Garcia, A. et al. Super-resolution structure of DNA significantly differs in buccal cells of controls and Alzheimer's patients. *J Cell Physiol* **232**, 2387-2395, doi:10.1002/jcp.25751 (2017).
- 33 Meaburn, K. J., Levy, N., Toniolo, D. & Bridger, J. M. Chromosome positioning is largely unaffected in lymphoblastoid cell lines containing emerin or A-type lamin mutations. *Biochem Soc Trans* **33**, 1438-1440, doi:10.1042/BST20051438 (2005).
- 34 Cremer, M. et al. Inheritance of gene density-related higher order chromatin arrangements in normal and tumor cell nuclei. *J Cell Biol* **162**, 809-820, doi:10.1083/jcb.200304096 (2003).
- 35 Krystosek, A. Repositioning of human interphase chromosomes by nucleolar dynamics in the reverse transformation of HT1080 fibrosarcoma cells. *Exp Cell Res* **241**, 202-209, doi:10.1006/excr.1998.4046 (1998).
- 36 Dixon, J. R. et al. Topological domains in mammalian genomes identified by analysis of chromatin interactions. *Nature* **485**, 376-380, doi:10.1038/nature11082 (2012).
- 37 Harmston, N. et al. Topologically associating domains are ancient features that coincide with Metazoan clusters of extreme noncoding conservation. *Nat Commun* **8**, 441, doi:10.1038/s41467-017-00524-5 (2017).
- 38 Speicher, M. R. & Carter, N. P. The new cytogenetics: blurring the boundaries with molecular biology. *Nat Rev Genet* **6**, 782-792, doi:10.1038/nrg1692 (2005).
- 39 Zuleger, N., Robson, M. I. & Schirmer, E. C. The nuclear envelope as a chromatin organizer. *Nucleus* **2**, 339-349, doi:10.4161/nucl.2.5.17846 (2011).
- 40 Blobel, G. Three-dimensional organization of chromatids by nuclear envelope-associated structures. *Cold Spring Harb Symp Quant Biol* **75**, 545-554, doi:10.1101/sqb.2010.75.004 (2010).



- 41 Heun, P., Laroche, T., Raghuraman, M. K. & Gasser, S. M. The positioning and dynamics of origins of replication in the budding yeast nucleus. *J Cell Biol* **152**, 385-400 (2001).
- 42 Gilbert, D. M. Replication timing and transcriptional control: beyond cause and effect. *Curr Opin Cell Biol* **14**, 377-383 (2002).
- 43 Gilbert, D. M. Nuclear position leaves its mark on replication timing. *J Cell Biol* **152**, F11-15 (2001).
- 44 Chow, J. C. & Heard, E. Nuclear organization and dosage compensation. *Cold Spring Harb Perspect Biol* **2**, a000604, doi:10.1101/cshperspect.a000604 (2010).
- 45 Ottaviani, A. et al. Identification of a perinuclear positioning element in human subtelomeres that requires A-type lamins and CTCF. *EMBO J* **28**, 2428-2436, doi:10.1038/emboj.2009.201 (2009).
- 46 Funabiki, H., Hagan, I., Uzawa, S. & Yanagida, M. Cell cycle-dependent specific positioning and clustering of centromeres and telomeres in fission yeast. *J Cell Biol* **121**, 961-976 (1993).
- 47 Hochstrasser, M., Mathog, D., Gruenbaum, Y., Saumweber, H. & Sedat, J. W. Spatial organization of chromosomes in the salivary gland nuclei of *Drosophila melanogaster*. *J Cell Biol* **102**, 112-123 (1986).
- 48 Ptak, C. & Wozniak, R. W. Nucleoporins and chromatin metabolism. *Curr Opin Cell Biol* **40**, 153-160, doi:10.1016/j.ceb.2016.03.024 (2016).
- 49 Gay, S. & Foiani, M. Nuclear envelope and chromatin, lock and key of genome integrity. *Int Rev Cell Mol Biol* **317**, 267-330, doi:10.1016/bs.ircmb.2015.03.001 (2015).
- 50 Bermejo, R. et al. The replication checkpoint protects fork stability by releasing transcribed genes from nuclear pores. *Cell* **146**, 233-246, doi:10.1016/j.cell.2011.06.033 (2011).
- 51 Goodarzi, A. A., Noon, A. T. & Jeggo, P. A. The impact of heterochromatin on DSB repair. *Biochem Soc Trans* **37**, 569-576, doi:10.1042/BST0370569 (2009).
- 52 Goodarzi, A. A. et al. ATM signaling facilitates repair of DNA double-strand breaks associated with heterochromatin. *Mol Cell* **31**, 167-177, doi:10.1016/j.molcel.2008.05.017 (2008).
- 53 Nagai, S. et al. Functional targeting of DNA damage to a nuclear pore-associated SUMO-dependent ubiquitin ligase. *Science* **322**, 597-602, doi:10.1126/science.1162790 (2008).

- 54 Oza, P., Jaspersen, S. L., Miele, A., Dekker, J. & Peterson, C. L. Mechanisms that regulate localization of a DNA double-strand break to the nuclear periphery. *Genes Dev* **23**, 912-927, doi:10.1101/gad.1782209 (2009).
- 55 Sung, P. Catalysis of ATP-dependent homologous DNA pairing and strand exchange by yeast RAD51 protein. *Science* **265**, 1241-1243 (1994).
- 56 Baumann, P. & West, S. C. Role of the human RAD51 protein in homologous recombination and double-stranded-break repair. *Trends Biochem Sci* **23**, 247-251 (1998).
- 57 Lisby, M., Mortensen, U. H. & Rothstein, R. Colocalization of multiple DNA double-strand breaks at a single Rad52 repair centre. *Nat Cell Biol* **5**, 572-577, doi:10.1038/ncb997 (2003).
- 58 Loeillet, S. et al. Genetic network interactions among replication, repair and nuclear pore deficiencies in yeast. *DNA Repair (Amst)* **4**, 459-468, doi:10.1016/j.dnarep.2004.11.010 (2005).
- 59 Ryu, T. et al. Heterochromatic breaks move to the nuclear periphery to continue recombinational repair. *Nat Cell Biol* **17**, 1401-1411, doi:10.1038/ncb3258 (2015).
- 60 Soutoglou, E. et al. Positional stability of single double-strand breaks in mammalian cells. *Nat Cell Biol* **9**, 675-682, doi:10.1038/ncb1591 (2007).
- 61 Moudry, P. et al. Nucleoporin NUP153 guards genome integrity by promoting nuclear import of 53BP1. *Cell Death Differ* **19**, 798-807, doi:10.1038/cdd.2011.150 (2012).
- 62 Kalocsay, M., Hiller, N. J. & Jentsch, S. Chromosome-wide Rad51 spreading and SUMO-H2A.Z-dependent chromosome fixation in response to a persistent DNA double-strand break. *Mol Cell* **33**, 335-343, doi:10.1016/j.molcel.2009.01.016 (2009).
- 63 Jasin, M. Homologous repair of DNA damage and tumorigenesis: the BRCA connection. *Oncogene* **21**, 8981-8993, doi:10.1038/sj.onc.1206176 (2002).
- 64 Trickett, A. J. & Butlin, R. K. Recombination suppressors and the evolution of new species. *Heredity (Edinb)* **73 ( Pt 4)**, 339-345 (1994).
- 65 Szostak, J. W., Orr-Weaver, T. L., Rothstein, R. J. & Stahl, F. W. The double-strand-break repair model for recombination. *Cell* **33**, 25-35 (1983).
- 66 Symington, L. S. & Gautier, J. Double-strand break end resection and repair pathway choice. *Annu Rev Genet* **45**, 247-271, doi:10.1146/annurev-genet-110410-132435 (2011).

- 67 *Ira, G., Malkova, A., Liberi, G., Foiani, M. & Haber, J. E. Srs2 and Sgs1-Top3 suppress crossovers during double-strand break repair in yeast. Cell* **115**, 401-411 (2003).
- 68 *Pâques, F. & Haber, J. E. Multiple pathways of recombination induced by double-strand breaks in Saccharomyces cerevisiae. Microbiol Mol Biol Rev* **63**, 349-404 (1999).
- 69 *Moore, J. K. & Haber, J. E. Cell cycle and genetic requirements of two pathways of nonhomologous end-joining repair of double-strand breaks in Saccharomyces cerevisiae. Mol Cell Biol* **16**, 2164-2173 (1996).
- 70 *Wu, L., Davies, S. L. & Hickson, I. D. Roles of RecQ family helicases in the maintenance of genome stability. Cold Spring Harb Symp Quant Biol* **65**, 573-581 (2000).
- 71 *Hickson, I. D. & Mankouri, H. W. Processing of homologous recombination repair intermediates by the Sgs1-Top3-Rmi1 and Mus81-Mms4 complexes. Cell Cycle* **10**, 3078-3085, doi:10.4161/cc.10.18.16919 (2011).
- 72 *Andersen, S. L. & Sekelsky, J. Meiotic versus mitotic recombination: two different routes for double-strand break repair: the different functions of meiotic versus mitotic DSB repair are reflected in different pathway usage and different outcomes. Bioessays* **32**, 1058-1066, doi:10.1002/bies.201000087 (2010).
- 73 *Gordenin, D. A. et al. Inverted DNA repeats: a source of eukaryotic genomic instability. Mol Cell Biol* **13**, 5315-5322 (1993).
- 74 *Mirkin, S. M. DNA structures, repeat expansions and human hereditary disorders. Curr Opin Struct Biol* **16**, 351-358, doi:10.1016/j.sbi.2006.05.004 (2006).
- 75 *Yu, X., Jacobs, S. A., West, S. C., Ogawa, T. & Egelman, E. H. Domain structure and dynamics in the helical filaments formed by RecA and Rad51 on DNA. Proc Natl Acad Sci U S A* **98**, 8419-8424, doi:10.1073/pnas.111005398 (2001).
- 76 *Mazin, A. V., Mazina, O. M., Bugreev, D. V. & Rossi, M. J. Rad54, the motor of homologous recombination. DNA Repair (Amst)* **9**, 286-302, doi:10.1016/j.dnarep.2009.12.006 (2010).
- 77 *Daley, J. M., Kwon, Y., Niu, H. & Sung, P. Investigations of homologous recombination pathways and their regulation. Yale J Biol Med* **86**, 453-461 (2013).
- 78 *Zapotoczny, G. & Sekelsky, J. Human Cell Assays for Synthesis-Dependent Strand Annealing and Crossing over During Double-Strand Break Repair. G3 (Bethesda)* **7**, 1191-1199, doi:10.1534/g3.116.037390 (2017).
- 79 *Bzymek, M., Thayer, N. H., Oh, S. D., Kleckner, N. & Hunter, N. Double Holliday junctions are intermediates of DNA break repair. Nature* **464**, 937-941, doi:10.1038/nature08868 (2010).

- 80 *Heyer, W. D. A new deal for Holliday junctions. Nat Struct Mol Biol* **11**, 117-119, doi:10.1038/nsmb0204-117 (2004).
- 81 *Biscotti, M. A., Olmo, E. & Heslop-Harrison, J. S. Repetitive DNA in eukaryotic genomes. Chromosome Res* **23**, 415-420, doi:10.1007/s10577-015-9499-z (2015).
- 82 *Hanahan, D. & Weinberg, R. A. The hallmarks of cancer. Cell* **100**, 57-70 (2000).
- 83 *Negrini, S., Gorgoulis, V. G. & Halazonetis, T. D. Genomic instability--an evolving hallmark of cancer. Nat Rev Mol Cell Biol* **11**, 220-228, doi:10.1038/nrm2858 (2010).
- 84 *Lamb, B. C., Saleem, M., Scott, W., Thapa, N. & Nevo, E. Inherited and environmentally induced differences in mutation frequencies between wild strains of *Sordaria fimicola* from "Evolution Canyon". Genetics* **149**, 87-99 (1998).
- 85 *Galhardo, R. S., Hastings, P. J. & Rosenberg, S. M. Mutation as a stress response and the regulation of evolvability. Crit Rev Biochem Mol Biol* **42**, 399-435, doi:10.1080/10409230701648502 (2007).
- 86 *Mekhail, K. & Moazed, D. The nuclear envelope in genome organization, expression and stability. Nat Rev Mol Cell Biol* **11**, 317-328, doi:10.1038/nrm2894 (2010).
- 87 *de Lange, T. How telomeres solve the end-protection problem. Science* **326**, 948-952, doi:10.1126/science.1170633 (2009).
- 88 *Murnane, J. P. Telomere dysfunction and chromosome instability. Mutat Res* **730**, 28-36, doi:10.1016/j.mrfmmm.2011.04.008 (2012).
- 89 *Van de Vosse, D. W. et al. A role for the nucleoporin Nup170p in chromatin structure and gene silencing. Cell* **152**, 969-983, doi:10.1016/j.cell.2013.01.049 (2013).
- 90 *Moyzis, R. K. et al. A highly conserved repetitive DNA sequence, (TTAGGG)<sub>n</sub>, present at the telomeres of human chromosomes. Proc Natl Acad Sci U S A* **85**, 6622-6626 (1988).
- 91 *Gilson, E., Laroche, T. & Gasser, S. M. Telomeres and the functional architecture of the nucleus. Trends Cell Biol* **3**, 128-134 (1993).
- 92 *Scherthan, H. Telomere attachment and clustering during meiosis. Cell Mol Life Sci* **64**, 117-124, doi:10.1007/s00018-006-6463-2 (2007).
- 93 *Taddei, A. & Gasser, S. M. Structure and function in the budding yeast nucleus. Genetics* **192**, 107-129, doi:10.1534/genetics.112.140608 (2012).

- 94 Therizols, P. et al. Telomere tethering at the nuclear periphery is essential for efficient DNA double strand break repair in subtelomeric region. *J Cell Biol* **172**, 189-199, doi:10.1083/jcb.200505159 (2006).
- 95 Guelen, L. et al. Domain organization of human chromosomes revealed by mapping of nuclear lamina interactions. *Nature* **453**, 948-951, doi:10.1038/nature06947 (2008).
- 96 Gonzalez-Suarez, I. et al. Novel roles for A-type lamins in telomere biology and the DNA damage response pathway. *EMBO J* **28**, 2414-2427, doi:10.1038/emboj.2009.196 (2009).
- 97 Branzei, D. & Foiani, M. Maintaining genome stability at the replication fork. *Nat Rev Mol Cell Biol* **11**, 208-219, doi:10.1038/nrm2852 (2010).
- 98 Bernstein, K. A. et al. Sgs1 function in the repair of DNA replication intermediates is separable from its role in homologous recombination repair. *EMBO J* **28**, 915-925, doi:10.1038/emboj.2009.28 (2009).
- 99 Liberi, G. et al. Rad51-dependent DNA structures accumulate at damaged replication forks in sgs1 mutants defective in the yeast ortholog of BLM RecQ helicase. *Genes Dev* **19**, 339-350, doi:10.1101/gad.322605 (2005).
- 100 Stark, J. M. & Jasin, M. Extensive loss of heterozygosity is suppressed during homologous repair of chromosomal breaks. *Mol Cell Biol* **23**, 733-743 (2003).
- 101 Iliakis, G. et al. Mechanisms of DNA double strand break repair and chromosome aberration formation. *Cytogenet Genome Res* **104**, 14-20, doi:10.1159/000077461 (2004).
- 102 Durkin, S. G. & Glover, T. W. Chromosome fragile sites. *Annu Rev Genet* **41**, 169-192, doi:10.1146/annurev.genet.41.042007.165900 (2007).
- 103 Hashash, N., Johnson, A. L. & Cha, R. S. Regulation of fragile sites expression in budding yeast by MEC1, RRM3 and hydroxyurea. *J Cell Sci* **124**, 181-185, doi:10.1242/jcs.077313 (2011).
- 104 Debatisse, M., Le Tallec, B., Letessier, A., Dutrillaux, B. & Brison, O. Common fragile sites: mechanisms of instability revisited. *Trends Genet* **28**, 22-32, doi:10.1016/j.tig.2011.10.003 (2012).
- 105 Szilard, R. K. et al. Systematic identification of fragile sites via genome-wide location analysis of gamma-H2AX. *Nat Struct Mol Biol* **17**, 299-305, doi:10.1038/nsmb.1754 (2010).
- 106 Bacolla, A., Wojciechowska, M., Kosmider, B., Larson, J. E. & Wells, R. D. The involvement of non-B DNA structures in gross chromosomal rearrangements. *DNA Repair (Amst)* **5**, 1161-1170, doi:10.1016/j.dnarep.2006.05.032 (2006).

- 107 Oakley, T. J. & Hickson, I. D. *Defending genome integrity during S-phase: putative roles for RecQ helicases and topoisomerase III. DNA Repair (Amst)* **1**, 175-207 (2002).
- 108 Lambert, S. & Carr, A. M. *Replication stress and genome rearrangements: lessons from yeast models. Curr Opin Genet Dev* **23**, 132-139, doi:10.1016/j.gde.2012.11.009 (2013).
- 109 Voineagu, I., Narayanan, V., Lobachev, K. S. & Mirkin, S. M. *Replication stalling at unstable inverted repeats: interplay between DNA hairpins and fork stabilizing proteins. Proc Natl Acad Sci U S A* **105**, 9936-9941, doi:10.1073/pnas.0804510105 (2008).
- 110 Bermejo, R., Lai, M. S. & Foiani, M. *Preventing replication stress to maintain genome stability: resolving conflicts between replication and transcription. Mol Cell* **45**, 710-718, doi:10.1016/j.molcel.2012.03.001 (2012).
- 111 García-Benítez, F., Gaillard, H. & Aguilera, A. *Physical proximity of chromatin to nuclear pores prevents harmful R loop accumulation contributing to maintain genome stability. Proceedings of the National Academy of Sciences*, doi:10.1073/pnas.1707845114 (2017).
- 112 Zhang, J. *Replication fork collapse triggers relocation of common fragile sites to the nuclear periphery and crossover recombination (Poster presented at: NCI Symposium on Chromosome Biology: Nuclear structure, Genome Integrity and Cancer (November 30-December, Natcher Auditorium, NIH Campus Bethesda, Maryland), 2016).*
- 113 Azvolinsky, A., Giresi, P. G., Lieb, J. D. & Zakian, V. A. *Highly transcribed RNA polymerase II genes are impediments to replication fork progression in Saccharomyces cerevisiae. Mol Cell* **34**, 722-734, doi:10.1016/j.molcel.2009.05.022 (2009).
- 114 Wang, J. D., Berkmen, M. B. & Grossman, A. D. *Genome-wide coorientation of replication and transcription reduces adverse effects on replication in Bacillus subtilis. Proc Natl Acad Sci U S A* **104**, 5608-5613, doi:10.1073/pnas.0608999104 (2007).
- 115 Wang, J. C. *Cellular roles of DNA topoisomerases: a molecular perspective. Nat Rev Mol Cell Biol* **3**, 430-440, doi:10.1038/nrm831 (2002).
- 116 Leonard, A. C. & Méchali, M. *DNA replication origins. Cold Spring Harb Perspect Biol* **5**, a010116, doi:10.1101/cshperspect.a010116 (2013).
- 117 Méchali, M. *Eukaryotic DNA replication origins: many choices for appropriate answers. Nat Rev Mol Cell Biol* **11**, 728-738, doi:10.1038/nrm2976 (2010).
- 118 Lemaitre, J. M., Danis, E., Pasero, P., Vassetzky, Y. & Méchali, M. *Mitotic remodeling of the replicon and chromosome structure. Cell* **123**, 787-801, doi:10.1016/j.cell.2005.08.045 (2005).

- 119 Courbet, S. et al. Replication fork movement sets chromatin loop size and origin choice in mammalian cells. *Nature* **455**, 557-560, doi:10.1038/nature07233 (2008).
- 120 Pope, B. D. et al. Topologically associating domains are stable units of replication-timing regulation. *Nature* **515**, 402-405, doi:10.1038/nature13986 (2014).
- 121 Newport, J. W., Wilson, K. L. & Dunphy, W. G. A lamin-independent pathway for nuclear envelope assembly. *J Cell Biol* **111**, 2247-2259 (1990).
- 122 Goldberg, M., Jenkins, H., Allen, T., Whitfield, W. G. & Hutchison, C. J. *Xenopus* lamin B3 has a direct role in the assembly of a replication competent nucleus: evidence from cell-free egg extracts. *J Cell Sci* **108 ( Pt 11)**, 3451-3461 (1995).
- 123 Spann, T. P., Moir, R. D., Goldman, A. E., Stick, R. & Goldman, R. D. Disruption of nuclear lamin organization alters the distribution of replication factors and inhibits DNA synthesis. *J Cell Biol* **136**, 1201-1212 (1997).
- 124 Moir, R. D., Spann, T. P., Herrmann, H. & Goldman, R. D. Disruption of nuclear lamin organization blocks the elongation phase of DNA replication. *J Cell Biol* **149**, 1179-1192 (2000).
- 125 Gant, T. M., Harris, C. A. & Wilson, K. L. Roles of LAP2 proteins in nuclear assembly and DNA replication: truncated LAP2beta proteins alter lamina assembly, envelope formation, nuclear size, and DNA replication efficiency in *Xenopus laevis* extracts. *J Cell Biol* **144**, 1083-1096 (1999).
- 126 Yang, L., Guan, T. & Gerace, L. Lamin-binding fragment of LAP2 inhibits increase in nuclear volume during the cell cycle and progression into S phase. *J Cell Biol* **139**, 1077-1087 (1997).
- 127 Gillespie, P. J., Khoudoli, G. A., Stewart, G., Swedlow, J. R. & Blow, J. J. ELYS/MEL-28 chromatin association coordinates nuclear pore complex assembly and replication licensing. *Curr Biol* **17**, 1657-1662, doi:10.1016/j.cub.2007.08.041 (2007).
- 128 Davuluri, G. et al. Mutation of the zebrafish nucleoporin *elys* sensitizes tissue progenitors to replication stress. *PLoS Genet* **4**, e1000240, doi:10.1371/journal.pgen.1000240 (2008).
- 129 Gao, N. et al. The nuclear pore complex protein *Elys* is required for genome stability in mouse intestinal epithelial progenitor cells. *Gastroenterology* **140**, 1547-1555.e1510, doi:10.1053/j.gastro.2011.01.048 (2011).
- 130 Margalit, A., Vlcek, S., Gruenbaum, Y. & Foisner, R. Breaking and making of the nuclear envelope. *J Cell Biochem* **95**, 454-465, doi:10.1002/jcb.20433 (2005).
- 131 Dessev, G., Palazzo, R., Rebhun, L. & Goldman, R. Disassembly of the nuclear envelope of *spisula* oocytes in a cell-free system. *Dev Biol* **131**, 496-504 (1989).

- 132 Dessev, G. & Goldman, R. Meiotic breakdown of nuclear envelope in oocytes of *Spisula solidissima* involves phosphorylation and release of nuclear lamin. *Dev Biol* **130**, 543-550 (1988).
- 133 Gant, T. M. & Wilson, K. L. Nuclear assembly. *Annu Rev Cell Dev Biol* **13**, 669-695, doi:10.1146/annurev.cellbio.13.1.669 (1997).
- 134 LaJoie, D. & Ullman, K. S. Coordinated events of nuclear assembly. *Curr Opin Cell Biol* **46**, 39-45, doi:10.1016/j.ceb.2016.12.008 (2017).
- 135 Nguyen, H. Q. & Bosco, G. Gene Positioning Effects on Expression in Eukaryotes. *Annu Rev Genet* **49**, 627-646, doi:10.1146/annurev-genet-112414-055008 (2015).
- 136 Gordon, M. R., Pope, B. D., Sima, J. & Gilbert, D. M. Many paths lead chromatin to the nuclear periphery. *Bioessays* **37**, 862-866, doi:10.1002/bies.201500034 (2015).
- 137 Peric-Hupkes, D. et al. Molecular maps of the reorganization of genome-nuclear lamina interactions during differentiation. *Mol Cell* **38**, 603-613, doi:10.1016/j.molcel.2010.03.016 (2010).
- 138 Talamas, J. A. & Capelson, M. Nuclear envelope and genome interactions in cell fate. *Front Genet* **6**, 95, doi:10.3389/fgene.2015.00095 (2015).
- 139 Borsos, M. & Torres-Padilla, M. E. Building up the nucleus: nuclear organization in the establishment of totipotency and pluripotency during mammalian development. *Genes Dev* **30**, 611-621, doi:10.1101/gad.273805.115 (2016).
- 140 Meister, P., Mango, S. E. & Gasser, S. M. Locking the genome: nuclear organization and cell fate. *Curr Opin Genet Dev* **21**, 167-174, doi:10.1016/j.gde.2011.01.023 (2011).
- 141 Reddy, K. L., Zullo, J. M., Bertolino, E. & Singh, H. Transcriptional repression mediated by repositioning of genes to the nuclear lamina. *Nature* **452**, 243-247, doi:10.1038/nature06727 (2008).
- 142 Finlan, L. E. et al. Recruitment to the nuclear periphery can alter expression of genes in human cells. *PLoS Genet* **4**, e1000039, doi:10.1371/journal.pgen.1000039 (2008).
- 143 Amendola, M. & van Steensel, B. Nuclear lamins are not required for lamina-associated domain organization in mouse embryonic stem cells. *EMBO Rep* **16**, 610-617, doi:10.15252/embr.201439789 (2015).
- 144 D'Angelo, M. A., Gomez-Cavazos, J. S., Mei, A., Lackner, D. H. & Hetzer, M. W. A change in nuclear pore complex composition regulates cell differentiation. *Dev Cell* **22**, 446-458, doi:10.1016/j.devcel.2011.11.021 (2012).



- 145 Bergqvist, C., Jafferli, M. H., Gudise, S., Markus, R. & Hallberg, E. An inner nuclear membrane protein induces rapid differentiation of human induced pluripotent stem cells. *Stem Cell Res* **23**, 33-38, doi:10.1016/j.scr.2017.06.008 (2017).
- 146 Cox, J. L. et al. *Banfl* is required to maintain the self-renewal of both mouse and human embryonic stem cells. *J Cell Sci* **124**, 2654-2665, doi:10.1242/jcs.083238 (2011).
- 147 Gesson, K., Vidak, S. & Foisner, R. Lamina-associated polypeptide (LAP)2 $\alpha$  and nucleoplasmic lamins in adult stem cell regulation and disease. *Semin Cell Dev Biol* **29**, 116-124, doi:10.1016/j.semcdb.2013.12.009 (2014).
- 148 Dorner, D. et al. Lamina-associated polypeptide 2 $\alpha$  regulates cell cycle progression and differentiation via the retinoblastoma-E2F pathway. *J Cell Biol* **173**, 83-93, doi:10.1083/jcb.200511149 (2006).
- 149 Markiewicz, E., Dechat, T., Foisner, R., Quinlan, R. A. & Hutchison, C. J. Lamin A/C binding protein LAP2 $\alpha$  is required for nuclear anchorage of retinoblastoma protein. *Mol Biol Cell* **13**, 4401-4413, doi:10.1091/mbc.E02-07-0450 (2002).
- 150 Raju, G. P., Dimova, N., Klein, P. S. & Huang, H. C. SANE, a novel LEM domain protein, regulates bone morphogenetic protein signaling through interaction with Smad1. *J Biol Chem* **278**, 428-437, doi:10.1074/jbc.M210505200 (2003).
- 151 Ishimura, A., Ng, J. K., Taira, M., Young, S. G. & Osada, S. Man1, an inner nuclear membrane protein, regulates vascular remodeling by modulating transforming growth factor beta signaling. *Development* **133**, 3919-3928, doi:10.1242/dev.02538 (2006).
- 152 Dedeic, Z., Cetera, M., Cohen, T. V. & Holaska, J. M. Emerin inhibits Lmo7 binding to the Pax3 and MyoD promoters and expression of myoblast proliferation genes. *J Cell Sci* **124**, 1691-1702, doi:10.1242/jcs.080259 (2011).
- 153 Markiewicz, E. et al. The inner nuclear membrane protein emerin regulates beta-catenin activity by restricting its accumulation in the nucleus. *EMBO J* **25**, 3275-3285, doi:10.1038/sj.emboj.7601230 (2006).
- 154 Gruenbaum, Y. & Foisner, R. Lamins: nuclear intermediate filament proteins with fundamental functions in nuclear mechanics and genome regulation. *Annu Rev Biochem* **84**, 131-164, doi:10.1146/annurev-biochem-060614-034115 (2015).
- 155 Moir, R. D., Yoon, M., Khuon, S. & Goldman, R. D. Nuclear lamins A and B1: different pathways of assembly during nuclear envelope formation in living cells. *J Cell Biol* **151**, 1155-1168 (2000).
- 156 Shimi, T. et al. The A- and B-type nuclear lamin networks: microdomains involved in chromatin organization and transcription. *Genes Dev* **22**, 3409-3421, doi:10.1101/gad.1735208 (2008).

- 157 Liu, J. et al. Essential roles for *Caenorhabditis elegans* lamin gene in nuclear organization, cell cycle progression, and spatial organization of nuclear pore complexes. *Mol Biol Cell* **11**, 3937-3947 (2000).
- 158 Lenz-Böhme, B. et al. Insertional mutation of the *Drosophila* nuclear lamin Dm0 gene results in defective nuclear envelopes, clustering of nuclear pore complexes, and accumulation of annulate lamellae. *J Cell Biol* **137**, 1001-1016 (1997).
- 159 Schulze, S. R. et al. A comparative study of *Drosophila* and human A-type lamins. *PLoS One* **4**, e7564, doi:10.1371/journal.pone.0007564 (2009).
- 160 van Engelen, B. G. et al. The lethal phenotype of a homozygous nonsense mutation in the lamin A/C gene. *Neurology* **64**, 374-376, doi:10.1212/01.WNL.0000149763.15180.00 (2005).
- 161 Camozzi, D. et al. Diverse lamin-dependent mechanisms interact to control chromatin dynamics. Focus on laminopathies. *Nucleus* **5**, 427-440, doi:10.4161/nucl.36289 (2014).
- 162 Worman, H. J. & Bonne, G. "Laminopathies": a wide spectrum of human diseases. *Exp Cell Res* **313**, 2121-2133, doi:10.1016/j.yexcr.2007.03.028 (2007).
- 163 Vidak, S. & Foisner, R. Molecular insights into the premature aging disease progeria. *Histochem Cell Biol* **145**, 401-417, doi:10.1007/s00418-016-1411-1 (2016).
- 164 Eriksson, M. et al. Recurrent de novo point mutations in lamin A cause Hutchinson-Gilford progeria syndrome. *Nature* **423**, 293-298, doi:10.1038/nature01629 (2003).
- 165 Ahmed, M. S., Ikram, S., Bibi, N. & Mir, A. Hutchinson-Gilford Progeria Syndrome: A Premature Aging Disease. *Mol Neurobiol*, doi:10.1007/s12035-017-0610-7 (2017).
- 166 Eisch, V., Lu, X., Gabriel, D. & Djabali, K. Progerin impairs chromosome maintenance by depleting CENP-F from metaphase kinetochores in Hutchinson-Gilford progeria fibroblasts. *Oncotarget* **7**, 24700-24718, doi:10.18632/oncotarget.8267 (2016).
- 167 Chojnowski, A. et al. Progerin reduces LAP2 $\alpha$ -telomere association in Hutchinson-Gilford progeria. *Elife* **4**, doi:10.7554/eLife.07759 (2015).
- 168 Wheaton, K. et al. Progerin-Induced Replication Stress Facilitates Premature Senescence in Hutchinson-Gilford Progeria Syndrome. *Mol Cell Biol* **37**, doi:10.1128/MCB.00659-16 (2017).
- 169 Hilton, B. A. et al. Progerin sequestration of PCNA promotes replication fork collapse and mislocalization of XPA in laminopathy-related progeroid syndromes. *FASEB J* **31**, 3882-3893, doi:10.1096/fj.201700014R (2017).

- 170 Gonzalo, S. & Kreienkamp, R. DNA repair defects and genome instability in Hutchinson-Gilford Progeria Syndrome. *Curr Opin Cell Biol* **34**, 75-83, doi:10.1016/j.ceb.2015.05.007 (2015).
- 171 McClintock, D. et al. The mutant form of lamin A that causes Hutchinson-Gilford progeria is a biomarker of cellular aging in human skin. *PLoS One* **2**, e1269, doi:10.1371/journal.pone.0001269 (2007).
- 172 Barton, L. J., Soshnev, A. A. & Geyer, P. K. Networking in the nucleus: a spotlight on LEM-domain proteins. *Curr Opin Cell Biol* **34**, 1-8, doi:10.1016/j.ceb.2015.03.005 (2015).
- 173 Wagner, N. & Krohne, G. LEM-Domain proteins: new insights into lamin-interacting proteins. *Int Rev Cytol* **261**, 1-46, doi:10.1016/S0074-7696(07)61001-8 (2007).
- 174 Segura-Totten, M. & Wilson, K. L. BAF: roles in chromatin, nuclear structure and retrovirus integration. *Trends Cell Biol* **14**, 261-266, doi:10.1016/j.tcb.2004.03.004 (2004).
- 175 Batsios, P., Ren, X., Baumann, O., Larochelle, D. A. & Gräf, R. *Src1* is a Protein of the Inner Nuclear Membrane Interacting with the Dictyostelium Lamin NE81. *Cells* **5**, doi:10.3390/cells5010013 (2016).
- 176 Lin, F. et al. MAN1, an inner nuclear membrane protein that shares the LEM domain with lamina-associated polypeptide 2 and emerin. *J Biol Chem* **275**, 4840-4847 (2000).
- 177 Lee, K. K. et al. Distinct functional domains in emerin bind lamin A and DNA-bridging protein BAF. *J Cell Sci* **114**, 4567-4573 (2001).
- 178 Liu, H. L., Osmani, A. H. & Osmani, S. A. The Inner Nuclear Membrane Protein *Src1* Is Required for Stable Post-Mitotic Progression into G1 in *Aspergillus nidulans*. *PLoS One* **10**, e0132489, doi:10.1371/journal.pone.0132489 (2015).
- 179 Kondé, E. et al. Structural analysis of the Smad2-MAN1 interaction that regulates transforming growth factor- $\beta$  signaling at the inner nuclear membrane. *Biochemistry* **49**, 8020-8032, doi:10.1021/bi101153w (2010).
- 180 Grund, S. E. et al. The inner nuclear membrane protein *Src1* associates with subtelomeric genes and alters their regulated gene expression. *J Cell Biol* **182**, 897-910, doi:10.1083/jcb.200803098 (2008).
- 181 Rodríguez-Navarro, S., Igual, J. C. & Pérez-Ortín, J. E. *SRC1*: an intron-containing yeast gene involved in sister chromatid segregation. *Yeast* **19**, 43-54, doi:10.1002/yea.803 (2002).
- 182 Ikegami, K., Egelhofer, T. A., Strome, S. & Lieb, J. D. *Caenorhabditis elegans* chromosome arms are anchored to the nuclear membrane via discontinuous

- association with LEM-2. *Genome Biol* **11**, R120, doi:10.1186/gb-2010-11-12-r120 (2010).
- 183 Barrales, R. R., Forn, M., Georgescu, P. R., Sarkadi, Z. & Braun, S. Control of heterochromatin localization and silencing by the nuclear membrane protein Lem2. *Genes Dev* **30**, 133-148, doi:10.1101/gad.271288.115 (2016).
- 184 Zhao, R., Bodnar, M. S. & Spector, D. L. Nuclear neighborhoods and gene expression. *Curr Opin Genet Dev* **19**, 172-179, doi:10.1016/j.gde.2009.02.007 (2009).
- 185 Osada, S., Ohmori, S. Y. & Taira, M. XMAN1, an inner nuclear membrane protein, antagonizes BMP signaling by interacting with Smad1 in *Xenopus* embryos. *Development* **130**, 1783-1794 (2003).
- 186 Liu, J. et al. MAN1 and emerin have overlapping function(s) essential for chromosome segregation and cell division in *Caenorhabditis elegans*. *Proc Natl Acad Sci U S A* **100**, 4598-4603, doi:10.1073/pnas.0730821100 (2003).
- 187 Barkan, R. et al. Ce-emerin and LEM-2: essential roles in *Caenorhabditis elegans* development, muscle function, and mitosis. *Mol Biol Cell* **23**, 543-552, doi:10.1091/mbc.E11-06-0505 (2012).
- 188 Brachner, A. & Foisner, R. Evolvement of LEM proteins as chromatin tethers at the nuclear periphery. *Biochem Soc Trans* **39**, 1735-1741, doi:10.1042/BST20110724 (2011).
- 189 Zheng, R. et al. Barrier-to-autointegration factor (BAF) bridges DNA in a discrete, higher-order nucleoprotein complex. *Proc Natl Acad Sci U S A* **97**, 8997-9002, doi:10.1073/pnas.150240197 (2000).
- 190 Segura-Totten, M., Kowalski, A. K., Craigie, R. & Wilson, K. L. Barrier-to-autointegration factor: major roles in chromatin decondensation and nuclear assembly. *J Cell Biol* **158**, 475-485, doi:10.1083/jcb.200202019 (2002).
- 191 Margalit, A., Segura-Totten, M., Gruenbaum, Y. & Wilson, K. L. Barrier-to-autointegration factor is required to segregate and enclose chromosomes within the nuclear envelope and assemble the nuclear lamina. *Proc Natl Acad Sci U S A* **102**, 3290-3295, doi:10.1073/pnas.0408364102 (2005).
- 192 Furukawa, K. et al. Barrier-to-autointegration factor plays crucial roles in cell cycle progression and nuclear organization in *Drosophila*. *J Cell Sci* **116**, 3811-3823, doi:10.1242/jcs.00682 (2003).
- 193 Towbin, B. D., Meister, P., Pike, B. L. & Gasser, S. M. Repetitive transgenes in *C. elegans* accumulate heterochromatic marks and are sequestered at the nuclear envelope in a copy-number- and lamin-dependent manner. *Cold Spring Harb Symp Quant Biol* **75**, 555-565, doi:10.1101/sqb.2010.75.041 (2010).

- 194 Cabanillas, R. et al. Néstor-Guillermo progeria syndrome: a novel premature aging condition with early onset and chronic development caused by BANF1 mutations. *Am J Med Genet A* **155A**, 2617-2625, doi:10.1002/ajmg.a.34249 (2011).
- 195 Mansharamani, M. & Wilson, K. L. Direct binding of nuclear membrane protein MAN1 to emerin in vitro and two modes of binding to barrier-to-autointegration factor. *J Biol Chem* **280**, 13863-13870, doi:10.1074/jbc.M413020200 (2005).
- 196 Caputo, S. et al. The carboxyl-terminal nucleoplasmic region of MAN1 exhibits a DNA binding winged helix domain. *J Biol Chem* **281**, 18208-18215, doi:10.1074/jbc.M601980200 (2006).
- 197 Pan, D. et al. The integral inner nuclear membrane protein MAN1 physically interacts with the R-Smad proteins to repress signaling by the transforming growth factor- $\beta$  superfamily of cytokines. *J Biol Chem* **280**, 15992-16001, doi:10.1074/jbc.M411234200 (2005).
- 198 Bourgeois, B. et al. Inhibition of TGF- $\beta$  signaling at the nuclear envelope: characterization of interactions between MAN1, Smad2 and Smad3, and PPM1A. *Sci Signal* **6**, ra49, doi:10.1126/scisignal.2003411 (2013).
- 199 Hattier, T., Andrulis, E. D. & Tartakoff, A. M. Immobility, inheritance and plasticity of shape of the yeast nucleus. *BMC Cell Biol* **8**, 47, doi:10.1186/1471-2121-8-47 (2007).
- 200 Yewdell, W. T., Colombi, P., Makhnevych, T. & Lusk, C. P. Luminal interactions in nuclear pore complex assembly and stability. *Mol Biol Cell* **22**, 1375-1388, doi:10.1091/mbc.E10-06-0554 (2011).
- 201 Yam, C., Gu, Y. & Oliferenko, S. Partitioning and remodeling of the *Schizosaccharomyces japonicus* mitotic nucleus require chromosome tethers. *Curr Biol* **23**, 2303-2310, doi:10.1016/j.cub.2013.09.057 (2013).
- 202 Steglich, B., Fillion, G. J., van Steensel, B. & Ekwall, K. The inner nuclear membrane proteins Man1 and Imal link to two different types of chromatin at the nuclear periphery in *S. pombe*. *Nucleus* **3**, 77-87 (2012).
- 203 Miyazono, K., ten Dijke, P. & Heldin, C. H. TGF- $\beta$  signaling by Smad proteins. *Adv Immunol* **75**, 115-157 (2000).
- 204 Bier, E. & De Robertis, E. M. EMBRYO DEVELOPMENT. BMP gradients: A paradigm for morphogen-mediated developmental patterning. *Science* **348**, aaa5838, doi:10.1126/science.aaa5838 (2015).
- 205 Bermeo, S., Al-Saedi, A., Kassem, M., Vidal, C. & Duque, G. The Role of the Nuclear Envelope Protein MAN1 in Mesenchymal Stem Cell Differentiation. *J Cell Biochem*, doi:10.1002/jcb.26096 (2017).

- 206 Pinto, B. S., Wilmington, S. R., Hornick, E. E., Wallrath, L. L. & Geyer, P. K. Tissue-specific defects are caused by loss of the *Drosophila* MAN1 LEM domain protein. *Genetics* **180**, 133-145, doi:10.1534/genetics.108.091371 (2008).
- 207 Couto, A. R. et al. A novel LEMD3 mutation common to patients with osteopoikilosis with and without melorheostosis. *Calcif Tissue Int* **81**, 81-84, doi:10.1007/s00223-007-9043-z (2007).
- 208 Hellemans, J. et al. Loss-of-function mutations in LEMD3 result in osteopoikilosis, Buschke-Ollendorff syndrome and melorheostosis. *Nat Genet* **36**, 1213-1218, doi:10.1038/ng1453 (2004).
- 209 Sannino, V., Kolinjivadi, A. M., Baldi, G. & Costanzo, V. Studying essential DNA metabolism proteins in *Xenopus* egg extract. *Int J Dev Biol* **60**, 221-227, doi:10.1387/ijdb.160103vc (2016).
- 210 Costanzo, V., Robertson, K. & Gautier, J. *Xenopus* cell-free extracts to study the DNA damage response. *Methods Mol Biol* **280**, 213-227, doi:10.1385/1-59259-788-2:213 (2004).
- 211 Gillespie, P. J., Gambus, A. & Blow, J. J. Preparation and use of *Xenopus* egg extracts to study DNA replication and chromatin associated proteins. *Methods* **57**, 203-213, doi:10.1016/j.ymeth.2012.03.029 (2012).
- 212 Busa, W. B. & Nuccitelli, R. An elevated free cytosolic Ca<sup>2+</sup> wave follows fertilization in eggs of the frog, *Xenopus laevis*. *J Cell Biol* **100**, 1325-1329 (1985).
- 213 Sannino, V., Pezzimenti, F., Bertora, S. & Costanzo, V. *Xenopus laevis* as Model System to Study DNA Damage Response and Replication Fork Stability. *Methods Enzymol* **591**, 211-232, doi:10.1016/bs.mie.2017.03.018 (2017).
- 214 Murray, A. W. Cell cycle extracts. *Methods Cell Biol* **36**, 581-605 (1991).
- 215 Bradford, M. M. A rapid and sensitive method for the quantitation of microgram quantities of protein utilizing the principle of protein-dye binding. *Anal Biochem* **72**, 248-254 (1976).
- 216 Mattaj, I. W. & Englmeier, L. Nucleocytoplasmic transport: the soluble phase. *Annu Rev Biochem* **67**, 265-306, doi:10.1146/annurev.biochem.67.1.265 (1998).
- 217 Macaulay, C. & Forbes, D. J. Assembly of the nuclear pore: biochemically distinct steps revealed with NEM, GTP gamma S, and BAPTA. *J Cell Biol* **132**, 5-20 (1996).
- 218 Bernis, C. & Forbes, D. J. Analysis of nuclear reconstitution, nuclear envelope assembly, and nuclear pore assembly using *Xenopus* in vitro assays. *Methods Cell Biol* **122**, 165-191, doi:10.1016/B978-0-12-417160-2.00008-4 (2014).

- 219 Webster, B. M. et al. *Chm7 and Heh1 collaborate to link nuclear pore complex quality control with nuclear envelope sealing. EMBO J* **35**, 2447-2467, doi:10.15252/embj.201694574 (2016).
- 220 Blow, J. J. & Watson, J. V. *Nuclei act as independent and integrated units of replication in a Xenopus cell-free DNA replication system. EMBO J* **6**, 1997-2002 (1987).
- 221 Mailand, N. & Diffley, J. F. *CDKs promote DNA replication origin licensing in human cells by protecting Cdc6 from APC/C-dependent proteolysis. Cell* **122**, 915-926, doi:10.1016/j.cell.2005.08.013 (2005).
- 222 Krasinska, L. & Fisher, D. *Replication initiation complex formation in the absence of nuclear function in Xenopus. Nucleic Acids Res* **37**, 2238-2248, doi:10.1093/nar/gkp081 (2009).
- 223 Jones, R. M. & Petermann, E. *Replication fork dynamics and the DNA damage response. Biochem J* **443**, 13-26, doi:10.1042/BJ20112100 (2012).
- 224 Ward, I. M. & Chen, J. *Histone H2AX is phosphorylated in an ATR-dependent manner in response to replicational stress. J Biol Chem* **276**, 47759-47762, doi:10.1074/jbc.C100569200 (2001).
- 225 Xu, Y. et al. *Histone H2A.Z controls a critical chromatin remodeling step required for DNA double-strand break repair. Mol Cell* **48**, 723-733, doi:10.1016/j.molcel.2012.09.026 (2012).
- 226 Pienta, K. J. & Coffey, D. S. *A structural analysis of the role of the nuclear matrix and DNA loops in the organization of the nucleus and chromosome. J Cell Sci Suppl* **1**, 123-135 (1984).
- 227 Vogelstein, B., Pardoll, D. M. & Coffey, D. S. *Supercoiled loops and eucaryotic DNA replicaton. Cell* **22**, 79-85 (1980).
- 228 Anderson, D. J., Vargas, J. D., Hsiao, J. P. & Hetzer, M. W. *Recruitment of functionally distinct membrane proteins to chromatin mediates nuclear envelope formation in vivo. J Cell Biol* **186**, 183-191, doi:10.1083/jcb.200901106 (2009).
- 229 Li, V. C., Ballabeni, A. & Kirschner, M. W. *Gap 1 phase length and mouse embryonic stem cell self-renewal. Proc Natl Acad Sci U S A* **109**, 12550-12555, doi:10.1073/pnas.1206740109 (2012).
- 230 Ahuja, A. K. et al. *A short G1 phase imposes constitutive replication stress and fork remodelling in mouse embryonic stem cells. Nat Commun* **7**, 10660, doi:10.1038/ncomms10660 (2016).
- 231 Hutchison, C. J. et al. *DNA replication and cell cycle control in Xenopus egg extracts. J Cell Sci Suppl* **12**, 197-212 (1989).

- 232 Alberio, R., Johnson, A. D., Stick, R. & Campbell, K. H. Differential nuclear remodeling of mammalian somatic cells by *Xenopus laevis* oocyte and egg cytoplasm. *Exp Cell Res* **307**, 131-141, doi:10.1016/j.yexcr.2005.02.028 (2005).
- 233 Cong, L. et al. Multiplex genome engineering using CRISPR/Cas systems. *Science* **339**, 819-823, doi:10.1126/science.1231143 (2013).
- 234 Zhang, X. H., Tee, L. Y., Wang, X. G., Huang, Q. S. & Yang, S. H. Off-target Effects in CRISPR/Cas9-mediated Genome Engineering. *Mol Ther Nucleic Acids* **4**, e264, doi:10.1038/mtna.2015.37 (2015).
- 235 Czechanski, A. et al. Derivation and characterization of mouse embryonic stem cells from permissive and nonpermissive strains. *Nat Protoc* **9**, 559-574, doi:10.1038/nprot.2014.030 (2014).
- 236 Azzalin, C. M., Reichenbach, P., Khoriantuli, L., Giulotto, E. & Lingner, J. Telomeric repeat containing RNA and RNA surveillance factors at mammalian chromosome ends. *Science* **318**, 798-801, doi:10.1126/science.1147182 (2007).
- 237 Younger, S. T. & Rinn, J. L. Silent pericentromeric repeats speak out. *Proc Natl Acad Sci U S A* **112**, 15008-15009, doi:10.1073/pnas.1520341112 (2015).
- 238 Breuer, M. & Ohkura, H. A negative loop within the nuclear pore complex controls global chromatin organization. *Genes Dev* **29**, 1789-1794, doi:10.1101/gad.264341.115 (2015).
- 239 Blow, J. J. & Sleeman, A. M. Replication of purified DNA in *Xenopus* egg extract is dependent on nuclear assembly. *J Cell Sci* **95 ( Pt 3)**, 383-391 (1990).
- 240 Yin, L., Locovei, A. M. & D'Urso, G. Activation of the DNA damage checkpoint in mutants defective in DNA replication initiation. *Mol Biol Cell* **19**, 4374-4382, doi:10.1091/mbc.E08-01-0020 (2008).
- 241 Musich, P. R. & Zou, Y. Genomic instability and DNA damage responses in progeria arising from defective maturation of prelamin A. *Aging (Albany NY)* **1**, 28-37, doi:10.18632/aging.100012 (2009).
- 242 Skoufias, D. A., Andreassen, P. R., Lacroix, F. B., Wilson, L. & Margolis, R. L. Mammalian mad2 and bub1/bubR1 recognize distinct spindle-attachment and kinetochore-tension checkpoints. *Proc Natl Acad Sci U S A* **98**, 4492-4497, doi:10.1073/pnas.081076898 (2001).
- 243 Potapova, T. A. et al. The reversibility of mitotic exit in vertebrate cells. *Nature* **440**, 954-958, doi:10.1038/nature04652 (2006).
- 244 Ying, Q. L., Nichols, J., Chambers, I. & Smith, A. BMP induction of Id proteins suppresses differentiation and sustains embryonic stem cell self-renewal in collaboration with STAT3. *Cell* **115**, 281-292 (2003).



- 245 Qi, X. et al. *BMP4 supports self-renewal of embryonic stem cells by inhibiting mitogen-activated protein kinase pathways. Proc Natl Acad Sci U S A* **101**, 6027-6032, doi:10.1073/pnas.0401367101 (2004).
- 246 Zhang, J. & Li, L. *BMP signaling and stem cell regulation. Dev Biol* **284**, 1-11, doi:10.1016/j.ydbio.2005.05.009 (2005).
- 247 Bandy, S., Farooq, Z., Rashid, R., Abdullah, E. & Altaf, M. *Role of Inner Nuclear Membrane Protein Complex Lem2-Nur1 in Heterochromatic Gene Silencing. J Biol Chem* **291**, 20021-20029, doi:10.1074/jbc.M116.743211 (2016).
- 248 Ganley, A. R. & Kobayashi, T. *Ribosomal DNA and cellular senescence: new evidence supporting the connection between rDNA and aging. FEMS Yeast Res* **14**, 49-59, doi:10.1111/1567-1364.12133 (2014).